Distribution Agreement

In presenting this dissertation as a partial fulfillment of the requirements for an advanced degree from Emory University, I hereby grant to Emory University and its agents the non-exclusive license to archive, make accessible, and display my dissertation in whole or in part in all forms of media, now or hereafter known, including display on the World Wide Web. I understand that I may select some access restrictions as part of the online submission of this dissertation. I retain all ownership rights to the copyright of the dissertation. I also retain the right to use in future works (such as articles or books) all or part of this dissertation.

_____

Lauren Smith Havel

Phosphorylation of N-terminal Mutant Huntingtin is Related to its Preferential Nuclear Accumulation in Striatal Neurons

By

Lauren Smith Havel
Doctor of Philosophy

Graduate Division of Biological and Biomedical Sciences
Genetics and Molecular Biology

_____
Xiao-Jiang Li, M.D., Ph.D.
Advisor

_____
Anthony W.S. Chan, DVM, Ph.D.
Committee Member

_____
Anita Corbett, Ph.D.
Committee Member

_____
Judith Fridovich-Keil, Ph.D.
Committee Member

_____
Junmin Peng, Ph.D.
Committee Member

Accepted:

_____
Lisa A. Tedesco, Ph.D.
Dean of the James T. Laney School of Graduate Studies

_____
Date

Phosphorylation of N-terminal Mutant Huntingtin is Related to its Preferential Nuclear Accumulation in Striatal Neurons

By

Lauren Smith Havel
B.S., Lehigh University, 2005

Advisor: Xiao-Jiang Li, M.D., Ph.D.

An ***abstract*** of
A dissertation submitted to the Faculty of the
James T. Laney School of Graduate Studies of Emory University
in partial fulfillment of the requirements for the degree of
Doctor of Philosophy

Graduate Division of Biological and Biomedical Sciences
Genetics and Molecular Biology

2011

Abstract

Phosphorylation of N-terminal Mutant Huntingtin is Related to its Preferential Nuclear Accumulation in Striatal Neurons

By Lauren Smith Havel

Huntington's disease (HD) is a fatal, late-onset neurodegenerative disease caused by a CAG repeat expansion of more than 37 in exon 1 of the gene encoding the huntingtin (htt) protein. Htt is a large 350 kDa protein that is normally localized to the cytoplasm. Cleavage of htt releases N-terminal fragments that can diffuse into the nucleus. In an HD KI mouse model, the striatum, which is the most profoundly affected brain region, shows preferential accumulation of N-terminal mutant htt. The nuclear localization of mutant N-terminal fragments leads to transcriptional dysregulation due to the binding of soluble mutant htt to various transcription factors. Compared to non-expanded N-terminal htt, mutant htt shows decreased binding to the nuclear pore proteins leading to nuclear accumulation. In this study, we found a negative correlation between fragment length and nuclear accumulation as well as toxicity. Recently, the first 17 amino acids (N17) of htt have been implicated in regulation of the subcellular distribution of htt. In this study, we found that compared to serine 13 (S13), serine 16 (S16) is more important in regulating the nuclear accumulation of htt. We generated phosphomimetic (S16D) and loss-of-phosphorylation (S16A) mutants, expressed them in HEK 293 cells and primary striatal neurons and found that phosphorylation increases nuclear accumulation and aggregation. We also found that compared to the cortex and cerebellum, the striatum is enriched for phosphorylated N-terminal htt. More specifically, the nuclei of the striatum appear to be enriched for phosphorylation activity when compared to the cytoplasm of striatal neurons. Mechanistically, our results show that phosphorylation of N-terminal mutant htt inhibits the interaction between htt and the nuclear pore in a fragment length dependent manner and that this interaction is weaker in the striatum than the cortex or cerebellum. Thus we have provided a novel mechanism for the preferential accumulation of N-terminal mutant htt in the striatal nuclei that will be important for the future development of HD therapeutics.

Phosphorylation of N-terminal Mutant Huntingtin is Related to its Preferential Nuclear Accumulation in Striatal Neurons

By

Lauren Smith Havel
B.S., Lehigh University, 2005

Advisor: Xiao-Jiang Li, M.D., Ph.D.

A ***dissertation*** submitted to the Faculty of the
James T. Laney School of Graduate Studies of Emory University
in partial fulfillment of the requirements for the degree of
Doctor of Philosophy

Graduate Division of Biological and Biomedical Sciences
Genetics and Molecular Biology

2011

ACKNOWLEDGEMENTS

I would like to thank my advisor, Xiao-Jiang Li for his support during my time as a graduate student in his lab. His willingness to help troubleshoot experiments was critical to my success and I am grateful that his door was always open for any question, no matter how trivial. I would also like to thank my co-PI Shihua Li who was always available and happy to answer any technical questions that arose during my experiments as well as provide protocols or ideas of where to find them for my experiments. I also owe a thank you to my committee who was always able to help me look at my data in a different way and come up with creative solutions to my experimental difficulties. I would also like to thank my awesome friends, both in Atlanta and in various other areas of the country, who always believed in me and provided me with a constant reminder of why I was here and how hard I worked to get here. I am also fortunate to have a wonderful family who never gave up on me and were always a great source of support. Even though they live 800 miles away, they were always a phone call away and willing to listen. Last but certainly not least I am thankful and lucky to have such a loving and caring husband who is always able to put a smile on my face. He always believed in me, even when I didn't believe in myself. I would never have made it through this process without his unconditional love and support and for that I am forever grateful.

TABLE OF CONTENTS

FIGURES AND TABLES

Chapter 1: General Introduction

Chapter 2: The size of huntingtin N-terminal fragment plays a role in nuclear accumulation of mutant htt

Chapter 3: Phosphorylation of serine 16 of huntingtin regulates its nuclear accumulation and toxicity

CHAPTER 1

General Introduction

1.1 The Polyglutamine Diseases

There are nine inherited polyglutamine repeat disorders including Huntington's disease (HD), Spinocerebellar Ataxia (SCA) 1-3, 6, 7, 17, Dentatorubral-pallidoluysian atrophy (DRPLA) and Spinal and bulbar muscular atrophy (SBMA). These affected disease proteins share no homology aside from a variable length polyglutamine (polyQ) tract. Despite the fact that these proteins have varying functions, subcellular localizations and normal CAG lengths, the polyQ diseases share several critical characteristics **(Table 1-1)**.

First, all of the diseases are caused by a polyQ expansion in the disease protein. Ample evidence shows that the expansion present in all of these diseases is a toxic gain-of-function mutation. For example, the expansion can result in aberrant interactions of the disease proteins with transcription factors such as Sp1 in the case of HD (Dunah et al., 2002; Li et al., 2002) and TFIIB in the case of SCA17 (Friedman et al., 2007). With the exception of SBMA, which is inherited in an X-linked recessive manner, most polyQ repeat disorders are autosomal dominant, meaning that the presence of one functional allele cannot compensate for the new function conferred by the mutated allele. Consistently, transgenic mice expressing exogenous mutant htt in the presence of normal mouse htt show severe neurological phenotypes (Davies et al., 1997; Schilling et al., 1999). In addition, although there is the embryonic death of homozygous htt knock-out mice, heterozygous htt knock-out mice live normally (Duyao et al., 1995; Nasir et al., 1995; Zeitlin et al., 1995). Despite this, loss-of-function of htt has been suggested to also play a role in HD pathogenesis (Cattaneo et al., 2001; Dragatsis et al., 2000). Support for htt loss-of-function playing a role in pathogenesis is that impaired axonal transport of

brain derived neurotrophic factor (BDNF) that results from the expression of polyQ expanded htt (Gauthier et al., 2004) can be rescued by the expression of full-length non-expanded htt. A gain-of-function and loss-of-function role of the expansion has also been observed in SBMA (Evert et al., 2003).

A second characteristic these polyQ diseases share is the formation of nuclear inclusions by the disease proteins, which in many cases are primarily cytoplasmic without the polyQ expansion (**Table 1-1)**. The role and composition of these inclusions is still a source of debate. Third, despite ubiquitous expression of the disease proteins, selective neurodegeneration is observed in all of these diseases and is largely unexplained (**Table 1-1)**. These similarities suggest that the polyQ repeat disorders may share some common pathogenic mechanisms.

HD, which will be the focus of this dissertation, is a rare but fatal disease affecting about 1 in 10,000 in populations of European origin (Harper, 1992). It is inherited in an autosomal dominant manner. Symptoms generally appear during midlife, although juvenile cases do occur with extremely long CAG repeat lengths of more than 50. The patient experiences motor and cognitive abnormalities as well as mood and personality changes. At a molecular level, the large 210 kb gene encoding the htt protein is *IT15*, which is mapped to chromosome 4 (Group, 1993). The htt protein is extremely large (~350 kDa) and contains a variable length polyQ tract of 17 to 34 glutamines encoded within the first exon of the HD gene. The mutant htt protein, however, contains more than 36 glutamines. A larger polyQ expansion leads to an earlier age of onset and more severe symptoms (Duyao et al., 1993). Furthermore, the instability of the

CAG/polyQ tract causes the length of the repeat to change frequently from one generation to another (Duyao et al., 1993; Group, 1993).

The exact function of non-expanded htt has not been conclusively determined; however, it is known to be crucial for development since homozygous htt knock-out mouse embryos die by day 7.5 (Duyao et al., 1995; Nasir et al., 1995; Zeitlin et al., 1995). Significant evidence has suggested that htt may act as a scaffolding protein that is necessary for vesicle transport. One study showed an interaction between non-expanded htt and huntingtin-associated protein (HAP-1) (Li et al., 1995), which associates with subunits of both kinesis and dynein, the proteins that bind to microtubules and carry vescicular cargo along axons (Li et al., 1998; McGuire et al., 2006). Furthermore, it has been demonstrated that non-expanded htt is required for the axonal transport of vesicles carrying BDNF, which is transported within the axons of cortico-striatal projecting neurons and is critical for cell survival (Gauthier et al., 2004). These studies strongly suggest a critical role of htt in neuronal trafficking; however, more work needs to be done to clearly define htt's exact role in this process. It is also likely that htt plays additional vital roles in the cell as it has many binding partners with a wide variety of functions.

Despite the fact that htt is expressed ubiquitously throughout the body, neurodegeneration initially affects the medium spiny neurons of the striatum then extends to other brain regions at later stages of the disease (de la Monte et al., 1988). In HD knock-in (KI) mice, nuclear aggregates of N-terminal htt appear in the striatum first then in the other brain regions during the later disease stages indicating that there is a correlation between nuclear htt aggregation and disease onset (DiFiglia et al., 1997). The role of these aggregates in the disease pathogenesis, however, is highly disputed.

Furthermore, it is possible that the role of the aggregates in the cell is partially determined by their location. The transgenic R6/2 HD mouse model, which overexpresses mutant htt under the control of the human htt promoter, shows significant and widespread aggregation of mutant htt in the striatum and cortex at a very young age (Davies et al., 1997; Li et al., 2001). Interestingly, when the mutant htt gene is endogenously expressed in a 72-80 CAG KI mouse (Shelbourne et al., 1999), neuronal htt aggregates are highly abundant in the nuclei of the striatum while weak or absent from other areas such as the cortex, cerebellum and hippocampus (Li et al., 2001). In addition to the nucleus, htt aggregates appear in the neuronal processes and axonal terminals of the striatum (Li et al., 2000).Why and how these fragments accumulate specifically in the nucleus of the striatum is a mystery that remains to be solved.

1.2 Nuclear Accumulation of huntingtin

Htt is a large protein of about 350 kDa that is primarily cytoplasmic (DiFiglia et al., 1995; Sharp et al., 1995; Trottier et al., 1995). Given the fact that nuclear inclusions are formed by mutant htt, htt must in some way be able to enter the nucleus. Substantial evidence has shown that the N-terminal portion of htt can accumulate in the nucleus (Cooper et al., 1998; DiFiglia et al., 1997; Lunkes et al., 2002; Wang et al., 2008a; Zhou et al., 2003). In support of this fact, the proteolysis of the disease protein to form truncation products that can form nuclear aggregates also occurs in other polyQ repeat disorders such as SCA-3, SBMA and DRPLA (Haacke et al., 2007; Schilling et al., 1999b; Wellington et al., 1998). Endogenous full-length htt is cleaved by caspases 2, 3 and 6 at amino acids 513, 552 and 586 as well as other proteolytic enzymes (Wellington

et al., 1998; Wellington et al., 2000) **(Figure 1-1).** Interestingly, the fragments generated by caspase cleavage are produced not only from mutant htt, but also from non-expanded htt (Kim et al., 2001; Wellington et al., 2002). This indicates that caspase cleavage may be a normal degradation process of htt but the accumulation of mutant htt fragments leads to neurotoxicity.

Later, calpains were shown to also cleave htt at sites near the caspase cleavage sites (Gafni and Ellerby, 2002; Kim et al., 2001) **(Figure 1-1)**. Expanded htt does appear to be cleaved by calpains to a greater extent than non-expanded htt indicating that this cleavage may be more critical to pathogenesis than caspase cleavage (Gafni and Ellerby, 2002). Subcellular fractionation using antibodies that specifically recognize the caspase and calpain derived fragments revealed that the fragments were present in both the cytoplasmic and nuclear fractions while full-length htt remained cytoplasmic (Gafni et al., 2004). Four very small fragments cleaved between amino acids 81 and 129 by aspartic proteases or other unknown proteases have also been identified (Lunkes et al., 2002; Ratovitski et al., 2007). Since these fragments are less than 35 kDa, they are small enough to passively diffuse into the nucleus.

Significant *In vivo* evidence shows that the numerous N-terminal htt fragments described above can be found in the nucleus where they form the nuclear inclusions, a pathological hallmark of HD (DiFiglia et al., 1997; Li et al., 2001; Saudou et al., 1998; Tanaka et al., 2006; Turmaine et al., 2000; Wang et al., 2008a; Zhou et al., 2003). Despite the presence of many htt fragments, it has yet to be determined which ones actually accumulate in the nucleus and exert a toxic effect in the cell. Analysis of the nuclear and cytoplasmic fractions of an HD 150Q KI mouse revealed the nuclear

enrichment of N-terminal htt fragments of less than 110 kDa and a smear on a western blot, which may consist of many bands due to the varying sizes as well as the oligimerization of the fragments (Zhou et al., 2003). Because of this, it is extremely difficult to determine the exact size of the nuclear htt fragments. Several *in vitro* studies have shown that size is a crucial determinant as to whether the fragment accumulates in the nucleus (Hackam et al., 1998; Ratovitski et al., 2009). These studies, however, focused on the formation of nuclear aggregates rather than the localization of soluble htt to the nucleus. Nonetheless, it is crucial to understand which fragments are more prone to nuclear accumulation and how it occurs because nuclear accumulation of htt has been strongly linked to neurotoxicity.

There are many lines of evidence, both *in vitro* and *in vivo,* showing that N-terminal mutant htt is sufficient to cause a neurological phenotype consistent with HD. *In vitro*, various cell lines (Cooper et al., 1998; Peters et al., 1999; Ratovitski et al., 2009) or primary striatal neurons (Saudou et al., 1998) transfected with N-terminal mutant htt show nuclear accumulation and an increase in cellular toxicity as a result. Additionally, inhibition of calpain cleavage in cells transfected with polyQ expanded htt with mutated calpain cleavage sites reduces cell toxicity (Gafni et al., 2004). Similarly, YAC transgenic HD mice expressing caspase-6 resistant mutant htt are protected from striatal neurodegeneration and neuronal dysfunction (Graham et al., 2006). *In vivo*, the transgenic R6/2 mouse, which expresses 150Q exon 1 (67 amino acids) htt, shows a progressive neurological phenotype including decreased brain size, decreased life span, involuntary movements, clasping and a decrease in body weight (Mangiarini et al., 1996).

If nuclear localization of the N-terminal fragments is a critical step in HD pathogenesis, targeting the expanded htt fragments to the nucleus should induce a neurological phenotype in mice. One such study created mice transgenic for 144Q exon 1 htt tagged with an N-terminal nuclear localization signal (NLS) and compared the phenotype of these mice to those tagged with a mutated NLS (Benn et al., 2005). While targeting of mutant htt to the nucleus clearly led to nuclear aggregation and an accelerated onset of the phenotype, their studies as well as others have suggested that cytoplasmic htt also contributes to toxicity (Benn et al., 2005; Hackam et al., 1999). Similarly, when an NLS was added to the N-terminus of a mouse expressing the first 171 amino acids of htt with 82Q (NLS-N171-82Q), a progressive neurological phenotype characterized by reduced body weight and life span, clasping, and reduced coordination and motor skills was accelerated compared to the N171-82Q mice, indicating that nuclear htt plays a toxic role in HD pathogenesis (Schilling et al., 2004). Importantly, the polyQ tract alone seems to be necessary and sufficient for a neurological phenotype in mice as the insertion of 146 CAG repeats into the murine *HPRT* gene (HPRTQ146) caused a late-onset neurological phenotype and also showed the presence of nuclear aggregates (Ordway et al., 1997). Furthermore, the addition of an NLS to the polyQ expanded HPRT protein caused an earlier onset of the neurological phenotype and inclusion formation while the addition of a nuclear export signal (NES) delayed the phenotype (Jackson et al., 2003). Together, these data support the role of nuclear N-terminal mutant htt in neurotoxicity.

1.3 N-terminal huntingtin

The first 17 amino acids (N17) of htt have been shown to play a crucial role in htt localization and aggregation (Rockabrand et al., 2007; Steffan et al., 2004). This sequence, which is immediately followed by the polyQ domain and then a proline rich region, is highly conserved among species suggesting a critical function in the htt protein. N17 htt tagged at the C-terminus with GFP expressed in cells remains almost entirely cytoplasmic mutant htt lacking N17 becomes highly nuclear, suggesting that N17 acts as a cytoplasmic retention signal (Rockabrand et al., 2007).

Consistent with the finding that htt contains a membrane association signal that targets htt to the ER and vesicles (Atwal et al., 2007), Rockbrand et al also found that both expanded and non-expanded htt co-localize with the ER. They also found that non-expanded htt interacts more strongly with the ER membrane than polyQ expanded htt (Rockabrand et al., 2007). They suggest that the decreased association of mutant htt with the ER would leave more mutant htt free to translocate to the nucleus, interfere with cellular processes and form aggregates. The membrane-associated signal is located in the N17 region of htt since a mutation that disrupts the helical structure of the N17 domain leads to significant nuclear accumulation of htt (Atwal et al., 2007). The N17 domain has also been shown to be required for htt aggregation as deletion of N17 or disruption of its structure reduces aggregation (Rockabrand et al., 2007). Additionally, TRiC, a chaperonin that has been shown to decrease htt aggregation and toxicity in cell culture, specifically binds the N17 domain (Tam et al., 2009). The same group also noted that N17 interacts with itself as well as the polyQ tract to initiate the aggregation process.

The mechanism by which htt enters the nucleus has yet to be defined, as a functional classical NLS in htt has not yet been identified (Xia et al., 2003). An NES at

the C-terminus of the protein has been identified but not part of the N-terminal region of htt that accumulates in the nucleus. It is also important to note that the nuclear aggregates are composed of N-terminal htt fragments that have already localized to the nucleus (Xia et al., 2003). Since both polyQ expanded and non-expanded N-terminal htt fragments can enter the nucleus but only the expanded protein becomes trapped there, nuclear export rather than nuclear import must be altered by the presence of the polyQ tract. This is shown in a study revealing that htt interacts via the N17 domain with Tpr, a nuclear pore protein. They found that this interaction is inhibited by a polyQ expansion as seen in the mutant htt protein (Cornett et al., 2005). Thus, the mutant N-terminal protein becomes trapped in the nucleus whereas the wild-type N-terminal protein can be exported out of the nucleus. This idea is supported by the observation that in PC12 cells stably transfected with either htt exon-1 containing either 20Q or 150Q, 20Q htt was primarily cytoplasmic while 150Q htt was mostly nuclear (Li et al., 1999).

1.4 Transcriptional Dysregulation

Due to the fact that many transcription factors contain glutamine-rich domains, it is logical to speculate that the polyQ domain in htt and other polyQ proteins may allow them to interact. Indeed, htt interacts with many transcription factors **(Table 1-2)**. Many of these transcription factors also co-localize with nuclear htt aggregates (Chai et al., 2001; Dunah et al., 2002; Perez et al., 1998; Shimohata et al., 2000; Yamanaka et al., 2008), leading many groups to support the sequestration hypothesis where transcription factors are depleted from the nucleus by interaction with the aggregates so they cannot perform their normal function. However, one of the most compelling pieces of evidence

disputing the sequestration hypothesis is that the formation of inclusions is insufficient to cause cell death (Saudou et al., 1998). Most other groups support the idea that the soluble form of htt interacts with the transcription factors such that these factors cannot perform their normal function.

All of the listed transcription factors with the exception of mSin3a are able to interact with the soluble form of htt in addition to the aggregated form. In the case of Sp1, for example, htt binds in a polyQ length-dependent manner where a polyQ expansion increases the interaction as compared to the non-expanded form (Li et al., 2002). The interaction between transcription factors and the polyQ expanded protein is not unique to HD. In SCA17, for example, polyQ expanded TBP aberrantly interacts with TFIIB and disrupts transcription of TFIIB controlled promoters (Friedman et al., 2007). The fact that only a few polyQ proteins associate with aggregates suggests that the interaction with soluble htt may be more relevant to HD pathogenesis. Furthermore, the co-localization of CBP with polyQ nuclear inclusions is controversial. In the case of SCA-1, CREB binding protein (CBP) does not to co-localize with nuclear polyQ aggregates (Chai et al., 2001). In the case of htt, however, one group found that CBP co-localizes to aggregates and also shows an altered cellular distribution in transfected cells and HD mouse models (Nucifora et al., 2001). Later on, however, the opposite findings were reported that CBP does not co-localize with htt aggregates in HD KI mice and the cellular distribution of CBP was not altered in the presence of mutant htt (Yu et al., 2002). Additionally, neither Sp1 nor TBP co-localize with htt aggregates in HD mice. One thing that may have led to these differences is that the first study used overexpressed protein in their *in vitro* cell studies and the transgenic R6/2 mouse, which overexpresses

N-terminal htt. This overexpression could lead to aberrant and irrelevant interactions of CBP with the aggregates. The second study, however, used the more relevant HD KI model that genetically recapitulates HD pathogenesis better and does not have the complication of htt overexpression. Similarly, in SCA1, ataxin-1 fragments aggregate in the nucleus, but CBP interacts with soluble ataxin-1 rather than the aggregated form (Chai et al., 2001). Altogether these data argue in favor of the hypothesis that the toxic nuclear species is the soluble polyQ protein that binds transcription factors so that they are unavailable to bind their respective promoters.

Due to the aberrant interactions between htt and transcription factors, many groups have investigated the transcriptional changes that occur in HD as well as other polyQ repeat disorders. Some of the first studies were done in cellular models of HD. For example, one study created a stably transfected PC12 model that expresses 150Q exon-1 htt. Htt was diffusely distributed throughout the nucleus and the cells showed transcriptional downregulation of several genes including GLAST, a molecule involved in glutamate uptake, TrkA/NGF and huntingtin associated protein (HAP1) (Li et al., 1999). In support of the nuclear toxicity of htt, these cells also showed defective neurite development and increased apoptosis. Another study showed the downregulation of brain derived neurotrophic factor, BDNF, a protein that is critical for the growth and differentiation of new neurons and synapses and contributes to long-term memory as it is highly active in the hippocampus and cortex (Zuccato et al., 2001). On a more global level, genes with Sp1-dependent promoters (Chen-Plotkin et al., 2006) such as the dopamine D2 receptor (DRD-2) or CRE-mediated promoters (Wyttenbach et al., 2001) are downregulated upon htt expression. Microarray analysis of striatal cells expressing

the N- terminal 548 amino acids of mutant htt also revealed the downregulation of genes involved in cholesterol and fatty acid biosynthesis as well as fatty acid oxidation (Sipione et al., 2002).

Since many of these studies were done in cell culture and did not measure global changes in mRNA expression to the full extent possible *in vivo*, microarrays were used to determine global transcriptional changes in HD mouse models. Analysis of the striatum of R6/2 mice compared to wild-type littermates showed the downregulation of genes in certain categories including signal transduction enzymes, calcium homeostasis and nuclear hormone receptors, which are all involved in processes that have been shown to be affected in HD (Luthi-Carter et al., 2000). Consistent with the idea that small N-terminal htt fragments localized to the nucleus are toxic is the observation that the YAC72 mouse model, which expresses full-length 72Q htt, shows less transcriptional alterations than the HD46 or HD 100 transgenic models expressing N-terminal mutant htt (Chan et al., 2002). Interestingly, another study found that much of the transcriptional dysregulation seems to be dependent on the polyQ tract length rather than the protein context. They analyzed changes in the levels of mRNA in mouse models of HD and DRPLA and found that many of the same genes were downregulated in both diseases (Luthi-Carter et al., 2002b). The fact that the YAC72 mice did not show the same gene expression changes as other transgenic HD mouse models suggests that transcriptional dysregulation seen in HD models is more likely mediated by short N-terminal mutant htt.

Interestingly, transcriptional dysregulation does not seem to be a problem limited to the striatum and cortex as one might expect. Instead, global dysregulation is seen in the cerebellum and even periphery tissues such as muscle, suggesting that transcriptional

dysregulation cannot explain the selective neurodegeneration that is seen in all polyQ repeat disorders (Chan et al., 2002; Luthi-Carter et al., 2002a; Luthi-Carter et al., 2002b). Recently, a study comparing transgenic HD mouse models and KI HD models expressing mutant htt showed that the same changes occurred, though mRNA levels changed at a later stage in the KI mice compared to the transgenic mice (Kuhn et al., 2007). These changes are also consistent with those seen in human HD postmortem tissue, indicating that the gene expression changes observed in HD mouse models are relevant to HD pathogenesis and may be an important factor in developing an effective therapeutic for HD or other polyQ repeat disorders.

Confirmation of these microarray results have consisted of northern blots to verify changes in mRNA levels (Chan et al., 2002; Luthi-Carter et al., 2002b; Sipione et al., 2002) as well experiments that measure the interaction between the transcription factor and its promoter in the presence of mutant or wild-type htt. Mutant htt reduces the binding of Sp1 to the NGFR (Li et al., 2002) and DRD-2 promoters (Chen-Plotkin et al., 2006), while wild-type htt had no effect. A similar study showed that in the presence of mutant htt, there is reduced binding between REST/NRSF and the *BDNF* promoter (Zuccato et al., 2003). Chromatin immunoprecipitation (ChIP) has also been used to show that the interaction of the transcription factor RAP30 with the D2 promoter is decreased in the presence of mutant htt (Zhai et al., 2005).

The decrease in mRNA levels of many genes has also led some groups to verify that the protein product levels of these transcripts were also reduced. A decreased protein level was verified in cells transfected with mutant htt for many genes containing a putative Sp1 binding site such as BDNF (Zuccato et al., 2001), NGF, which consists of

the $p75^{NTR}$ and TrkA subunits (Li et al., 1999), and various other proteins (Luthi-Carter et al., 2002a). Since much of the work so far has focused on changes in mRNA levels, it will be critical to continue focusing on the altered protein levels and their roles in pathogenesis of the polyQ repeat disorders.

1.5 Misfolding and Aggregation of PolyQ Proteins

It is well established that N-terminal fragments of htt, as well as other polyQ proteins, become misfolded. Since correct protein folding is crucial for proper function, the misfolding results in altered function and protein interactions as well as aggregation and toxicity. Molecular chaperones are the proteins responsible for maintaining proper folding of cellular proteins. In HD, chaperone levels have proven to be crucial in regulating the aggregation of htt as well as the phenotypes. For example, several chaperones such as hsp70 and hsp40 are downregulated in the R6/2 mouse model of HD (Hay et al., 2004). Furthermore, overexpression of hsp40 but not hsp70 reduces the aggregation of polyQ proteins and decreases toxicity in cell culture (Jana et al., 2000; Kobayashi et al., 2000; Zhou et al., 2001). Overexpression of either hsp40 or hssp70 also suppressed neurodegeneration in addition to aggregation in *Drosophila* where expanded htt or ataxin-3 was expressed (Chan et al., 2000; Kazemi-Esfarjani and Benzer, 2000; Warrick et al., 1999). The same studies have been carried out in mouse and produced similar results for *SCA1* and *SBMA* mice (Adachi et al., 2003; Cummings et al., 2001). In HD mice, however, there have been conflicting reports. An earlier study showed that overexpression of exogenous Hsp70 in R6/2 HD mice did not significantly alter the phenotype (Hay et al., 2004), but in a later study where endogenous hsp70 was knocked

out in the R6/2 HD mouse, there was a significant reduction in motor abilities, survival and other physical phenotypes (Wacker et al., 2009). This finding raises the possibility that the source (endogenous versus exogenous) of hsp70 may modulate HD symptoms differently.

For several reasons, many investigators have suggested that the mechanism by which chaperones reduce htt induced toxicity is through the reduction of aggregated polyQ protein. First, hsp40 and hsp70, among other chaperones, co-localize with the nuclear inclusions formed by misfolded polyQ protein (Adachi et al., 2003; Hay et al., 2004; Jana et al., 2000; Kobayashi et al., 2000; Wyttenbach et al., 2000). Secondly, the fact that overexpressing the chaperones in various polyQ disease models suppresses aggregation indicates that the aggregates may be the source of toxicity.

The role of aggregates in the pathogenesis of HD, however, is widely disputed. Mounting evidence suggests that soluble rather than aggregated htt is the toxic species within the nucleus. In support of this theory is the proposed alternative method for how chaperones reduce toxicity. Two studies showed that although hsp40 reduces htt aggregation in transiently transfected HEK 293 cells, it also decreases caspase activity, which is indicative of reduced apoptosis (Lotz et al.; Zhou et al., 2001). Furthermore, hsp40, but not hsp70, reduced aggregation whereas both chaperones significantly reduced caspase activity suggesting that the inhibition of apoptosis activation may be the mechanism by which chaperones inhibit neurodegeneration. In another study, hsp40 was shown to reduce the aberrant interaction between soluble mutant htt and Sp1 caused by misfolding of the htt protein, suggesting again that polyQ mediated toxicity may not be caused by nuclear aggregation (Cornett et al., 2006). Other studies support either the

protective or neutral role of nuclear aggregates by showing that the presence of nuclear aggregates does not correlate with cell death (Gutekunst et al., 1999; Saudou et al., 1998). In fact, some data indicate a protective role of aggregates because striatal neurons transiently transfected with mutant htt that formed inclusions earlier survived longer (Arrasate et al., 2004). This study did not indicate whether they took into consideration the localization of the aggregates, and the possibility remains that aggregates may play different roles depending on their localization.

Since the accumulation of misfolded proteins in the cell has deleterious effects, there are two important systems in the cell to clear misfolded proteins. One is the ubiquitin proteasome system (UPS) that recognizes proteins marked for degradation by the presence of a ubiquitin tag. The other is autophagy where the protein is engulfed by autophagasome that is then fused with a lysosome for protein degradation. These systems may fail to remove misfolded polyQ proteins, leading to accumulation of the proteins. Although some studies initially showed that the expression of mutant htt results in global impairment of the UPS (Bennett et al., 2007; Venkatraman et al., 2004), significant evidence now demonstrates that the UPS is not globally impaired in HD animal models. When the proteasomal activity was measured in R6/2 HD mice and WT controls, there was no significant decrease in UPS activity in R6/2 mice (Bett et al., 2006). Crossing a transgenic mouse model of SCA7 (Bowman et al., 2005) or HD (Bett et al., 2009) with a transgenic mouse expressing a ubiquitin GFP reporter construct and analyzing the GFP levels as a measure of proteasome function revealed no global impairment of the UPS. There is, however, some UPS impairment localized to specific neuronal regions such as the synapses (Wang et al., 2008b), suggesting that UPS

impairment may depend on the subcellular localization. Several groups have observed an age-dependent decrease in proteasome activity that may partially explain the late-onset of the disease as well as the progressive accumulation of mutant polyQ protein that causes the inclusion bodies to increase in size with age (Tonoki et al., 2009; Tydlacka et al., 2008; Zhou et al., 2003).

The role of autophagy in the pathology of polyQ repeat disorders has yet to be defined. Significant evidence shows that autophagy can remove mutant htt and its activation can improve the phenotype of HD mice. One of the earlier experiments treated HD-N171-82Q mice and a *Drosophila melanogaster* model of HD with rapamycin, which activates autophagy. They found that rapamycin treatment reduced neurodegeneration in the fly model and improved the motor deficits characteristic of HD mice (Ravikumar et al., 2004). Treatment with rapamycin also decreased aggregation in the striatum of the mice. In a later study, interrupting the formation of autophagosomes and thus inhibiting autophagy enhanced the toxicity observed in cellular and *Drosophila* models of HD (Ravikumar et al., 2008). Increasing the formation of autophagosomes, on the other hand, enhanced the neurodegeneration in the HD *Drosophila* model. Consistent with the fact that autophagy generally clears large or long-lived cytoplasmic protein complexes or damaged organelles; cytoplasmic aggregates seemed to be more prone to degradation by autophagy than nuclear aggregates because of the absence of autophagy in the nucleus (Iwata et al., 2005). More recent evidence, however, has cast doubt on these ideas as rapamycin treatment inhibited htt aggregation in both autophagy deficient and proficient cells (King et al., 2008). Additionally, the presence of mutant htt in the brains of HD mice expressing N-terminal or full-length htt does not cause a significant change

in the conversion of LC3-I to LC3-II, which is a marker for autophagy activation (Li et al., 2010). Similar to the UPS, some evidence suggests the potential for an age-dependent decline in autophagy activity. Beclin 1, for example, is the protein necessary for the formation of autophagosomes and has been found to co-localize with htt aggregates in HD R6/2 mice. Expression levels of Beclin 1 also appear to decrease over time in both HD and control human brains (Shibata et al., 2006). This raises possibility that like the UPS, the system regulating autophagy becomes less active with age, making the brains of HD patients more vulnerable to mutant htt accumulation later in life. Altogether, it can be agreed upon that the machinery necessary for clearing misfolded proteins such as mutant htt becomes dysregulated, leading the mutant protein to accumulate over time in neuronal cells.

1.6 Post-Translational Modifications of Huntingtin

As discussed in the previous section, proper protein folding is crucial to the function of the protein. Since post-translational modifications play an important role in protein folding, any change in modifications can cause misfolding and potentially toxicity. In the case of htt, several post-translational modifications occur in the highly conserved N-terminal 17 amino acids. Ubiquitination was the first to be discovered after htt was found to interact with the ubiquitin-conjugating enzyme, E2-25K, which interestingly is enriched in the striatum and cortex; the most profoundly affected brain regions in HD (Kalchman et al., 1996). Later it was noted that in a *Drosophila* model of HD, the inhibition of htt ubiquitination enhanced the neurodegeneration already seen in the HD flies. In the same study, lysines (K) 6 and 9 of the N-terminus of htt were found

to be sumoylated **(Figure 1-2)**. Increasing the amount of sumoylation in the HD flies enhanced neurodegeneration (Steffan et al., 2004). Together these data suggest that ubiquitination of N-terminal htt is protective whereas sumoylation is toxic. They also raise the possibility that ubiquitination may compete with sumoylation to protect cells from degeneration. More recently, it was proposed that Rhes (Ras Homolog Enriched in Striatum), which localizes specifically to the striatum, interacts with mutant htt, induces sumoylation of htt, decreases aggregation and increases cytotoxicity (Subramaniam et al., 2009). This data is also consistent with the theory that large aggregates may not be the toxic species in HD pathology.

Another major post-translational modification that has been studied in the context of the htt protein is phosphorylation. Initially, a mass spectrometry screen was performed to map the phosphorylation sites common to both mutant and WT full-length htt. Several novel sites were identified but the most N-terminal amino acid showing phosphorylation was amino acid 421 (Schilling et al., 2006), which was also identified by another group and shown to be important for axonal transport (Colin et al., 2008; Zala et al., 2008) **(Figure 1-2)**. As discussed in a previous section, the fragments that accumulate in the nucleus are mostly small N-terminal fragments, suggesting that if phosphorylation affects the localization of N-terminal mutant htt, there are probably some phosphorylated sites closer to the N-terminus.

Recently, another group used mass spectrometry to analyze any phosphorylation sites within exon 1 (the N-terminal 67 amino acids of htt) and identified threonine 3 (T3) as the most common phosphorylation site (Aiken et al., 2009) **(Figure 1-2)**. As seen in cell culture and an HD *Drosophila* model, phosphorylation of T3 is necessary for

aggregation. Interestingly, the T3 residue seems to play a role in toxicity but not through phosphorylation. Most likely, T3 is important to the tertiary structure of the N-terminus. Also within the first 17 amino acids lie two serine (S) residues: S13 and S16, which are also subject to phosphorylation **(Figure 1-2)**. There is conflicting evidence on the role of the phosphorylation state of these residues in HD pathogenesis. Two groups mutated both S13 and S16 to either alanine to generate a loss of phosphorylation mutant or aspartic acid to generate a phosphomimetic mutant, but one group expressed the constructs in cell culture (Thompson et al., 2009) while the other group produced a BACHD mouse expressing both point mutations (Gu et al., 2009). According to the Thompson et al study, phosphorylation of both residues increases the nuclear localization of N-terminal htt and also targets mutant htt to lysosomes or the proteasome for clearance. According to the Gu et al group, phosphorylation of both residues decreases aggregation and toxicity of mutant htt. Importantly, both of these studies looked at the double mutants rather than the single S13 or S16 mutants. There are also many fundamental differences between these studies, which will be discussed in depth later, that cause the role of N-terminal htt phosphorylation to remain unclear.

This dissertation will focus on the factors impacting striatal specific nuclear accumulation of N-terminal mutant htt fragments. In chapter 1, the impact of fragment size will be explored to determine which fragments are capable of accumulating in the nucleus and exerting a toxic effect. Chapter 2 will look specifically at the effect of S16 phosphorylation on the localization, aggregation and toxicity of mutant htt. Chapter 3 will focus on the mechanism of nuclear accumulation of N-terminal mutant htt. The data

will show that N-terminal mutant htt phosphorylated at S16 is enriched in the nuclei of the striatum and that it becomes trapped in the nucleus due to impaired binding to the nuclear export machinery. Overall, this body of work provides a novel mechanism for the striatal specific accumulation of N-terminal mutant htt fragments.

Table 1-1

PolyQ Disease	Normal CAG Repeats	Mutant CAG Repeats	Disease protein	Subcellular distribution	Affected brain region [a]	Known or putative protein function
Huntington's Disease (HD)	6 – 34	36 – 121	Huntingtin (htt)	Cytoplasmic	Striatum	Scaffolding and axonal transport (Li et al, 2004)
Spinocerebellar Ataxia 1 (SCA1)	6 – 44	39 - 82	Ataxin-1	Nuclear	Cerebellum (Purkinje cells)	Transcription co-repressor (Tsai et al., 2004)
Spinocerebellar Ataxia 2 (SCA2)	15 – 24	32 – 200	Ataxin-2	Cytoplasmic	Cerebellum (Purkinje cells)	RNA Metabolism (Ralser et al., 2005)
Spinocerebellar Ataxia 3 (SCA3/MJD)	12 – 39	61 – 84	Ataxin-3	Cytoplasmic	Spinal cord and brain stem	Poly-ubiquitin editing enzyme (Mao et al., 2005)
Spinocerebellar Ataxia 6 (SCA6)	4 – 19	10 – 33	$CACNA1_A$	Membrane Associated	Cerebellum (Purkinje cells)	Main subunit of voltage-gated Ca^{2+} Channel
Spinocerebellar Ataxia 7 (SCA7)	4 – 35	37 – 306	Ataxin-7	Nuclear	Cerebellum (Purkinje cells)	Unknown
Dentatorubral-pallidoluysian atrophy (DRPLA)	7 - 34	49 – 88	Atrophin-1	Nuclear and cytoplasmic	Cerebellum (Purkinje cells)	Transcripton regulation (Wood et al., 2000)
Spinal and bulbar muscular atrophy (SBMA)	9 – 36	38 – 62	Androgen Receptor (AR)	Nuclear	Spinal cord and brain stem	Nuclear hormone receptor
Spinocerebellar Ataxia 17 (SCA17)	25 - 42	47 - 63	TATA binding Protein (TBP)	Nuclear	Cerebellum	Transcription Factor

[a] **The** primary brain region that is affected is listed, but other regions can be affected at late stages of the disease.

Figure 1-1

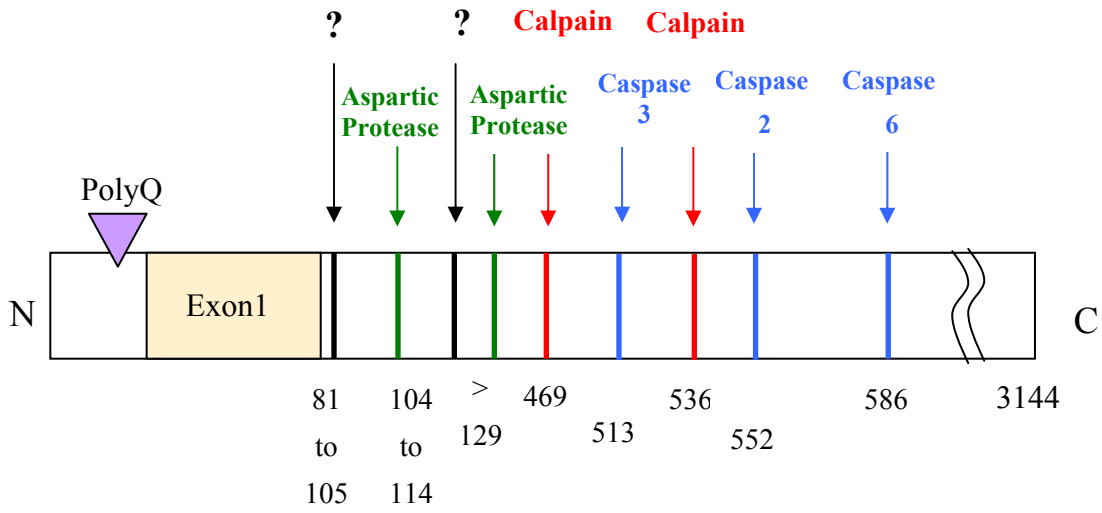
?
?
Calpain
Calpain
Aspartic Protease
Aspartic Protease
Caspase 3
Caspase 2
Caspase 6
PolyQ
N
Exon1
C
81 to 105
104 to 114
> 129
469
513
536
552
586
3144

Figure 1-1. Protease cleavage sites in the huntingtin protein. Htt is cleaved by caspases (blue) at the residues marked at the bottom of the construct (amino acids 513, 552 and 586). It is also independently cleaved by calpains (red) at the marked residues (469, 536). Towards the N-terminus, four protease cleavage products have been identified and mapped to short regions as marked below the construct. The specific proteases (black or green) responsible for the cleavage at these sites have not been determined yet.

Table 1-2

Transcription Factor/Co-factor	Co-localization with Aggregates?	Interaction with Soluble htt?	Region htt binds to	Reference
p53	+	+	polyproline	(Steffan et al., 2000)
Sp1	+	+	aa 1 - 171	(Li et al., 2002)
TAFII130/TAF4	+	+	aa 1 - 480	(Dunah et al., 2002)
CBP	+	+	aa 1 - 588	(Steffan et al., 2000)
CtBP		+	?	(Kegel et al., 2002)
REST-NRSF		+	aa 1 - 548	(Zuccato et al., 2003)
NF-κB		+	HEAT repeats	(Takano and Gusella, 2002)
NCOR		+	aa 1 - 171	(Boutell et al., 1999)
TBP	+	+	?	(Huang et al., 1998)
CA150	+	+	?	(Holbert et al., 2001)
HYPB		+	polyproline	(Faber et al., 1998)
RAP30		+	polyproline	(Zhai et al., 2005)
mSin3a	+		aa 1 - 171	(Boutell et al., 1999)
NF-YA,C	+	?	?	(Yamanaka et al., 2008)

Figure 1-2

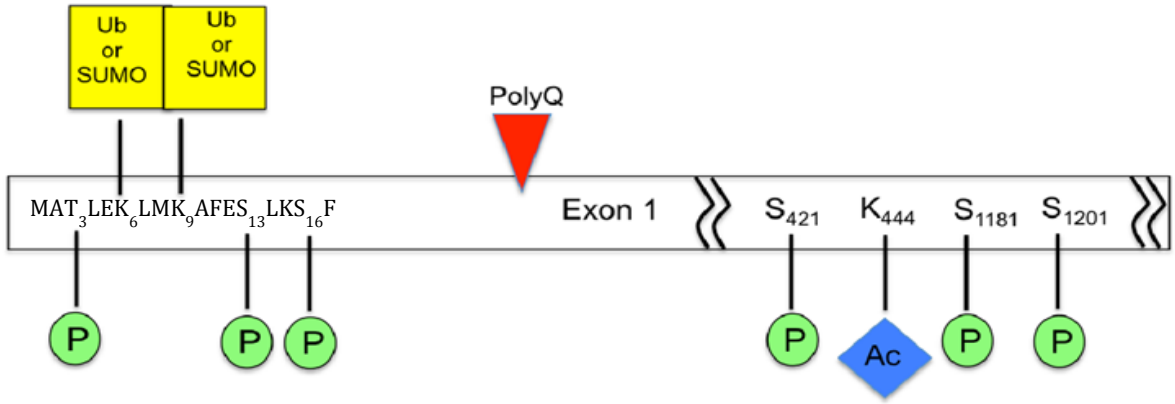
Ub
or
SUMO
Ub
or
SUMO
PolyQ
MAT3LEK6LMK9AFES13LKS16F
Exon 1
S421
K444
S1181
S1201
P
P
P
P
Ac
P
P

Figure 1-2 Post-translational modifications of htt. A diagram showing the various known post-translational modifications found in N-terminal htt. The yellow squares mark lysines that are subject to both ubiquitination and sumoylation. The green circles mark serines or threonines that are known to be phosphorylated. The blue diamonds mark lysines known to be a substrate for acetylation. The number at several of the amino acid residues denotes the amino acid number within the htt protein that is subject to modifications.

CHAPTER 2

The size of N-terminal huntingtin plays a role in nuclear accumulation of mutant huntingtin.

This chapter presents work published as: Lauren S Havel, Chuan-En Wang, Brandy Wade, Brenda Huang, Shihua Li and Xiao-Jiang Li (2011) *Hum Mol Genet* Apr 1;20(7):1424-37. Lauren Havel performed all of the experiments in this chapter with the exception of the culturing of primary neurons, which was done by Chuan-En Wang (figure 2-3). Xiao-Jiang Li and Shihua Li helped with experimental design. Xiao-Jiang Li played a key role in the preparation of the manuscript.

2.1 Abstract

An expansion of the polyglutamine (polyQ) tract to more than 37 glutamines encoded within exon 1 of the huntingtin (htt) protein results in the late-onset neurodegenerative disorder known as Huntington's Disease (HD). An important pathological feature of this disease is the accumulation of N-terminal mutant htt in neuronal nuclei, resulting in the formation of intranuclear aggregates as well as transcriptional dysregulation. The size of the htt fragments that accumulate in the nuclei and cause nuclear toxicity, however, is not known. Here we show in a semi-quantitative manner that size plays a critical role in the nuclear accumulation of N-terminal mutant htt. We also show that the size of the fragment is important for the ability of htt to exert its toxic effect in the nucleus.

2.2 Introduction

A unifying factor among the polyQ repeat disorders is the presence of intranuclear inclusions consisting of the various truncated forms of the mutant polyQ protein as well as other proteins. How these fragments localize to the nucleus and become trapped there still remains to be investigated. Although the possibility remains that htt contains a nuclear localization signal (NLS), no classical NLS has been identified (Hackam et al., 1999; Xia et al., 2003). The most compelling mechanism supporting a passive diffusion mechanism is that the size of the fragments determines whether htt accumulates in the nucleus. It has been established that proteins <40 kDa can freely pass through the nuclear pore whereas proteins >40 kDa generally rely on active transport (Allen et al., 2000). Sometimes proteins lacking a functional NLS can bind to another protein with a

functional NLS to allow nuclear entry. Some early immunocytochemical evidence from experiments done in cell culture indicated that a small amount of full-length htt can be found in the nucleus (De Rooij et al., 1996; Hoogeveen et al., 1993); however, the amount is so small that it can barely be detected by traditional biochemical methods. In support of this, several studies used a subcellular fractionation approach to show that the nucleus and perinucleus of human and HD mouse samples are enriched for N-terminal fragments < 75 kDa but not full-length htt (DiFiglia et al., 1997; Zhou et al., 2003). Because expanded polyQ tracts retard the migration of mutant polyQ proteins in the SDS gel, those N-terminal htt fragments <75 kDa are likely equivalent to the fragments <40 kDa, which can passively diffuse through the nuclear pore. The larger fragments are likely localized to the perinucleus. This is supported by a previous study that showed htt accumulates at the perinucleus where it undergoes caspase cleavage, allowing translocation to the nucleus (Sawa et al., 2005).

The polyQ domain appears to have a large effect on the nuclear accumulation of mutant htt. One study introduced 146 CAG repeats into the mouse hypoxanthine phosphoribosyltransferase gene (*Hprt*) in a transgenic mouse and observed the formation of nuclear inclusions as well as a progressive neurological phenotype similar to that of HD mice (Ordway et al., 1997). Interestingly, when an NLS was added to the same $Hprt^{146CAG}$ gene, the phenotype worsened and nuclear inclusions appeared earlier than those formed by non-NLS tagged $Hprt^{146CAG}$. On the contrary, the addition of a nuclear export signal (NES) delayed the phenotype as well as the formation of nuclear inclusions (Jackson et al., 2003). Also in support of the polyQ tract being crucial for their nuclear aggregation is that all of the mutant polyQ proteins, despite their very different functions

and sequences outside of the polyQ tract, are able to form nuclear inclusions resulting in a progressive neurological phenotype in humans and mouse models. Together these data suggest that the polyQ tract allows nuclear accumulation and toxicity to occur. This is not to say that other regions of the protein do not have an effect on aggregation and toxicity but instead that the polyQ tract is sufficient to cause proteins to accumulate in the nucleus. For example, the first 17 amino acids of htt (N17), which directly precede the polyQ tract, have been shown be important for the aggregation process (Tam et al., 2009). Therefore, there may by regions outside of the polyQ tract that can modify the aggregation and toxicity exerted by the polyQ tract.

The nuclear toxicity caused by the accumulation of N-terminal mutant htt fragments is supported by experiments in cell culture as well as various mouse models. In cell culture, using an NLS to target mutant htt to the nucleus increased cell loss and nuclear accumulation of htt while using an NES to promote nuclear export decreased cell loss and nuclear accumulation of htt (Peters et al., 1999). Similar experiments were carried out in mice where an NLS was added to either exon 1 of htt (Benn et al., 2005) or to N171-82Q htt in HD transgenic mice (Schilling et al., 2004). Targeting mutant htt fragments to the nucleus accelerated the disease onset and increased the formation of nuclear inclusions. Combined with the numerous studies showing aberrant interactions between nuclear htt fragments and transcription factors, these data indicate that N-terminal htt accumulates in the nuclei and plays a toxic role.

Despite this knowledge regarding the factors that impact nuclear aggregation and the composition of the intranuclear aggregates, the specific size of the N-terminal fragment(s) that can accumulate in the nucleus remains unknown. Our hypothesis is that

smaller N-terminal htt fragments are more prone to nuclear accumulation than longer fragments. Although some studies have addressed this to a certain extent, they were all qualitatively based on immunocytochemistry data. We wanted to carry out a more quantitative study to reveal which htt fragments localize to the nucleus and cause toxicity. Furthermore, many of the previous nuclear localization studies focused on the exon 1 portion of htt, which consists of only the first 67 amino acids of htt plus an expanded polyQ tract. Our study, however, uses longer fragments of 208, 300 or 500 amino acids. We convincingly show that fragments as small as 300 amino acids display nuclear accumulation and the 208 fragment of htt causes significant nuclear toxicity to transfected cells.

2.3 Materials and Methods

Cell culture and transient transfection – HEK 293 cells were cultured in Dulbecco's modified Eagle's medium supplemented with 10% FBS, 100 μg/mL penicillin, 100 units/mL streptomycin and 250 μg/μL fungizone amphotericin B. Cells were incubated at 37ºC in 5% CO_2. Cells were plated in a 6-well plate for western blotting or 12-well plate for immunocytochemistry. At a confluency of 70% the cells were transfected with 1-2 μg/well (6-well plate) or 0.5-1 μg/well (12-well plate) of DNA and lipofectamine (Invitrogen) for 48 hours.

Plasmids - A PRK-HA vector expressing htt fragments with N-terminal lengths of 208, 300 or 500 amino acids with a polyQ tract of either 120Q or 23Q was used to transfect HEK 293 cells. These constructs are HA tagged at the C-terminus.

Antibodies – mEM48, a mouse monoclonal, rEM48 and a rabbit polyclonal antibody, which recognize the N-terminus (amino acids 1-256) of htt were used for western blotting and immunocytochemistry at a dilution of 1:100 or 1:1000 respectively. An anti-HA antibody was also used at 1: 1000 (Cell signaling) for both western blotting and immunocytochemistry. Additional antibodies used for western blotting were against GAPDH at 1: 20,000(Ambion), TBP N-12 at 1: 1000 (Santa Cruz). Secondary antibodies, which were used at a concentration of 1: 5000, were peroxidase-conjugated donkey anti-mouse or donkey anti-rabbit IgG (H+L) from Jackson ImmunoResearch (West Grove, PA).

Immunocytochemistry – Transfected HEK 293 cells were fixed with 4% paraformaldehyde (PFM) for 15 minutes then permeabilized and blocked for 1 hour with 3% BSA and 0.2% triton X-100 in 1X PBS. Cells were washed 3 times with 1X PBS then incubated overnight with mEM48 (1:100 dilution) in 3% BSA in 1X PBS at 4ºC. After 3 washes with 1X PBS, the cells were incubated for 1 hour at 4ºC with secondary antibodies conjugated to Alexa flour 488 dye (Invitrogen) or rhodamine red (Jackson Immunoresearch laboratories. DNA was visualized using Hoechst staining (Molecular Probes) at a dilution of 1:5000. Fluorescent images were obtained using a Zeiss

microscope (Axiaovert 200 MOT) with a digital camera (Hamamatsu Orca-100) and Openlab software (Improvision Inc).

Primary neuron culture and transfection - Neurons from the striatum and cortex of E18 rats were isolated and washed in Hanks Balanced Salt Solution (HBSS; Invitrogen). Neurons were treated with 2.5% trypsin in HBSS at 37ºC for 10 minutes then cultured in sterile filtered neurobasal media (2 mM L-glutamine, 2% B-27 supplement, 100 units/mL streptomycin and 100 units/mL penicillin) on poly-D lysine coated plates. At 50-70% confluence in a 12-well plate, the cells were transfected with 2 μg DNA/well and lipofectamine 2000 (Invitrogen). After 5 hours the transfection reagent was removed and replaced with half fresh neurobasal media and half pre-transfection neurobasal media.

Nuclear Fractionation and Western Blotting - To isolate the nuclear fraction from transfected HEK 293 cells, the cells were collected and incubated on ice for 10 minutes in buffer A (20mM Tris-HCl pH 7.4, 10mM NaCl, 3mM $MgCl_2$, 1mM PMSF, 10mM NaF, 0.2mM $NaVO_3$ and 1:100 protease inhibitor cocktail (P8340, Sigma)). Cells were passed through a 22gg syringe 15 times to release the cytoplasmic protein. Cells were centrifuged at 12,000g for 30 seconds to collect the intact nuclei. The supernatant was clarified at 13,000 RPM for 5 minutes and saved as the cytoplasmic fraction. The nuclei were washed with buffer A 3 times and lysed in PBS lysis buffer (1X PBS, 1% Triton X-100 and 1:100 protease inhibitor cocktail (P8340, Sigma)).

To analyze the fractions by western blotting, the protein from each of the fractions was added to SDS sample buffer and resolved on a 4-12% tris-glycine polyacrylamide

gel (Invitrogen). The proteins were transferred to nitrocellulose membrane and blocked with 5% milk in 1X PBS for an hour at room temperature before incubation with primary antibody overnight at 4ºC in 1X PBS with 3% BSA. After washing 3 times for 5 minutes with 1X PBS, the membrane was incubated with horseradish peroxidase (HRP) conjugated secondary antibody (Jackson Laboratories) at 1:5000 for 1 hour at room temperature. The membrane was washed several times with 1X PBS, exposed to the ECL reagent and exposed to autoradiography film (Denville Scientific). Band intensity was calculated with densitometry software (U-SCAN).

Cell viability assay - An MTS assay kit (Promega G3850) was used to measure cell viability. Transfected HEK 293 cells were collected and washed in cold serum free media. The cells were resuspended in 1 mL serum free media per well. 75 µL of the cells plus the MTS reagent were added to a well of a 96-well plate in triplicate. After 30 minutes at 37°C, a SpectraMax Plus plate reader (Molecular Devices) was used to quantify color changes corresponding to cell viability.

Statistical analysis - Results generated from three or more independent experiments and expressed as the mean ±SD and were analyzed for statistical significance using a two-tailed Student's t-test.

2.4 Results

We wanted to evaluate the effect of N-terminal htt size on the nuclear accumulation and toxicity of mutant htt. To this end, we generated N-terminal htt

constructs of varying N-terminal lengths with a polyQ tract of either 23Q or 120Q, which were also tagged at the C-terminus with HA (N208, N300 and N500) **(Figure 2-1A).** To verify expression of these constructs, we transiently transfected HEK 293 cells with each of the 120Q- N208, N300 and N500 constructs for 48 hours. Analysis by western blotting with the mEM48 antibody against the N-terminus of htt showed nearly equal and robust expression (**Figure 2-1B)**. Due to the instability of the polyQ tract of htt, it is highly prone to shortening during amplification. After sequencing, N300 htt was found to have a polyQ repeat shortened to 100Q. It is known that the polyQ length used for experiments in both cell culture and mouse models has to be much longer than the number of repeats (40-50 CAG/glutamine) seen in a typical adult onset HD patient in order to enhance the phenotype and decrease the age of onset. (Orr and Zoghbi, 2007). We therefore believe that this slight shortening will not have a significant effect on the effects of mutant htt.

In order to look at the subcellular localization of the various htt fragments, we transiently transfected HEK 293 cells with the previously described N208, N300 or N500 mutant htt fragments containing 100-120Q as well as the 23Q-N208 fragment as a control. We visualized the localization of htt using immunocytochemistry with both the mEM48 and anti-HA antibodies and took pictures of representative cells **(Figure 2-2)**. We found that although there was no difference in the localization of soluble mutant htt, there was an obvious difference in the localization of the aggregates. Cells transfected with the smaller fragments (N208 and N300) showed the presence of nuclear aggregates as marked by the arrows. The aggregates formed by the larger 500 fragments, on the other hand, were mostly cytoplasmic.

We wanted to confirm this finding in neuronal culture so we cultured primary striatal neurons from an embryonic day 18 rat and transiently transfected them with the same N-terminal htt fragments and used immunocytochemistry with the mEM48 and anti-HA antibodies to analyze the subcellular localization of mutant htt **(Figure 2-3)**. Similar to the results from the transfection of HEK 293 cells, the smaller fragments showed more nuclear accumulation than the larger fragments. Interestingly, while the N208 construct did aggregate whereas the others did not, which is consistent with our previous results, the subcellular localization of the smaller soluble mutant htt was also more nuclear than the larger soluble htt. We were able to see a difference in localization of the soluble mutant htt in the primary neurons but not HEK 293 cells because transfected protein expresses better in HEK 293 cells than primary neurons and the overexpression of mutant htt increases its propensity to aggregate. In HEK 293 cells, the soluble htt that localizes to the nucleus likely aggregates immediately whereas in the primary neurons, which expresses a lower level of transfected htt, the aggregation process is slower. An alternative explanation is that the differences are due to cell type differences.

Another interesting observation we made is that in some transfected cells showing the presence of nuclear aggregates, some aggregates were labeled by mEM48 but not the anti-HA antibody **(Figure 2-4)**. This indicates that these aggregates are made of proteolytic cleavage products of htt from transfected htt fragments. While it is possible that the HA tag is simply hidden within the aggregates, we do not believe this is the case because we saw that a small number of aggregates could be labeled by the anti-HA antibody regardless of the N-terminal length of transfected htt.

In order to evaluate any differences in subcellular localization in a more quantitative manner, we transfected HEK 293 cells with the 120Q-N208, N300 or N500 htt fragments for 48 hours. We performed a subcellular fractionation on the samples to separate the nuclear from cytoplasmic fractions and analyzed the fractions by western blotting with the mEM48 antibody **(Figure 2-5A)**. The purity of the fractions was verified by probing the same blot with an antibody against TBP as the nuclear marker and GAPDH as the cytoplasmic marker. Notably, the bands appearing below the intact htt (marked by the bracket) are N-terminal degradation products resulting from further proteolytic cleavage. Importantly, these products are enriched in the nuclear fraction, which is consistent with fractionation data from a 150Q HD KI mouse, which also shows enrichment of small N-terminal degradation and cleavage products in the nucleus (Zhou et al., 2003). We used densitometry software to quantify the band intensity of the intact N-terminal htt fragments (marked by the arrow). To quantify nuclear htt levels, we first accounted for expression level differences by dividing the nuclear or cytoplasmic densitometry value by the densitometry value of the total fraction. Then we calculated the ratio of nuclear: cytoplasmic intact htt to determine the amount of nuclear htt relative to cytoplasmic htt **(Figure 2-5B)**. As the western blot indicates, we found that the ratio of nuclear: cytoplasmic htt was significantly higher for the shorter N208 and N300 fragments compared to the longer N500 fragment. This data is also consistent with the immunocytochemistry data discussed earlier.

Since N-terminal htt that localizes to the nucleus has been shown to exert a toxic effect through transcriptional dysregulation, we wanted to determine if the size of the fragment also has an effect on the nuclear toxicity of mutant htt. We transfected HEK

293 cells with the 120Q-N208, N300 or N500 htt fragments for 48 hours then collected the cells for a cell viability assay known as the MTS assay. The MTS assay is a colormetric assay that measures cell viability according to the ability of the cell's dehydrogenase enzymes to convert the MTS compound to formazan. Consistent with the previous data that smaller fragments are more prone to nuclear accumulation and the idea that N-terminal htt accumulates in the nucleus to exert a toxic function, we observed that the shorter N208 fragment is significantly more toxic to the cells than the longer N300 or N500 fragments **(Figure 2-6A)**. We also used a small portion of the cells from each sample for a western blot with the mEM48 antibody to verify equal expression of each of the constructs **(Figure 2-6B)**. Although the expression levels are not exactly equal, they are still relevant because N300 htt expressed better than N208 htt but still resulted in significantly higher cell viability levels. Therefore, the results from this experiment may underestimate rather than overestimate the effect of htt size on the toxicity of nuclear htt.

Altogether, these data indicate that N208 mutant htt is able to accumulate in the nucleus and decrease cell viability, which is consistent with the prevailing toxic fragment hypothesis discussed earlier. The mechanism by which this accumulation and toxicity occur, however, remains to be determined.

2.5 Discussion

N-terminal Fragment Size and Nuclear Accumulation of Mutant htt

While previous work by other groups has looked at the effect of size on nuclear accumulation, our study offers a more detailed and quantitative analysis of the nuclear accumulation of mutant N-terminal htt derived from proteolytic cleavage. We show by

immunocytochemistry that the smaller N208 and N300 fragments are able to form nuclear inclusions when overexpressed in HEK 293 cells. This data is consistent with several other studies in cell culture showing that small fragments can accumulate in the nucleus. Two of these studies used an even smaller fragment containing only exon 1 (the first 67 amino acids) or the first 171 amino acids of htt (Cooper et al., 1998; Peters et al., 1999). Another study from our lab used N208 htt with different polyQ lengths and used immunocytochemistry to find that the number of nuclear inclusions increased with polyQ length (Li and Li, 1998).

This is the first study using a subcellular fractionation method to quantify any differences in nuclear accumulation between N-terminal htt fragments of different lengths. This study also has the added advantage of using constructs with a C-terminal HA tag which allows us to track any proteolytic cleavage events that may happen either prior to or after nuclear translocation. We, like many others, found evidence of further htt cleavage that is visible in our immunocytochemistry data **(Figures 2-2 and 2-4)** as well as our subcellular fractionation data, which shows a smear of N-terminal htt fragments (marked by the bracket) that are shorter than the intact transfected form marked by the arrow **(Figure 2-5)**. Other labs studying caspase or calpain cleavage noticed the formation of cleavage products and their propensity to form nuclear inclusions (Lunkes et al., 2002; Ratovitski et al., 2009; Ratovitski et al., 2007). Interestingly, Ratovitski et al (2009) concluded that htt proteolysis is likely a heterogeneous process producing fragments of several lengths. This is consistent with our data showing a loss of the HA tag in some but not all of the aggregates. It is also

consistent with *in vivo* data showing that in the nuclear fractions of 150Q HD KI mice, there is a smear of N-terminal fragments that appears below 75 kDa (Zhou et al., 2003).

N-terminal htt Fragment Size and Toxicity

We also make the important connection between mutant htt fragment size, nuclear accumulation and toxicity. While cytoplasmic htt certainly causes toxicity, especially in terms of axonal transport and synapse function, nuclear htt plays a crucial role in cytotoxicity primarily through transcriptional dysregulation. We showed that in transfected HEK 293 cells, smaller fragments exert a more toxic effect. Notably, both the N208 and N300 htt fragments showed nuclear accumulation according to our immunocytochemistry **(Figure 2-2)** and subcellular fractionation **(Figure 2-5)** data but the N208 fragment was the only one to show significant toxicity in transiently transfected cells **(Figure 2-6)**. This is likely due to the fact that more N208 than N300 htt was localized to the nucleus.

The dependence of nuclear localization of N-terminal fragment size is consistent with a trend we have observed in common HD mouse models where expression of shorter fragments leads to a more severe and earlier onset phenotype than expression of longer fragments or full-length htt. The transgenic R6/2 mouse, for example, overexpresses mutant htt with 150 glutamines and shows a very severe phenotype, a drastically decreased lifespan of 3-4 months, and the early appearance of nuclear inclusions (Mangiarini et al., 1996). Another transgenic HD model is the HD N171-82Q mouse expressing the first 171 amino acids of htt with 82 glutamines. This mouse shows a less severe phenotype than the R6/2 mouse, a lifespan of about 6-7 months and the early

appearance of nuclear inclusions (Schilling et al., 1999a). The 150Q knock-in (KI) mouse, which expresses full-length htt with 150 glutamines under the endogenous promoter, exhibits a very mild and late-onset phenotype, has a fairly long lifespan of more than 18 months and only shows the presence of nuclear inclusions after about 8 months of age (Lin et al., 2001). These data emphasize that idea that shorter N-terminal fragments that can accumulate in the nucleus are more toxic than larger fragments.

Figure 2-1

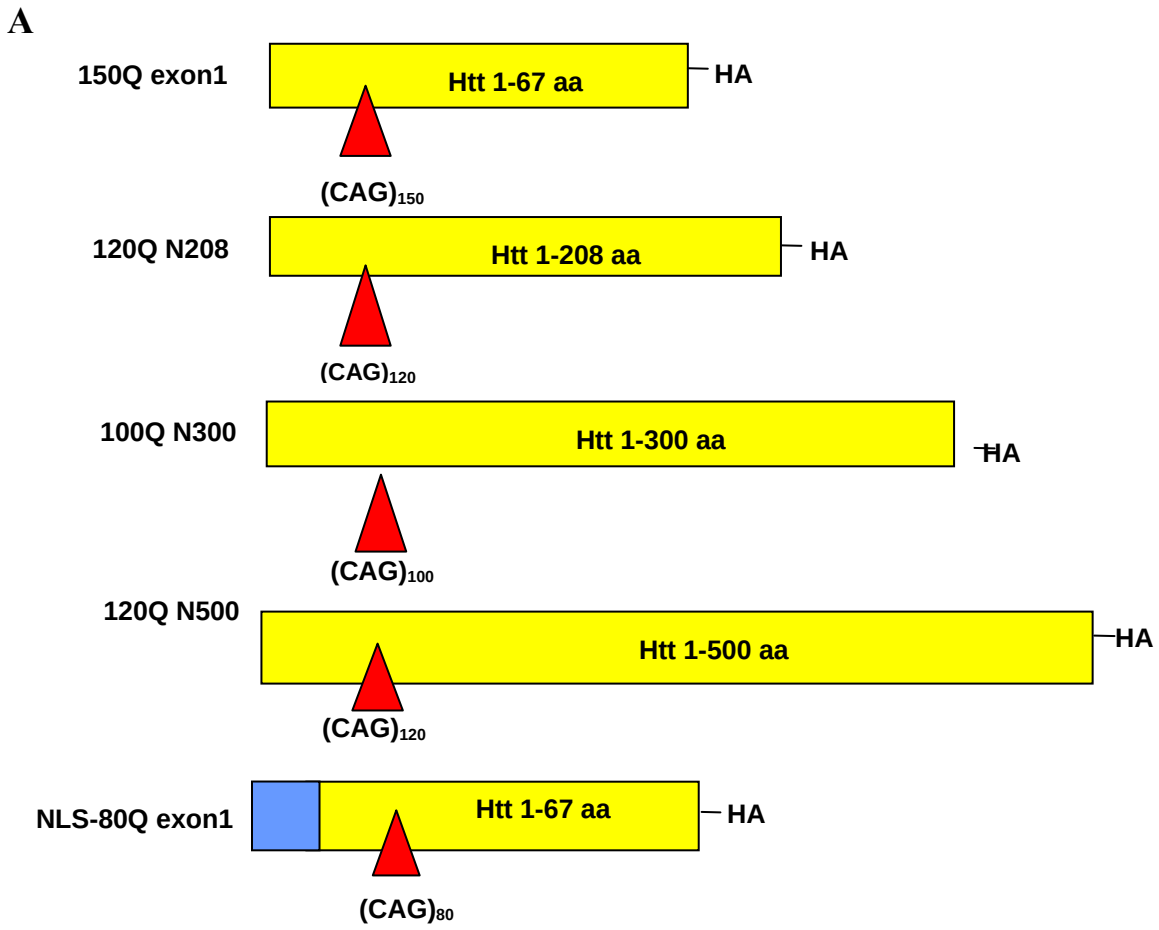
A
150Q exon1
Htt 1-67 aa
HA
(CAG)150
120Q N208
Htt 1-208 aa
HA
(CAG)120
100Q N300
Htt 1-300 aa
HA
(CAG)100
120Q N500
Htt 1-500 aa
HA
(CAG)120
NLS-80Q exon1
Htt 1-67 aa
HA
(CAG)80

B

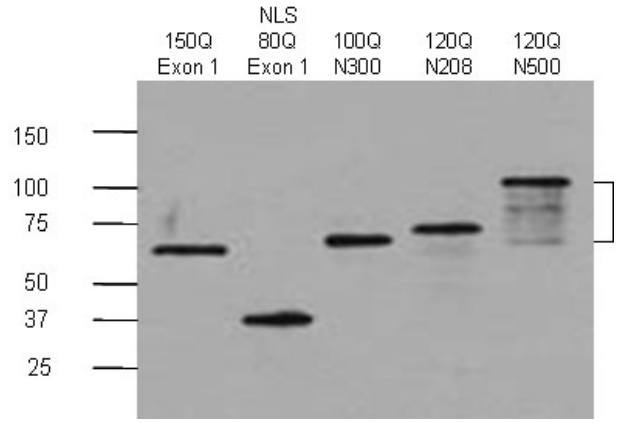
150Q Exon 1
NLS 80Q Exon 1
100Q N300
120Q N208
120Q N500
150
100
75
50
37
25

Figure 2-1. Expression of N-terminal huntingtin fragments. (A) N-terminal htt fragments of varying lengths were cloned into a pRK vector and include a polyQ expansion of either 100Q or 120Q and a C-terminal HA tag. The fragments consisted of the first 67 (exon 1), 208, 300 or 500 amino acids of htt in addition to the polyQ tract. **(B)** A western blot probed with mEM48 showing about equal expression each of the constructs mentioned above in HEK 293 cells. The bracket marks degraded N-terminal htt fragments formed from the larger fragments.

Figure 2-2

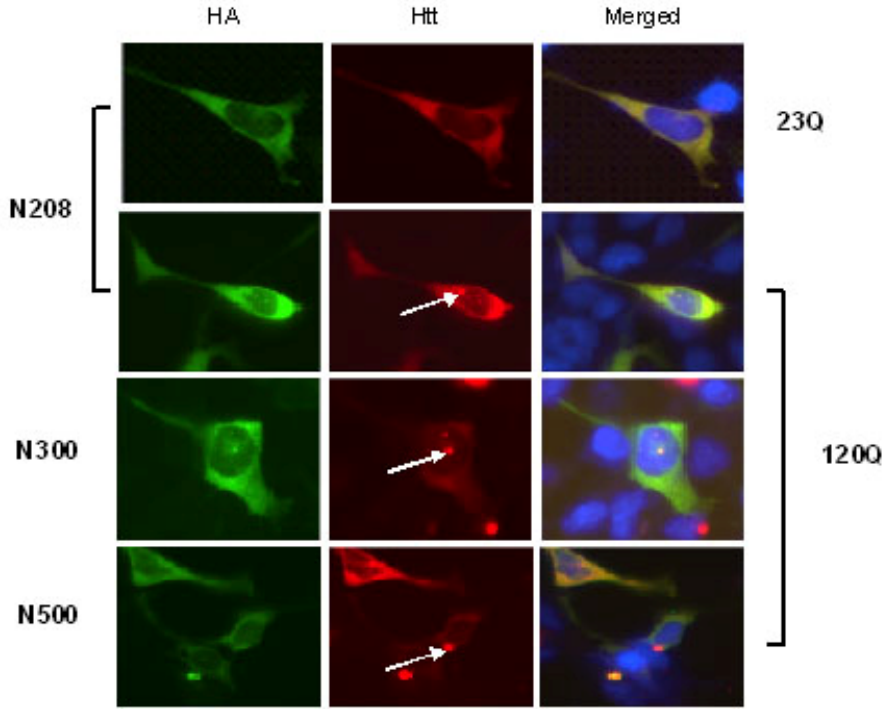

Figure 2-2. Nuclear accumulation of N-terminal mutant htt in HEK 293 cells. 120Q N208, N300, N500 or 23Q N208 htt were expressed in HEK 293 cells for 48 hours and co-stained with rEM48 to label htt (red), anti-HA to label the HA tag (green) and Hoechst dye to label the DNA. N208 and N300 N-terminal mutant htt showed more nuclear aggregation (marked by arrows) than the larger N500 fragment.

Figure 2-3

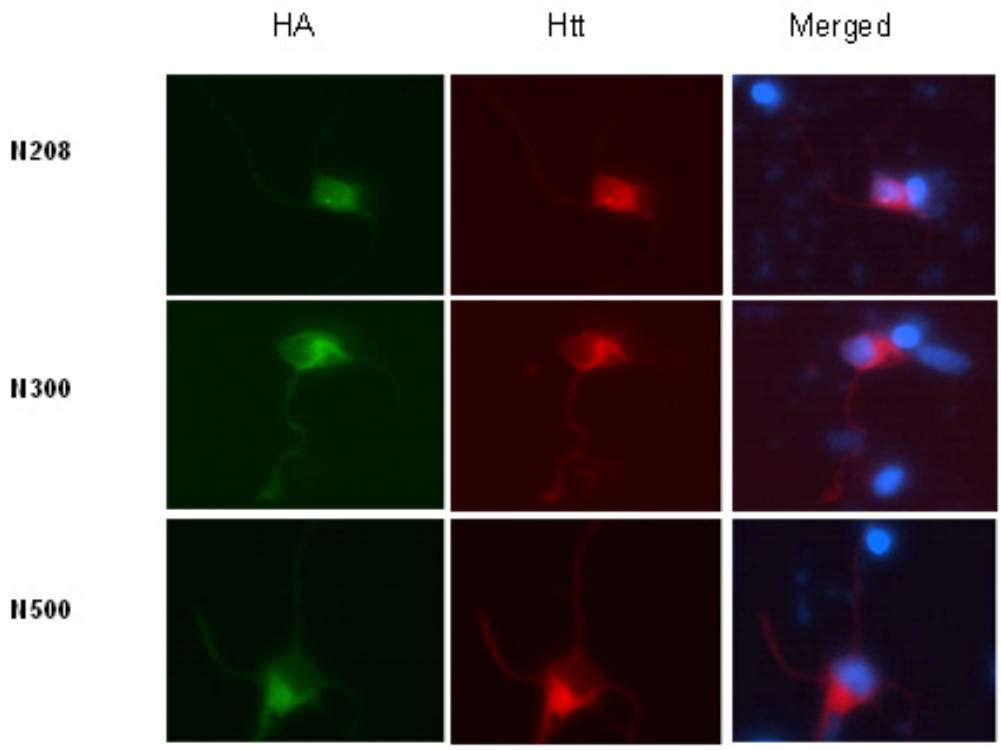

Figure 2-3. Nuclear accumulation of N-terminal mutant htt in primary striatal neurons. 120Q N208, N300 or N500 htt were expressed in embryonic rat primary striatal neurons. The cells were stained with rEM48 to label htt (red), anti-HA to label the HA tag (green) and Hoechst to label DNA. The small N208 fragment was diffuse throughout the neuron while the larger N300 and N500 fragments were localized primarily to the cytoplasm. The shorter N208 fragment also formed a small perinuclear aggregate while the longer fragments did not form any aggregates.

Figure 2-4

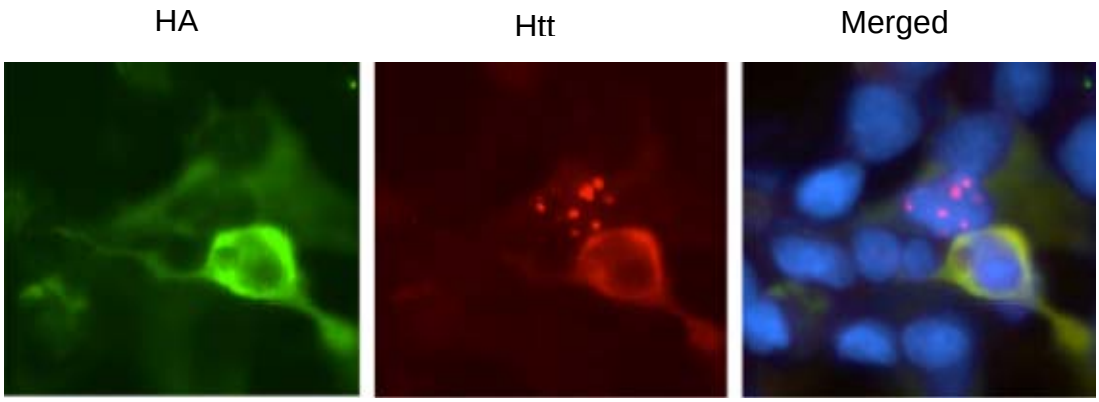

Figure 2-4. Proteolytic N-terminal htt fragments form nuclear aggregates. C-terminally HA tagged 120Q N208 htt was expressed in HEK 293 cells for 48 hours then fixed and stained with rEM48 for htt (red), anti-HA (green) and Hoechst for the DNA. The nuclear aggregates formed by this htt fragment were labeled by the mEM48 antibody but not the anti-HA antibody.

Figure 2-5

A

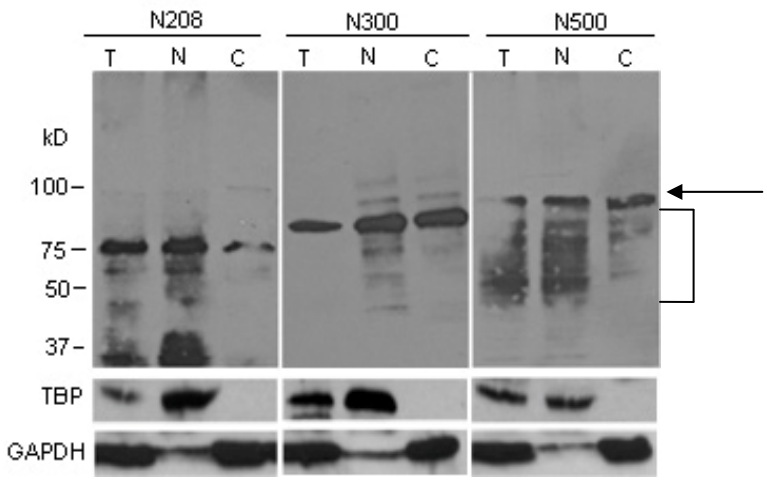
N208
N300
N500
T
N
C
T
N
C
T
N
C
kD
100
75
50
37
TBP
GAPDH

B

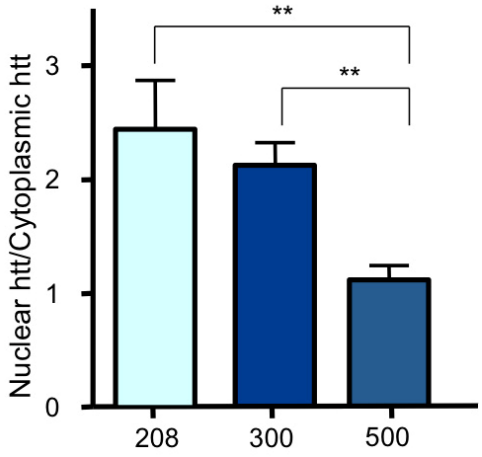
**
**
Nuclear htt/Cytoplasmic htt
3
2
1
0
208
300
500

Figure 2-5. Subcellular distribution of N-terminal mutant Htt. (A) 120Q N208, N300 or N500 htt were expressed in HEK 293 cells for 48 hours. Subcellular fractionation was used to separate the nuclear from the cytoplasmic regions. The fractions were analyzed by western blotting with the mEM48 antibody. The purity of the fractionation was verified by probing for TBP (the nuclear marker) and GAPDH (the cytoplasmic marker). The arrow marks the intact soluble N-terminal htt fragment while the bracket marks the degraded fragments that form. **(B)** Densitometry was used to determine the intensity of the bands for each fraction. To normalize for variable expression of the constructs, the ratio was calculated for both the nuclear: total and cytoplasmic: total. The graph shows the ratio of nuclear: cytoplasmic soluble htt. For densitometry purposes we used the intact version of the soluble htt. There was a statistically significant difference between the nuclear localization of both the N208 and N300 compared to the N500 htt fragment. ** $p < 0.05$

Figure 2-6

A

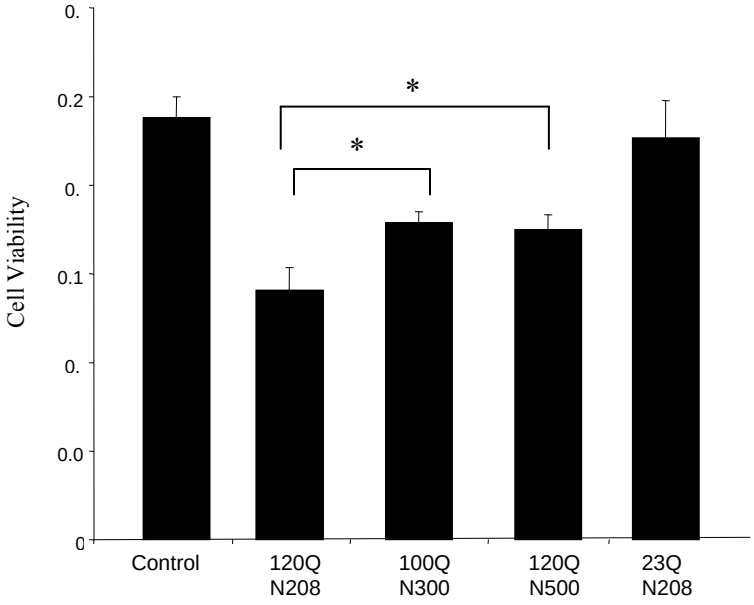
Cell Viability
0.
0.2
0.
0.1
0.
0.0
0
*
*
Control
120Q N208
100Q N300
120Q N500
23Q N208

B

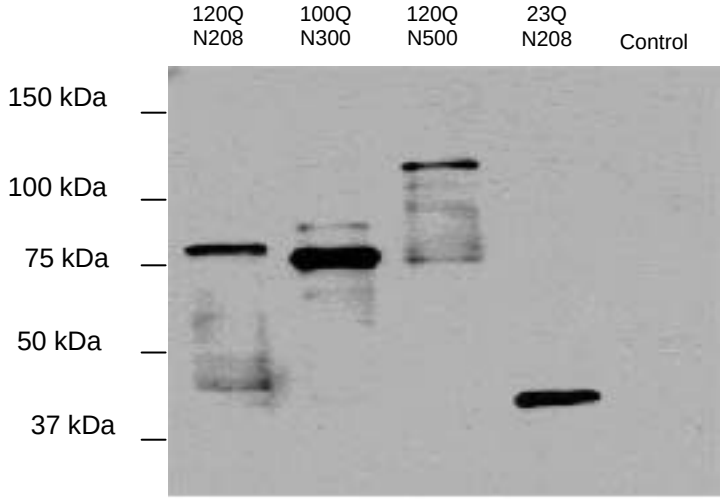
120Q N208
100Q N300
120Q N500
23Q N208
Control
150 kDa
100 kDa
75 kDa
50 kDa
37 kDa

Figure 2-6. Cell Viability of HEK 293 cells expressing N-terminal mutant htt. (A) HEK 293 cells were transfected with 120Q N208, N300, N500 or 23Q N208 htt for 48 hours. An MTS assay was used to determine cell viability. The shorter 120Q N208 htt fragment was significantly more toxic to the cells than the longer N300 or N500 htt fragments. Cells transfected with the pRK vector served as the positive control. * $p < 0.05$ **(B)** Expression of the N-terminal htt fragments was verified using western blotting with the mEM48 antibody against htt.

CHAPTER 3

Phosphorylation of serine 16 of huntingtin regulates its nuclear accumulation and toxicity

This chapter presents work published as: Lauren S Havel, Chuan-En Wang, Brandy Wade, Brenda Huang, Shihua Li and Xiao-Jiang Li (2011) *Hum Mol Genet,* Apr 1;20(7):1424-37. Lauren Havel performed all of the experiments in this chapter with the exception of the culturing of primary neurons, which was done by Chuan-En Wang (figure 2-3). Additionally, Brandy Wade assisted in the generation of the 23Q S13A and S13D constructs as well as the caspase assay. Xiao-Jiang Li and Shihua Li helped with experimental design. Xiao-Jiang Li played a key role in the preparation of the manuscript.

3.1 Abstract

The first 17 amino acids of huntingtin (htt), which directly precede the polyQ tract, are highly conserved across most species, indicating that they are crucial for the function of the htt protein. Within this 17 amino acid region are three potential phosphorylation sites: threonine (T) 3, Serine (S) 13 and S16. Previous studies in cell culture and mouse models have used double S13 and S16 loss of phosphorylation and phosphomimetic mutants to show that phosphorylation of N-terminal htt is important for htt's subcellular localization, aggregation, and clearance. In this study we will explore the role of S16 phosphorylation in the nuclear localization, aggregation, and toxicity of mutant htt. We generated the loss of phosphorylation mutants, S16A and S13A, as well as phosphomimetic mutants, S16D and S13D. We show that the S16 residue appears to be more important for regulating the subcellular localization of mutant htt than the S13 residue. Expression of the S16 mutants in HEK 293 cells and primary striatal neurons showed the phosphorylation of S16 is critical for the nuclear accumulation of mutant htt.

3.2 Introduction

The high degree of conservation across species of the first 17 amino acids of htt (N17) suggests an important role in the protein's function. This region of the protein has recently become a focus of research in the HD field. The N17 region has been shown to exclude htt from the nucleus (Rockabrand et al., 2007) and actually target htt to the ER and other vesicles (Atwal et al., 2007). ER stress is thought to cause N-terminal htt to be released from the ER membrane and transported into the nucleus. Based on these findings, the N17 region clearly plays a crucial role in the subcellular localization of

mutant htt. The mechanisms allowing this transport and resulting in accumulation of N-terminal htt in the nucleus are not yet well defined.

One study showed that the chaperonin protein, TRiC, binds to N17 and blocks aggregation. Thus, suppression of chaperonin proteins such as TRiC, which could occur as a result of aging among other reasons, may provide a favorable environment for nuclear accumulation. Additionally, once mutant N-terminal htt localizes to the nucleus, its binding to the nuclear export proteins has been shown to be impaired compared to non-expanded N-terminal htt (Cornett et al., 2005). This allows mutant htt to become trapped and thus accumulate in nuclei while non-expanded N-terminal htt can still pass through the nuclear pore back into the cytoplasm. The factors regulating such transport and binding have not yet been identified.

A recent idea is that regulation occurs through post-translational modifications of N-terminal htt. In addition to two substrates for both sumoylation and ubiquitination at lysines 6 and 9 (Steffan et al., 2004), there are also three potential substrates for phosphorylation: threonine (T) 3, Serine (S) 13 and 16. One *in vitro* study found that T3 phosphorylation is necessary for mutant htt aggregation but did not analyze its effect on nuclear localization (Aiken et al., 2009). The other two putative phosphorylation sites within the N17 region have been studied in combination but neither has been studied individually. An *in vitro* study showed that phosphorylation of S13 and S16 increased nuclear localization and also increased clearance by the ubiquitin proteasome system (UPS) or autophagy (Thompson et al., 2009). This study, however, did not address neurotoxicity, aggregation or a mechanism for nuclear accumulation. Furthermore, the

fact that S16 phosphorylation targets htt for degradation is not consistent with the increase in nuclear accumulation resulting from phosphorylation.

Another *in vivo* study produced a BAC transgenic mouse with serines 13 and 16 both mutated to either alanine (BACHD AA) to produce a double loss of phosphorylation mutant or aspartic acid (BACHD DD) to produce a double phosphomimetic mutant (Gu et al., 2009). They concluded that phosphorylation of both serine residues inhibited the formation of aggregates and improved motor function suggesting that phosphorylation is actually protective. This study, however, did not specifically address nuclear accumulation of mutant htt. The two studies are also conflicting since Thompson et al showed phosphorylation increased nuclear localization, which would be expected to increase the toxicity of the protein. Gu et al, however, shows that S13 and S16 phosphorylation is protective. Therefore there is still much work to do to fully understand how phosphorylation of N-terminal htt influences HD pathogenesis.

Since the involvement of the individual serine residues in mutant htt nuclear accumulation and toxicity have not yet been analyzed, we chose to produce individual phosphomimetic (S13D or S16D) or loss of phosphorylation (S13A or S16A) mutants to determine which serine residue plays a more important role in nuclear localization of htt. We found that phosphorylation of S16 is more important for increasing the nuclear accumulation and aggregation of N-terminal mutant htt. Thus, we focused the rest of our experiments on the effect of S16 on nuclear accumulation and toxicity of mutant N-terminal htt.

3.3 Materials and Methods

Cell culture, transient transfection and drug treatments– HEK 293 cells were cultured in Dulbecco's modified Eagle's medium supplemented with 10% FBS, 100 μg/mL penicillin, 100 units/mL streptomycin and 250 μg/μL fungizone amphotericin B. Cells were incubated at 37ºC in 5% CO_2. Cells were plated in a 6-well plate for western blotting or 12-well plate for immunocytochemistry. At a confluency of 70% the cells were transfected with 1-2 μg/well (6-well plate) or 0.5-1 μg/well (12-well plate) of DNA and lipofectamine (Invitrogen) for 48 hours. Okadaic acid (OA) was prepared in DMSO at a stock concentration of 120 μM. Transfected cells were treated with OA in serum free media for 4 hours at a final concentration of 50 nM or 100 nM.

Plasmids - Site-directed mutagenesis was performed on the HA tagged 120Q N208 htt construct in a pRK cloning vector to replace serine 16 with alanine (A16) and aspartic acid (D16) in the htt constructs. The PCR was carried out in two rounds in order to introduce both the point mutation and the cloning site. Primers for the first round were designed as follows to introduce the point mutation:

5'ATGAAAGCCTTCGAGTCCCTCAAGGCCTTCCAG-3' (forward, S16A)

5'ATGAAAGCCTTCGAGTCCCTCAAGGACTTCCAG-3' (forward, S16D)

5'ATGAAAGCCTTCGAGGCCCTCAAGGACTTCCAG-3' (forward, S13A)

5'ATGAAAGCCTTCGAGGACCTCAAGGACTTCCAG-3' (forward, S13D)

5'ATTTCCTTATAGAGCTCGAGCTGTAACCTTGGAAGATTAGAATCC -3' (reverse).

The PCR program used for the first round of PCR was as follows

1) 3 minutes - 96°C

2) 45 seconds - 96°C

3) 45 seconds - 66°C

4) 1 minute - 72°C

5) Repeat steps 2-4 for 35 cycles

6) 5 minutes - 72°C

The product was gel purified using Ultrafree DA collumns (Millipore) and used for a second round of PCR to introduce the BamHI cloning site into the construct for insertion into the pRK-HA vector. The primers were designed as follows:

5'-ATTTCCTTATAGAGCTCGAGCTGTAACCTTGGAAGATTAGAATCC-3' (Forward)

5'TAGGATCCGCCATGGCGACCCTGGAAAAGCTGATGAAGGCCTTCGAG TCCCTC-3' (Reverse)

The PCR program used was

1) 3 minutes - 96°C

2) 45 seconds - 96°C

3) 1 minutes - 61°C

4) 1 minutes – 72°C

5) Steps 2-4 were repeated 35 times

6) 5 minutes - 72°C

The PCR product was then gel purified using Ultrafree-DA collumns (Millipore) and

ligated into the pRK-HA vector. The constructs were sequenced through Macrogen to confirm the correct mutations.

Antibodies – mEM48, a mouse monoclonal antibody, which recognizes the N-terminus (amino acids 1-256) of htt was used for western blotting and immunocytochemistry at a dilution of 1:100. Additional antibodies used were against GAPDH at 1: 20,000 (Ambion), TBP N-12 at 1:1000 (Santa Cruz), Sp1 at 1:1000 (Chemicon) and TFIIB at 1:2500 (Santa Cruz). Secondary antibodies, which were used at a concentration of 1: 5000, used were peroxidase-conjugated donkey anti-mouse or donkey anti-rabbit IgG (H+L) from Jackson ImmunoResearch (West Grove, PA).

Immunocytochemistry – Transfected HEK 293 cells were fixed with 4% paraformaldehyde (PFM) for 15 minutes then permeabilized and blocked for 1 hour with 3% BSA and 0.2% triton X-100 in 1X PBS. Cells were washed 3 times with 1X PBS then incubated overnight with mEM48 (1:100 dilution) in 3% BSA in 1X PBS at 4ºC. After 3 washes with 1X PBS, the cells were incubated for 1 hour at 4ºC with secondary antibodies conjugated to Alexa flour 488 dye (Invitrogen) or rhodamine red (Jackson Immunoresearch laboratories. DNA was visualized using Hoechst staining (Molecular Probes) at a dilution of 1:5000. Fluorescent images were obtained using a Zeiss microscope (Axiaovert 200 MOT) with a digital camera (Hamamatsu Orca-100) and Openlab software (Improvision Inc).

Primary neuron culture and transfection - Neurons from the striatum and cortex of E18 rats were isolated and washed in Hanks Balanced Salt Solution (HBSS; Invitrogen). Neurons were treated with 2.5% trypsin in HBSS at 37ºC for 10 minutes then cultured in sterile filtered neurobasal media (2 mM L-glutamine, 2% B-27 supplement, 100 units/mL streptomycin and 100 units/mL penicillin) on poly-D lysine coated plates. At 50-70% confluence in a 12-well plate, the cells were transfected with 2 μg DNA/well and lipofectamine 2000 (Invitrogen). After 5 hours, the transfection reagent was removed and replaced with half fresh neurobasal media and half pre-transfection neurobasal media.

Nuclear Fractionation and Western Blotting - To isolate the nuclear fraction from transfected HEK 293 cells, the cells were collected and incubated on ice for 10 minutes in buffer A (20mM Tris-HCl pH 7.4, 10mM NaCl, 3mM $MgCl_2$, 1mM PMSF, 10mM NaF, 0.2mM $NaVO_3$ and 1:100 protease inhibitor cocktail (P8340, Sigma)). Cells were passed through a 22gg syringe 15 times to release the cytoplasmic protein. Cells were centrifuged at 12,000g for 30 seconds to collect the intact nuclei. The supernatant was clarified at 13,000 RPM for 5 minutes and saved as the cytoplasmic fraction. The nuclei were washed with buffer A 3 times and lysed in PBS lysis buffer (1X PBS, 1% Triton X-100 and 1:100 protease inhibitor cocktail (P8340, Sigma)).

To analyze the fractions by western blotting, the protein from each of the fractions was added to SDS sample buffer and resolved on a 4-12% tris-glycine polyacrylamide gel (Invitrogen). The proteins were transferred to nitrocellulose membrane and blocked with 5% milk in 1X PBS for an hour at room temperature before incubation with primary

antibody overnight at 4ºC in 1X PBS with 3% BSA. After washing 3 times with 1X PBS, the membrane was incubated with horseradish peroxidase (HRP) conjugated secondary antibody (Jackson Laboratories) at 1:5000 for 1 hour at room temperature. The membrane was washed several times with 1X PBS, exposed to the ECL reagent and exposed to autoradiography film (Denville Scientific). Band intensity was calculated with densitometry software (U-SCAN).

Cell viability assay - An MTS assay kit (Promega G3850) was used to measure cell viability. Transfected HEK 293 cells were collected and washed in cold serum free media. The cells were resuspended in 1 mL serum free media per well. 75 µL of the cells plus the MTS reagent were added to a well of a 96-well plate in triplicate. After 30 minutes at 37ºC, a SpectraMax Plus plate reader (Molecular Devices) was used to quantify color changes corresponding to cell viability.

Caspase-3 Assay - Transfected HEK 293 cells were lysed in cell lysis buffer (10mM Tris-HCl pH 7.4, 10mM NaH_2PO_4/Na_2HPO_4 pH 7.5, 130mM NaCl, 1% Triton X-100 and 10mM NaPPi). Cells were broken open by repeated freeze/thaw cycles with dry ice/100% EtOH and a 37ºC water bath. The lysates were clarified at 16,000 RPM for 5 minutes at 4ºC. Protein lysate and 200 µL assay buffer (40mM PIPES, 200mM NaCl, 20mM DTT, 2mM EDTA, 0.2% Chaps and 20% sucrose; pH7.4) were added to a total volume of 400 µL and incubated at 37 ºC for 1 hour. The reactions were transferred to a 96-well plate to be read by a fluorescent plate reader (FLUOstar galaxy) in triplicate.

Statistical analysis - Results generated from three or more independent experiments are expressed as the mean ±SD and were analyzed for statistical significance using a two-tailed Student's t-test.

3.4 Results

First we wanted to determine whether S16 or S13 is more important in regulating the subcellular localization of mutant htt. To this end we generated loss of phosphorylation (serine to alanine) and phosphomimetic (serine to aspartic acid) mutants for both the S16 and S13 residues by site-directed mutagenesis using PCR with primers including the desired mutation **(Figure 3-1).** We produced these mutants in both the 120Q and 23Q htt constructs using the HA-tagged N208 htt construct described in chapter 2 because this htt fragment was able to accumulate in the nuclei of both HEK 293 cells and primary striatal neurons. To determine which residue plays a larger role in the subcellular distribution of htt, we transiently transfected WT-, S16A-, S16D-, S13A- or S13D-htt containing 23Q in HEK 293 cells and performed immunocytochemistry with the mEM48 antibody **(Figure 3-2)**. Since replacing S16 but not S13 with the phosphomimetic aspartic acid residue (D) resulted in increased nuclear localization of 23Q-N208 htt, we concluded that S16 is more important than S13 in regulating N-terminal htt nuclear localization. Also in support of this conclusion is that S16A-htt showed a reduction in nuclear localization compared to both WT and S16D-htt, whereas the S13A-htt did not.

Since we concluded that S16 plays a more important role than S13 in the nuclear localization of N-terminal htt, we wanted to see if we saw a similar difference with the

polyQ expanded 120Q-S16, -S16A and -S16D htt constructs. We transiently transfected HEK 293 cells with these htt constructs for 48 hours and performed immunocytochemistry using the mEM48 antibody **(Figure 3-3)**. Interestingly, we noticed that while 120Q-S16 and -S16D htt showed significant nuclear aggregation (marked by arrows), 120Q-S16A htt showed very little nuclear aggregation. When nuclear aggregates were present they were very small in comparison to the aggregates formed by 120Q-S16 and -S16D htt, indicating that S16 is important for both nuclear localization and aggregation of mutant htt.

We wanted to verify that these differences occur in primary neurons as well. We therefore transiently transfected primary striatal neurons cultured from an embryonic day 18 rat with 120Q-S16 and -S16A htt and performed immunocytochemistry with the mEM48 antibody **(Figure 3-4)**. Like in the HEK 293 cells, representative transfected primary neurons show that 120Q-S16 htt formed large nuclear aggregates whereas 120Q-S16A htt showed no nuclear aggregates. Interestingly, in the neuronal environment, we see a difference in soluble as well as aggregated mutant htt localization. This is likely due to cell type differences and also htt expression level differences. HEK 293 cells likely show more htt aggregates because of their higher transfection efficiency compared to that of primary neurons. Based on these data and the fact that cultured primary neurons are more relevant to the brain neuronal cells, we conclude that S16 is important for the regulation of the nuclear localization and aggregation of mutant htt.

Since the previous immunocytochemistry data is qualitative and shows a limited number of cells, we wanted to generate more quantitative data to verify our immunocytochemistry data. To this end, we transfected HEK 293 cells with 120Q-S16, -

S16A and -S16D N-terminal htt for 48 hours. The cells were gently scraped and subjected to subcellular fractionation to separate the nuclear and cytoplasmic fractions. The fractions were analyzed by western blotting using the mEM48 antibody **(Figure 3-5A)**. The blot shown is representative of several replicates. We used densitometry to quantify the band intensity of the nuclear aggregated htt for each sample. To rule out the influences of varying expression levels of the constructs, we normalized the aggregated htt levels to the intact soluble htt levels (marked by the arrow). Quantification indicated that S16- and S16D-htt show increased nuclear aggregation compared to S16A-htt (**Figure 3-5B**). The bands below the intact soluble band (marked by the bracket) are degraded htt fragments resulting from further cleavage. Interestingly, S16-htt shows increased degradation compared to S16A-htt, as evidenced by the degradation products marked by the bracket on the western blot. This is consistent with the *in vitro* data generated by Thompson et al (2009) showing that N-terminal phosphorylation targets htt to the lysosomes and autophagasomes.

Together these data indicate that S16 is important for the nuclear localization and aggregation of N-terminal mutant htt. To test whether it is phosphorylation rather than a structural change that causes the localization differences between the S16- and S16A-htt, we treated HEK 293 cells transfected with 120Q-S16 or -S16A htt for 4 hours with 50 or 100 nM okadaic acid (OA), a phosphatase inhibitor that can increase cellular phosphorylation. We performed immunocytochemistry on the treated and untreated (control) cells with the mEM48 antibody and found that with increasing concentrations of OA, the levels of nuclear S16-htt increased while there was no change in the levels of nuclear S16A-htt, which is unable to be phosphorylated at S16 (**Figure 3-6**). This

indicates that phosphorylation of S16 is in fact a regulator of N-terminal mutant htt nuclear accumulation. To quantitatively assess whether phosphorylation of S16 is responsible for nuclear accumulation of mutant htt, we performed a subcellular fractionation on OA-treated and control HEK 293 cells transfected with either 120Q-S16 or S16A-htt. The fractions were analyzed by western blotting with the mEM48 antibody **(Figure 3-7A)**. We quantified nuclear enrichment of the soluble htt by using densitometry to measure the band intensity of soluble htt (marked by the arrow) in each fraction and calculating the ratio of nuclear: total htt (**Figure 3-7B**). In agreement with the immunocytochemistry data, treatment with OA increased the nuclear localization of S16 but not S16A N-terminal htt. It is also important to note that the same trend holds true for aggregated htt. Interestingly, the effect of S16 phosphorylation on mutant htt localization seems to be specific to N-terminal fragments since there was no significant change in the localization of full-length endogenous htt (marked by the arrow head) in HEK 293 cells.

To see if phosphorylation at S16 also regulates the localization of normal htt fragments, we performed immunocytochemistry with the mEM48 antibody on OA-treated or control HEK 293 cells transfected with 23Q-S16 or 23Q-A16 (**Figure 3-8**). We saw a trend similar to cells transfected with 120Q-htt where OA treatment increased the nuclear localization of 23Q-S16 htt but had no effect on the localization of 23Q-S16A N-terminal htt. Since the change was subtle by immunocytochemistry, we quantitatively measured the change in localization caused by phosphorylation of S16 using subcellular fractionation of OA-treated or control HEK 293 cells transfected with either 23Q-S16 or -S16A htt (**Figure 3-9A**). Densitometry was used to measure the intensity of each of the

htt bands. The amount of nuclear enrichment for each htt fragment was determined by calculating the ratio of nuclear: total htt (**Figure 3-9B**). Not surprisingly, we found that OA-treatment also increased the nuclear accumulation of 23Q-S16 but not 23Q-S16A htt, indicating that phosphorylation of S16 also regulates the nuclear localization of non-expanded N-terminal htt.

Since nuclear localization of mutant htt has been linked to nuclear toxicity, we also wanted to analyze how phosphorylation of S16 of mutant htt affects cell viability. To this end we used an MTS assay, which is a colorimetric assay measuring the activity of cellular dehydrogenase enzymes that convert the MTS reagent to a purple formazan product as an indicator of cell viability. We transfected HEK 293 cells with 120Q-S16, -S16A or -S16D htt for 48 hours, scraped the cells, exposed them to the MTS reagent in triplicate and measured the amount of formazan produced. Surprisingly, we found that 120Q-S16A htt significantly reduced cell viability relative to 120Q-S16 and -S16D htt (**Figure 3-10A**). Equal expression of the 120Q-htt constructs was verified using western blotting with the mEM48 antibody (**Figure 3-10B**). The dehydrogenase activity measured by the MTS assay assesses mitochondrial function to reflect cell viability. We therefore decided to try a different technique independent of mitochondrial activity to measure cell viability. Since DNA fragmentation is a late sign of cell death, we measured the amount of DNA fragmentation in HEK 293 cells transfected with 120Q-S16, 120Q-S16A or 23Q-S16 htt and performed immunocytochemistry with the mEM48 antibody (**Figure 3-11A**). As seen by the arrows, which mark healthy nuclei, and the arrowhead, which marks nuclei with fragmented DNA, cells transfected with 120Q-S16 htt showed increased cell viability compared to those transfected with S16A-htt. We

scored viable cells by counting those with no visible DNA fragmentation for each of the 120Q-S16 and 120Q-S16A htt transfections and found that transfection of 120Q-S16 htt led to a statistically significant increase in cell viability compared to the transfection of 120Q-S16A htt (**Figure 3-11B**). Since DNA fragmentation is a late stage indicator of cell death, we decided to look at an earlier indicator of apoptosis: caspase-3 activity. We transfected HEK 293 cells with 120Q-S16, 120Q-S16A, 120Q-S16D or 23Q-S16 htt for 48 hours and as a positive control treated untransfected cells with staurosporine to induce cell death (**Figure 3-12**). Surprisingly, we found no significant difference in the caspase-3 activities of cells transfected with the 120Q-htt mutants, though S16-htt slightly increased caspase-3 activity compared to S16A-htt. Increased caspase activity by nuclear htt has been reported previously (Li et al., Hum Mol Genet. 2000), but S16A-htt may produce more cytoplasmic toxicity thereby reducing cell viability.

3.5 Discussion

In this study we show that phosphorylation of S16 increases the nuclear localization and aggregation of mutant N-terminal htt. Consistent with previous studies showing that phosphorylation targets mutant htt to lysosomes or proteasomes (Thompson et al., 2009), we also show that S16 phosphorylation decreases the stability of mutant htt as evidenced by the large increase in the number of degraded N-terminal htt products seen by western blotting (**Figure 3-5A**).

Although other work has been published regarding N-terminal htt phosphorylation, there are some differences between our approaches and findings. One important difference between our studies is that both Thompson et al (2009) and Gu et al

(2009) used double S13 and S16 mutants whereas we focused solely on S16 phosphorylation and its effects. Thompson et al also saw that phosphorylation increases nuclear accumulation and Gu et al showed that phosphorylation decreases aggregation in their transgenic mice. This reduction in aggregation could be due to the lower levels of transgenic S13,16D-htt expressed compared to S13,16A-htt and S13,16-htt. It is also possible that while S16 increases htt nuclear localization as evidenced by our transfection of HEK293 cells with the 23Q S16 and S13 mutant constructs (**Figure 3-2**), S13 can inhibit htt aggregation. Since our S16A construct decreased aggregation, our study provides evidence for the specific role of S16 phosphorylation on nuclear htt accumulation and aggregation.

There are also some remaining questions regarding the effect of phosphorylation of N-terminal htt and toxicity. The BACHD AA mouse showed a worse phenotype than the BACDH DD mouse in the work by Gu et al. Their results suggest that mimicking phosphorylation of S13 and S16 can reduce htt toxicity in transgenic mice. However, their data also show that BACDH DD mice express mutant htt at a lower level than BACDH AA mice, suggesting that the phenotype differences may be caused by variance in transgenic htt expression levels and transgene insertion into different chromosomal regions. In our studies, *in vitro* cell viability assays also showed that phosphorylation appears to be protective against mutant htt induced toxicity. While we were surprised by these results due to its inconsistency with previous findings showing that nuclear targeting of htt increases mutant htt induced toxicity, there are several possible explanations for this result.

First and most likely is that in our *in vitro* assays using HEK 293 cells, most of transfected htt is in the cytoplasm. The subcellular localization of transiently transfected htt in non-neuronal cells is different from the abundant nuclear accumulation of mutant htt in the neuronal cells in aged mouse or human brains. Although we did not specifically study the effect of phosphorylated htt on cytoplasmic toxicity, it is possible that S16 phosphorylation is protective when mutant htt is localized to the cytoplasm and this protective effect masks the small amount of toxicity caused by the limited nuclear translocation of mutant htt. This idea is supported by our immunocytochemistry data of HEK 293 cells transfected with the S16-, S16A- and S16D-htt mutants where much of the soluble mutant htt remains either perinuclear or cytoplasmic (**Figure 3-3**). The mutant htt that is localized to the nucleus is mostly sequestered into large aggregates. Also in support of this theory is that the BACHD AA and BACHD DD mice show varying expression levels (Gu et al., 2009). The BACHD DD mice expressed full-length htt at a lower level than the BACHD AA mice. The toxicity observed in the BACHD AA mice may be due to cytoplasmic toxicity of phosphorylated mutant htt since a loss of phosphorylation reduces nuclear accumulation of mutant htt. The reduced htt expression in the BACHD DD mice may not allow the detection of toxicity exerted by nuclear N-terminal htt.

A second possibility is potential cell type differences as mentioned above. The localization of soluble mutant htt differed greatly in primary striatal neurons (**Figure 3-4**) whereas in HEK 293 cells, which were used for the toxicity studies, the differences in localization between S16- and S16A-htt was limited to the nuclear aggregates (**Figure 3-3**). It would be useful to look at toxicity in transfected primary neurons, however, this is

difficult because the transfection efficiency of primary neurons is too low for biochemical assays. Cell type has already been shown to impact cell viability as evidenced by the production of various types of HD animal models. For example, although HD mouse models show nuclear aggregation of htt as well as a progressive neurological phenotype, they do not show overt neuronal death. Recently, however, HD transgenic pigs expressing 105Q N208 htt show apoptosis, indicating that cell types in different species can determine mutant htt-mediated neuropathology (Yang et al., 2010).

A third possibility is that the nuclear aggregates are protective. This would be consistent with the data generated by Gu et al (2009) where mutating both S13 and S16 to aspartic acid improved the motor function of BACHD mice (Gu et al., 2009)(Gu et al., 2009)(Gu et al., 2009)(Gu et al., 2009)(Gu et al., 2009)(Gu et al., 2009)(Gu et al., 2009)(Gu et al., 2009). As I discussed earlier, however, aggregated htt could be protective or toxic based on the subcellular localization. Nuclear htt aggregation may reduce the interactions of mutant htt with other transcription factors to prevent gene transcriptional dysregulation whereas cytoplasmic htt aggregates can physically interfere with trafficking in neuronal processes. It is clear that more work needs to be done both *in vitro* and *in vivo* to determine the role of S16 phosphorylation in cell toxicity and HD pathogenesis.

Figure 3-1

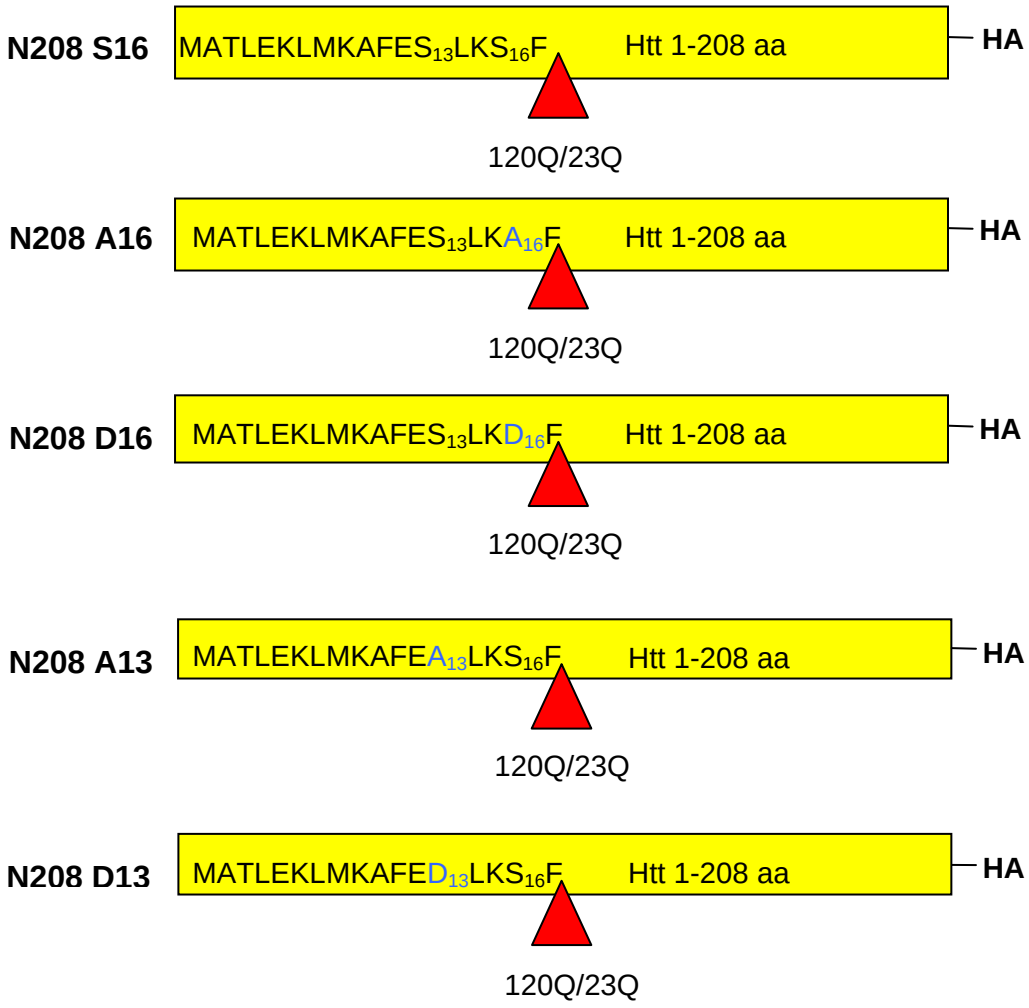
N208 S16
MATLEKLMKAFES13LKS16F
Htt 1-208 aa
HA
120Q/23Q
N208 A16
MATLEKLMKAFES13LKA16F
Htt 1-208 aa
HA
120Q/23Q
N208 D16
MATLEKLMKAFES13LKD16F
Htt 1-208 aa
HA
120Q/23Q
N208 A13
MATLEKLMKAFEA13LKS16F
Htt 1-208 aa
HA
120Q/23Q
N208 D13
MATLEKLMKAFED13LKS16F
Htt 1-208 aa
HA
120Q/23Q

Figure 3-1. N-terminal htt constructs containing mutations that affect their phosphorylation state. Site directed mutagenesis was used to mutate either serine 13 (S13) or serine 16 (S16) of N208-120Q or -23Q htt to alanine (A) to create loss of phosphorylation mutants. The same residues were also mutated to aspartic acid (D) to create phosphomimetic mutants. All of these mutants also contain a C-terminal HA tag.

Figure 3-2

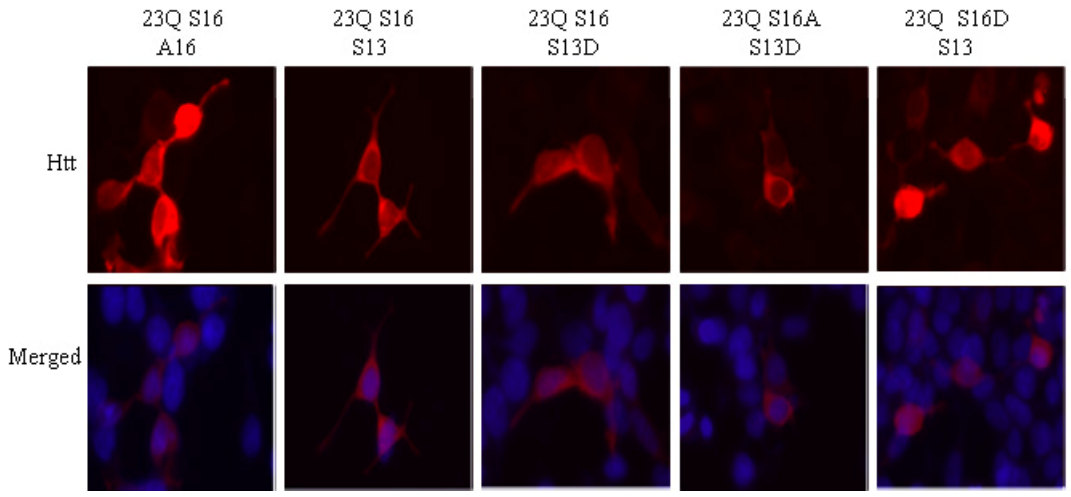
23Q S16
A16
23Q S16
S13
23Q S16
S13D
23Q S16A
S13D
23Q S16D
S13
Htt
Merged

Figure 3-2. Expression of the 23Q-S13 and -S16 htt mutants in HEK 293 cells. 23Q WT-, S13A-, S13D-, S16A- and S16D-htt were expressed in HEK 293 cells for 48 hours than stained with mEM48 for htt and Hoechst for DNA to analyze the localization of htt for each of the mutants. The S13A and S13D mutants had a similar cytoplasmic distribution of htt. The S16D mutant however was much more nuclear than the S16A mutant indicating that the S16 residue of htt may be important for htt's localization.

Figure 3-3

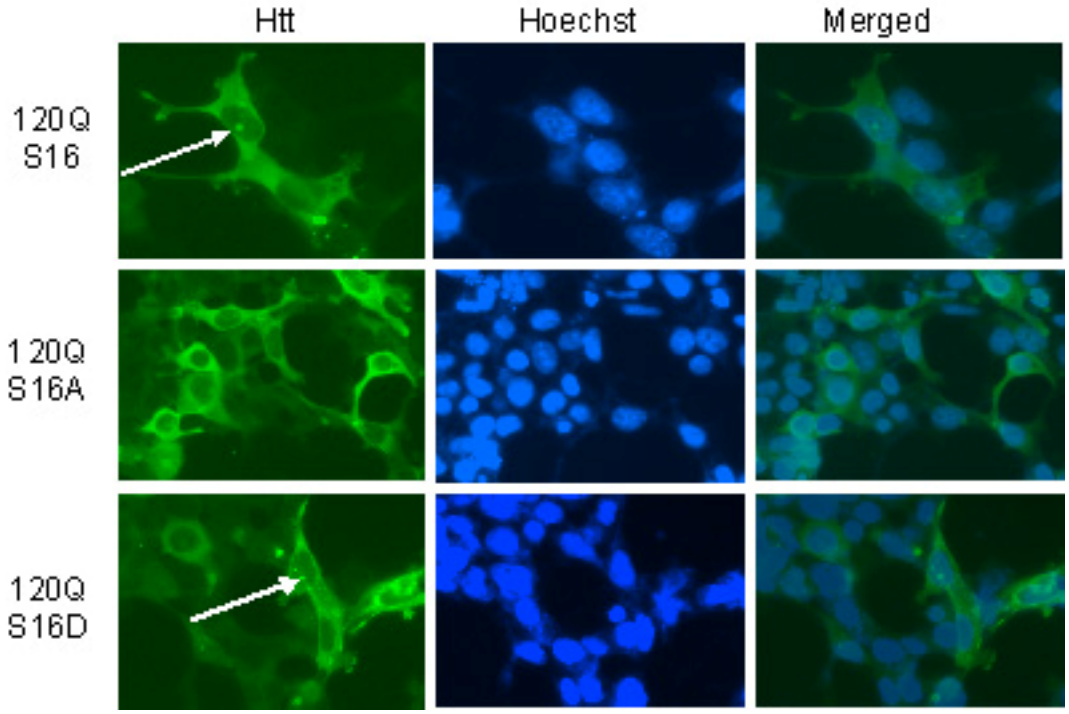

Figure 3-3. Expression of the 120Q-S16 htt mutants in HEK 293 cells. 120Q-S16, -S16A and -S16D htt were expressed in HEK 293 cells for 48 hours then stained with mEM48 for htt and Hoechst for DNA. S16- and S16D-htt showed large nuclear aggregates as marked by the arrows. S16A-htt, however, showed very few nuclear aggregates suggesting that the S16 residue may be important for nuclear aggregation of htt.

Figure 3-4

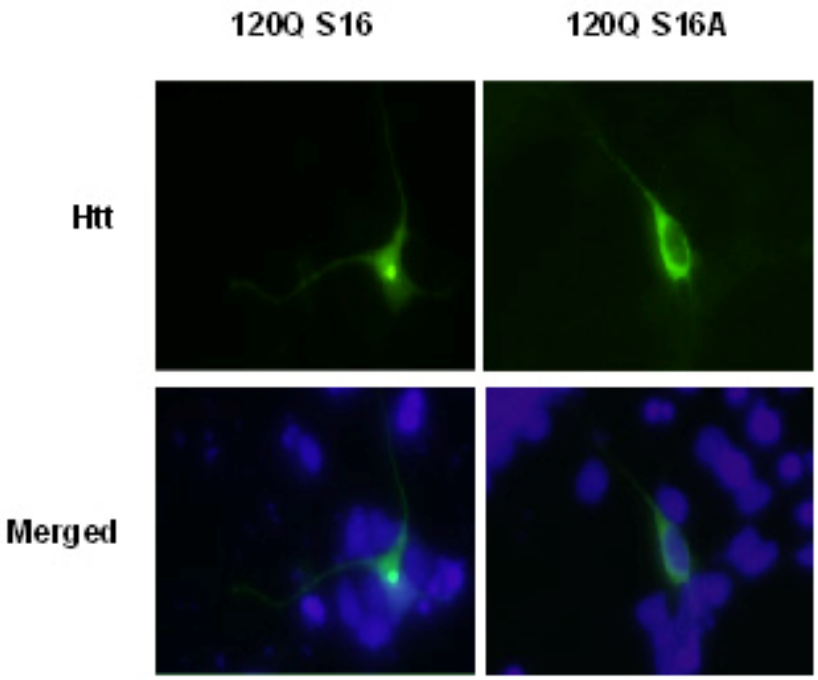

Figure 3-4. Expression of 120Q-S16 htt mutants in primary striatal neurons. 120Q-S16 and 120Q-S16A htt were expressed in embryonic rat primary striatal neurons for 48 hours. They were stained with mEM48 to label htt and Hoechst to label DNA. The cells expressing 120Q-S16 showed both nuclear and cytoplasmic staining with a perinuclear aggregate. The cells expressing -S16A htt, however, showed primarily cytoplasmic staining with no visible aggregation.

Figure 3-5

A

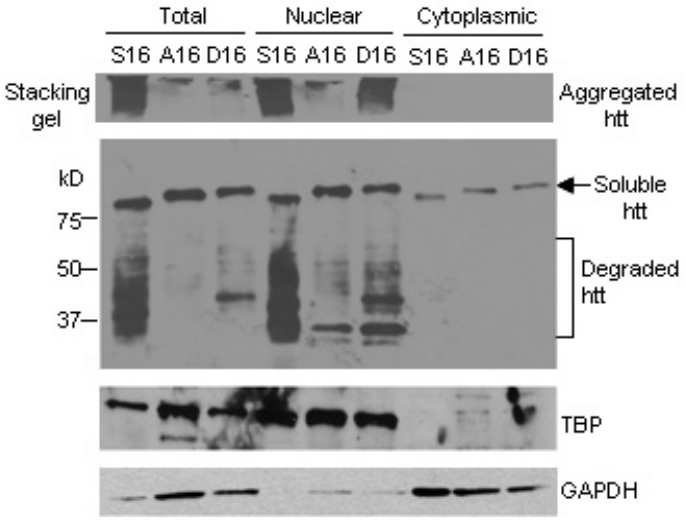
Total
Nuclear
Cytoplasmic
S16 A16 D16 S16 A16 D16 S16 A16 D16
Stacking gel
Aggregated htt
kD
75
50
37
Soluble htt
Degraded htt
TBP
GAPDH

B

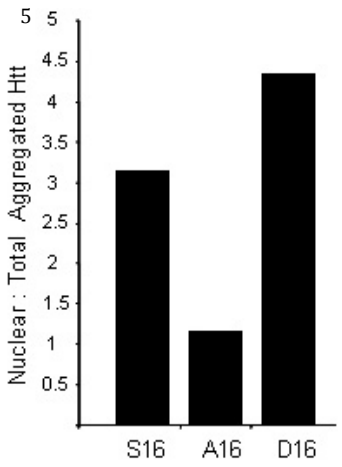
Nuclear : Total Aggregated Htt
5
4.5
4
3.5
3
2.5
2
1.5
1
0.5
S16
A16
D16

Figure 3-5. Subcellular distribution of the S16 htt mutants in HEK 293 cells. (A) HEK 293 cells were transfected with 120Q-S16, -S16A and -S16D htt for 48 hours. Subcellular fractionation was used to separate the nuclear and cytoplasmic fractions. The distribution of htt among the fractions was analyzed by western blotting using the mEM48 antibody. The purity of the fractions was verified by probing for TBP as the nuclear marker and GAPDH as the cytoplasmic marker. The upper panel of the blot represents the aggregated htt that remains in the stacking gel. The middle panel represents the soluble htt. The upper band is the intact form of the N-terminal htt (marked by the arrow) and the bands below it are the degraded N-terminal products (marked by the bracket). **(B)** Densitometry was used to measure the intensity of the bands for both the aggregated and intact soluble htt for a representative blot. To control for variable expression between the constructs, the ratio of aggregated htt to soluble htt was calculated. The nuclear: total ratio of the normalized aggregated htt was then calculated and graphed to determine nuclear enrichment of the N-terminal htt aggregates. Both S16- and S16D-htt showed increased nuclear aggregation compared to S16A-htt.

Figure 3-6

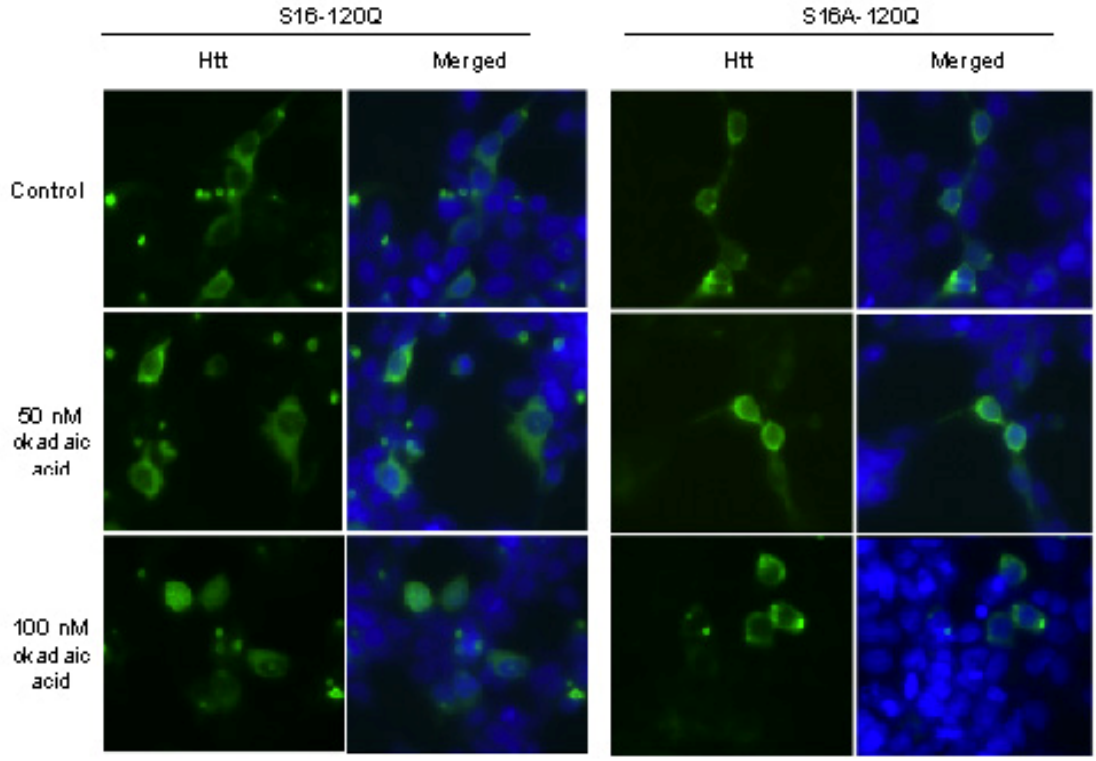
S16-120Q
S16A-120Q
Htt
Merged
Htt
Merged
Control
50 nM okadaic acid
100 nM okadaic acid

Figure 3-6. Okadaic acid treatment of HEK 293 cells expressing 120Q-S16 htt mutants. HEK 293 cells were transfected with 120Q-S16 or 120Q-S16A htt for 48 hours then treated in serum free media for 4 hours with 50 nM or 100 nM okadaic acid (OA) to increase total cellular phosphorylation. The cells were fixed and stained with the mEM48 antibody to label htt and Hoechst to label the DNA. The okadaic acid treatment increased the nuclear localization of soluble 120Q-S16 htt but had no effect on the localization of 120Q-S16A htt indicating that phosphorylation of S16 is important for the nuclear accumulation of mutant htt.

Figure 3-7

A

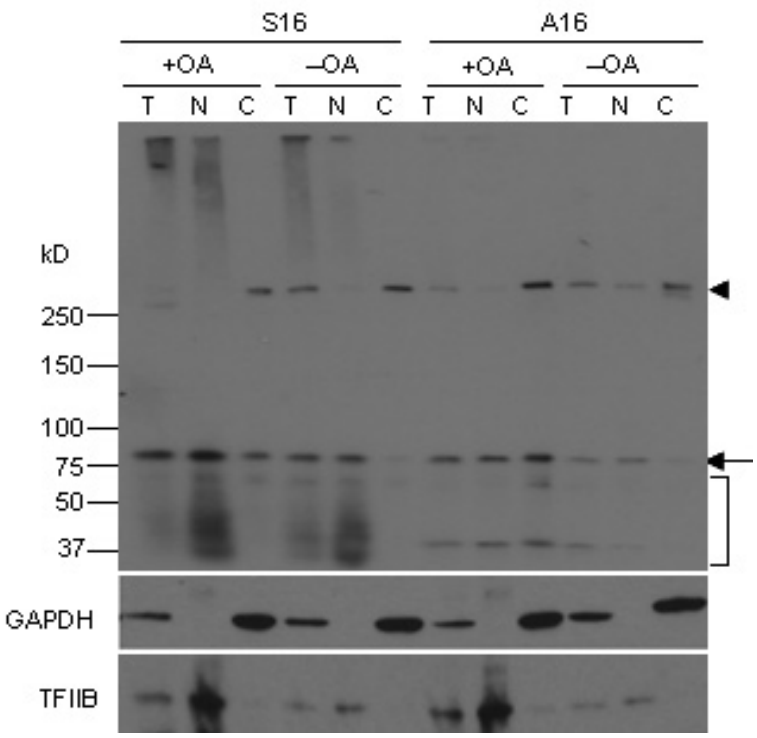
S16
A16
+OA
–OA
+OA
–OA
T N C T N C T N C T N C
kD
250
150
100
75
50
37
GAPDH
TFIIB

B

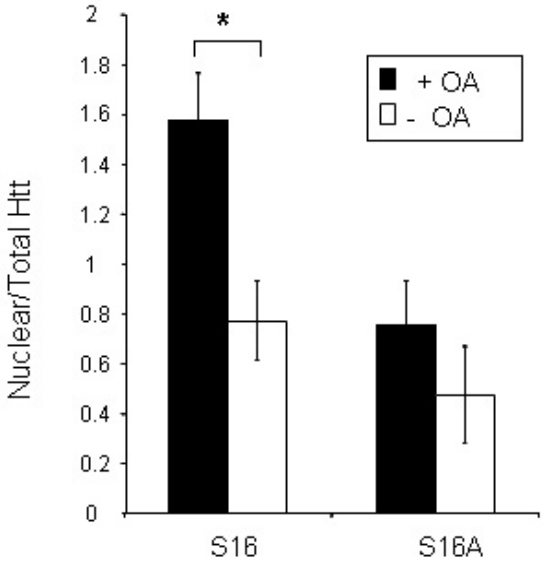
Nuclear/Total Htt
2
1.8
1.6
1.4
1.2
1
0.8
0.6
0.4
0.2
0
*
+ OA
- OA
S16
S16A

Figure 3-7. Subcellular distribution of N-terminal 120Q-S16 htt mutants in okadaic acid treated HEK 293 cells. (A) HEK 293 cells were transfected with 120Q-S16 or -S16A htt for 48 hours then treated with either 100 nM okadaic acid or DMSO for 4 hours in serum free media. Subcellular fractionation was performed to separate the nuclear and cytoplasmic fractions. The distribution of htt among the fractions was analyzed by western blotting using the mEM48 antibody against htt. The purity of the fractions was analyzed by probing for TFIIB as the nuclear marker and GAPDH as the cytoplasmic marker. The arrowhead marks endogenous full-length htt and the arrow marks intact transfected N-terminal htt. The bracket marks the degraded N-terminal htt fragments. **(B)** Densitometry was used to measure the intensity of the soluble intact N-terminal htt bands marked by the arrow. To determine the nuclear enrichment of each of the constructs (+ OA and –OA), the ratio of soluble nuclear: soluble total htt was calculated. OA treatment significantly increased the nuclear localization of the 120Q-S16 but not 120Q-S16A N-terminal htt. The distribution of full-length htt (marked by the arrowhead) remained unaltered by OA treatment indicating that phosphorylation of htt only affects the nuclear distribution of N-terminal mutant htt. * $p < 0.05$.

Figure 3-8

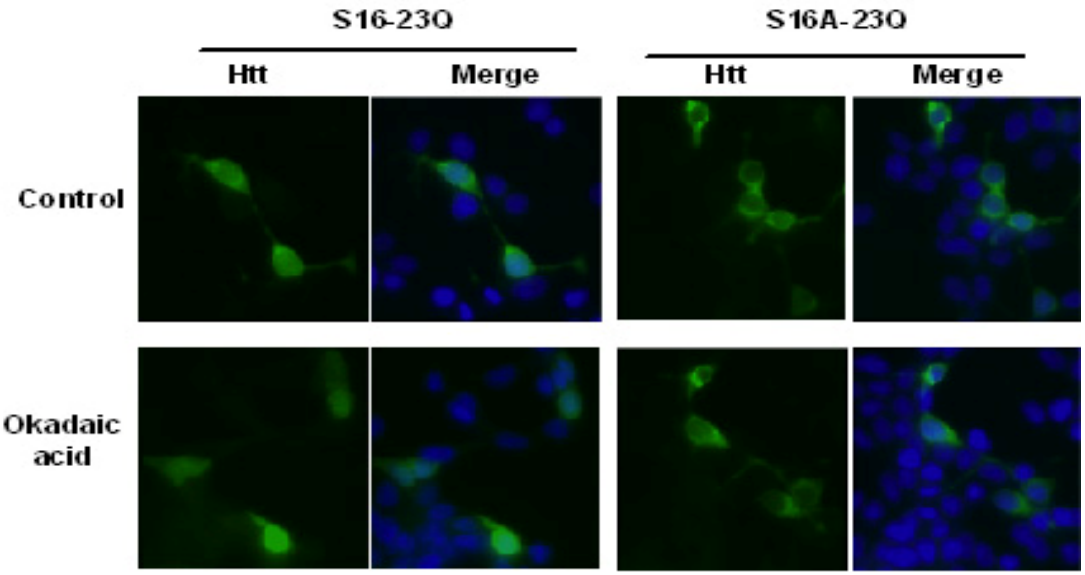

Figure 3-8. Okadaic acid treatment of HEK 293 cells expressing 23Q-S16 htt mutants. HEK 293 cells were transfected with 23Q-S16 or 23Q-S16A htt for 48 hours then treated in serum free media for 4 hours with 100 nM okadaic acid (OA) to increase total cellular phosphorylation. The cells were fixed and stained with the mEM48 antibody to label htt and Hoechst to label the DNA. The okadaic acid treatment increased the nuclear localization of 23Q-S16 htt but had no effect on the 23Q-S16A htt indicating that phosphorylation of S16 is important for the nuclear accumulation of non-expanded htt.

Figure 3-9

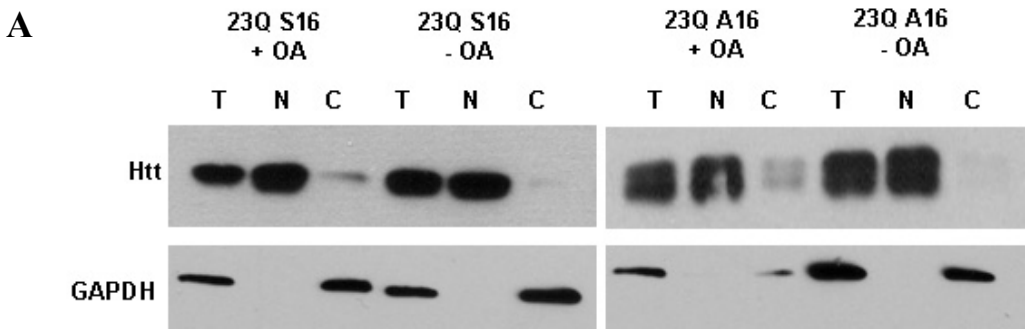
A
23Q S16
+ OA
23Q S16
- OA
23Q A16
+ OA
23Q A16
- OA
T N C T N C T N C T N C
Htt
GAPDH

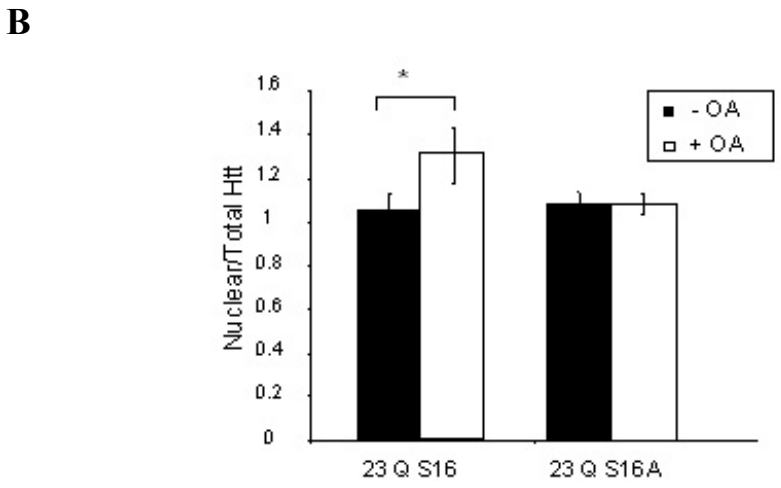
B
*
- OA
+ OA
Nuclear/Total Htt
1.6
1.4
1.2
1
0.8
0.6
0.4
0.2
0
23 Q S16
23 Q S16A

Figure 3-9. Subcellular distribution of N-terminal 23Q-S16 htt mutants in okadaic acid treated HEK 293 cells. (A) HEK 293 cells were transfected with 23Q-S16 or 23Q-S16A htt for 48 hours then treated with either 100 nM okadaic acid (OA) or DMSO for 4 hours in serum free media. Subcellular fractionation was used to separate the nuclear and cytoplasmic fractions. The distribution of htt among the fractions was analyzed by western blotting using the mEM48 antibody against htt. The purity of the fractions was analyzed by probing for GAPDH as the cytoplasmic marker. **(B)** Densitometry was used to measure the intensity of the N-terminal htt band. To determine the nuclear enrichment of each of the constructs (+ OA and –OA), the ratio of nuclear: total htt was calculated. OA treatment significantly increased the nuclear localization of the 23Q-S16 but not the 23Q-S16A N-terminal htt. * $p < 0.05$.

Figure 3-10

A

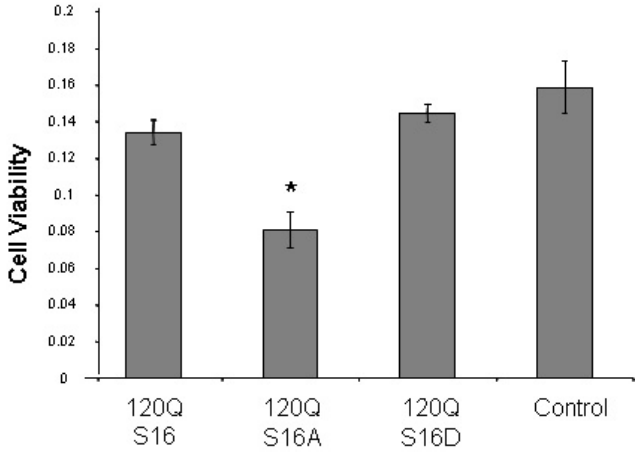

B

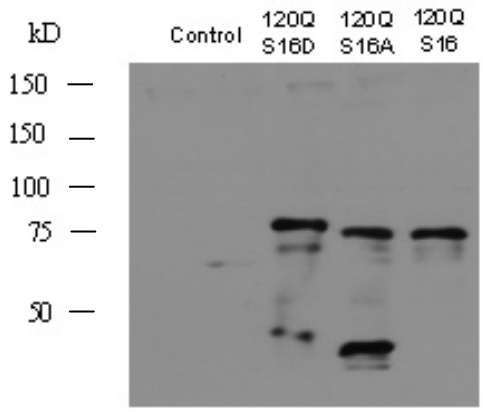

Figure 3-10. Cell viability of HEK 293 cells expressing 120Q-S16 htt mutants. (A) HEK 293 cells were transfected with 120Q-S16, -S16A or -S16D for 48 hours. The control was cells transfected with the pRK vector alone. The cells were scraped for an MTS assay to determine differences in cell viability caused by expression of the different S16 N-terminal htt mutants. Expression of 120Q-S16A caused significantly more cell death than either the 120Q-S16 or -S16D htt constructs. * $p < 0.005$. (N=3) **(B)** Similar expression levels of each of the S16 htt mutants were verified by western blotting with the mEM48 antibody against htt.

Figure 3-11

A

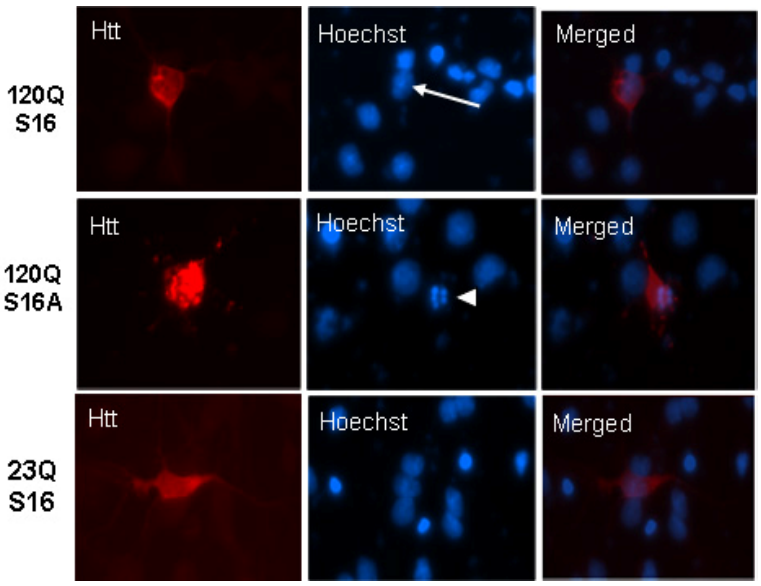

B

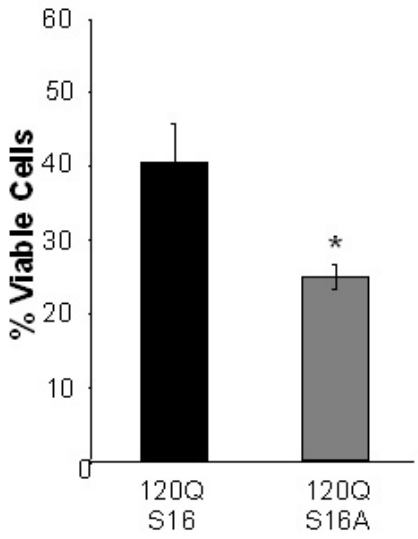

Figure 3-11. DNA fragmentation of HEK 293 cells transfected with S16-htt mutants. (A) HEK 293 cells were transfected with 120Q-S16, 120Q-S16A or 23Q-S16 htt for 48 hours. Cells were fixed and stained with mEM48 to label htt and Hoechst to label the DNA. The cells transfected with 120Q-S16 and 23Q-S16 htt showed more intact nuclei than the cells expressing 120Q-S16A htt. The arrows mark intact nuclei and the arrowhead marks fragmented nuclei. **(B)** For each well of HEK 293 cells transfected with either 120Q-S16 or 120Q-S16A, the number of cells containing fragmented nuclei and cells containing intact nuclei were counted. Cells containing fragmented nuclei were considered dead while those containing intact nuclei were considered viable (N=200). The percentage of viable cells was calculated and graphed. 120Q-S16A N-terminal htt was significantly more toxic than 120Q-S16 htt. * $p < 0.05$.

Figure 3-12

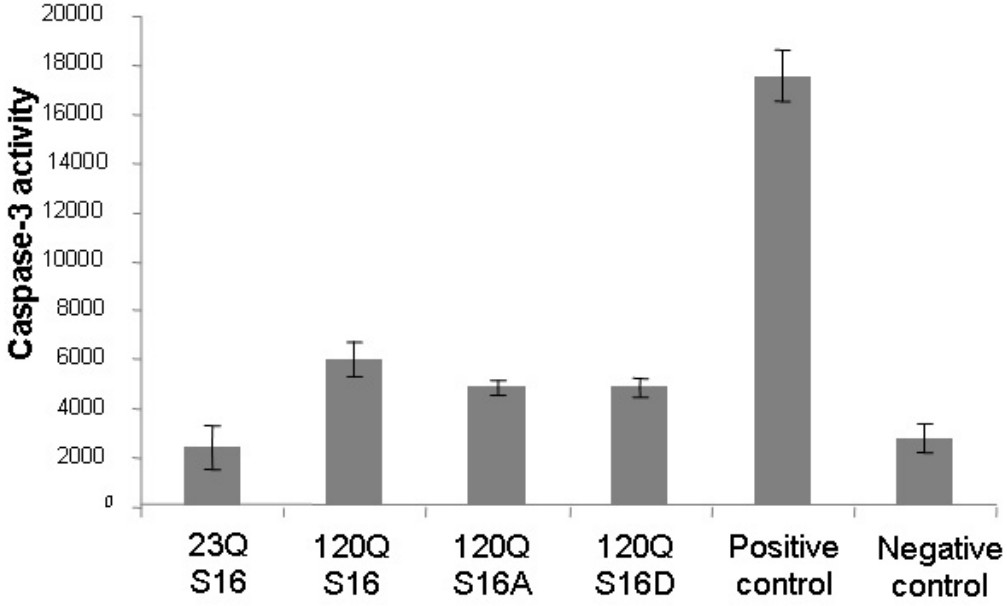
Caspase-3 activity
20000
18000
16000
14000
12000
10000
8000
6000
4000
2000
0
23Q S16
120Q S16
120Q S16A
120Q S16D
Positive control
Negative control

Figure 3-12. Caspase-3 activity in HEK 293 cells transfected with the S16 N-terminal htt constructs. HEK 293 cells were transfected with 120Q-S16, -S16A, -S16D or 23Q-S16 htt for 48 hours. Untransfected cells treated with 0.5 μM staurosporine to induce cell death served as the positive control. Untransfected cells alone served as the negative control. The caspase-3 activity was determined in each of the samples as a measure of cell death. There were no significant differences in cell viability between cells transfected with 120Q-S16, -S16A or -S16D htt.

CHAPTER 4

Mutant huntingtin phosphorylated at serine 16 is enriched in the nuclei of the striatum

This chapter presents work published as: Lauren S Havel, Chuan-En Wang, Brandy Wade, Brenda Huang, Shihua Li and Xiao-Jiang Li (2011) *Hum Mol Genet,* Apr 1;20(7):1424-37. Lauren Havel performed all of the experiments in this chapter with the exception of the immunocytochemical staining of the HD 140Q KI mice, which was done by Chuan-En Wang (figures 4-7 and 4-8). Brenda Huang also assisted me in optimizing conditions for GST pulldown between of phosphorylated huntingtin and Tpr (Figure 4-11) Xiao-Jiang Li and Shihua Li helped with experimental design. Xiao-Jiang Li played a key role in the preparation of the manuscript.

4.1 Abstract

Huntington's disease (HD) initially causes selective neurodegeneration of the striatum. In HD 140Q knock-in (KI) mice, the striatum also shows preferential accumulation of N-terminal mutant huntingtin (htt). While various hypotheses have been proposed, this preferential accumulation is not entirely understood. We have previously shown that phosphorylation of htt at serine 16 increases the nuclear accumulation of N-terminal mutant htt in cultured cells and neurons. In this *in vivo* study we show that mutant N-terminal htt phosphorylated at serine 16 is enriched in the striatum of HD KI 140Q mice. We also show that phosphorylation of htt inhibits the interaction between htt and the nuclear pore protein, Tpr, which is involved in nuclear export, thus trapping phosphorylated htt in the nucleus. While previous work in the HD research field has addressed the nuclear accumulation of htt, preferential accumulation in the striatum has not been resolved. This work provides important insight into the mechanism by which htt becomes preferentially trapped in the striatal nuclei.

4.2 Introduction

The mechanisms underlying selective neurodegeneration of striatal neurons is an important phenomenon that remains to be investigated. An important observation made by many groups has been that htt, which is normally cytoplasmic, is observed in the nuclei of brain cells in HD patients (DiFiglia et al., 1997; Gutekunst et al., 1999) and HD mouse models (Li et al., 2000; Li et al., 2001; Lin et al., 2001; Schilling et al., 1999a; Wheeler et al., 2002). Additionally, the HD KI mouse model that expresses full-length mutant htt, shows preferential accumulation N-terminal mutant htt in the striatal neurons.

This suggests that the selective neurodegeneration may be correlated with the localization of mutant htt to the nucleus of striatal neurons. The selective neurodegeneration phenomenon and the aberrant localization of polyQ expanded proteins to the nucleus is not exclusive to HD but is observed in other polyQ repeat diseases such as SCA1, 3, 7, 17, DRPLA and SBMA (Orr and Zoghbi, 2007). Neither the mechanism for the preferential accumulation of N-terminal in the striatal nuclei nor the link between nuclear accumulation and selective neurodegeneration is understood. One study has recently been trying to shed light on the cause of striatal specific neurodegeneration. This study showed that the striatal specific protein, Rhes, induces sumoylation of N-terminal htt (Subramaniam et al., 2009), which is thought to induce toxicity (Steffan et al., 2004). This study, however, did not address the striatal specific nuclear localization and accumulation of N-terminal mutant htt.

Understanding the mechanism leading to the nuclear accumulation of N-terminal htt is crucial because the nuclear accumulation of mutant htt occurs prior to the onset of neurological symptoms in HD mouse brains (Zhou et al., 2003). The observation that nuclear export rather than nuclear import is altered by the presence of an expanded polyQ tract represents some mechanistic insight (Cornett et al., 2005). In this study, the polyQ expansion was shown to inhibit the interaction between N-terminal htt and the nuclear pore protein Tpr, thus leaving the mutant htt trapped in the nucleus to accumulate. Non-expanded N-terminal htt can, however efficiently bind to Tpr allowing it to freely diffuse in and out of the nucleus. Other studies analyzing proteasome function in HD mouse models have shown that rather than global impairment of the ubiquitin proteasome system (UPS), there is an age-dependent decrease in UPS activity (Tydlacka et al., 2008;

Zhou et al., 2003). Combined with the observation that UPS activity is lower in the nucleus than the cytoplasm (Zhou et al., 2003), it is clear that age and subcellular dependent UPS activity plays a key role in the nuclear accumulation of mutant htt. The question of why the striatal neurons show preferential htt accumulation is still open to investigation. If the formation and nuclear accumulation of mutant htt could be prevented early on, the disease could be prevented or at least delayed or occur with less severe symptoms.

In the following experiments, we have explored factors contributing to the striatal specific accumulation of small phosphorylated N-terminal htt fragments. We have used the HD KI 140Q mouse model to show striatal enrichment of the kinase or other factor acting on S16 of N-terminal htt as well as phosphorylated N-terminal htt. We also show that S16 phosphorylation decreases the interaction between Tpr and mutant htt and that the interaction between Tpr and htt is decreased in the striatum compared to the cortex or cerebellum. Together these findings suggest a potential mechanism for the preferential accumulation of N-terminal htt in the striatum. In addition to providing novel information to help us understand the pathogenesis of HD, this work may also aid in the development of an effective therapeutic for the treatment of HD.

4.3 Materials and Methods

Animals - All animal procedures were approved by the Institutional Animal Care and Use Committee of Emory University. Full-length mutant htt knock-in (CAG140) mice were provided by Dr. Michael Levine at UCLA (Hickey et al., 2008) and were

maintained in the animal facility at Emory University in accordance with institutional guidelines.

Cell culture, transient transfection and drug treatments –HEK 293 cells were cultured in Dulbecco's modified Eagle's medium supplemented with 10% FBS, 100 μg/mL penicillin, 100 units/mL streptomycin and 250 μg/μL fungizone amphotericin B. Cells were incubated at 37ºC in 5% CO_2. Cells were plated in a 6-well plate for western blotting or 12-well plate for immunocytochemistry. At a confluency of 70% the cells were transfected with 1-2 μg/well (6-well plate) or 0.5-1 μg/well (12-well plate) of DNA and lipofectamine (Invitrogen) for 48 hours. For phosphorylation studies, okadaic acid (OA) (Sigma) was used to treat transfected cells in serum free media for 4 hours at a final concentration of 100nM.

Antibodies and Peptides – mEM48, a mouse monoclonal, which recognizes the N-terminus (amino acids 1-256) of htt was used for western blotting and immunocytochemistry at a dilution of 1: 100. A polyclonal antibody against phospho-serine 16 of huntingtin was generated using a peptide containing amino acids 5-22 of huntingtin that is phosphorylated at serine 16 (LEKLMKAFESLKS_pFQQ) produced by AnaSpec and used for western blotting and immunocytochemistry at a dilution of 1: 10. Additional antibodies used were against γ-tubulin at 1: 20,000 (Sigma), Sp1 at 1:1000 (Millipore), GAPDH at 1: 20,000 (Ambion), 1C2 at 1: 2500 (Millipore), TBP N-12 at 1:500 (Santa Cruz) and GST at 1:1000 (produced by the laboratory of Xiao-Jiang and Shihua Li (Cornett et al., 2005)). Secondary antibodies, which were used at a

concentration of 1: 5000, were peroxidase-conjugated donkey anti-mouse or donkey anti-rabbit IgG (H+L) from Jackson ImmunoResearch (West Grove, PA). N-terminally biotin tagged S16 and A16 peptides of the first 17 amino acids of huntingtin (MATLEKLMKAFESLKSF or MATLEKLMKAFESLKAF) were generated by AnaSpec for phosphorylation analysis.

***In vitro* phosphorylation assay and dot blotting**- The striatum, cortex, and cerebellum from a wild-type male and female C3/BL6 mouse of 4-8 months of age were homogenized in Nonidet P-40 lysis buffer (50 mM Tris-HCl (pH7.4), 50 mM NaCl, 0.2% Triton X-100, 1% Nonidet P-40, 1 mM PMSF, 1:100 protease inhibitor cocktail (P8340, Sigma), 10 mM NaF, and 0.2 mM $NaVO_3$) at 2 mg/mL. The S16 and A16 peptides or N208-S16 and N208-A16 htt immunoprecipitated from transfected HEK 293 cells were incubated in 1X kinase buffer (20 mM HEPES (pH7.6), 5 mM $MgCl_2$, 55 mM KCl, and 10 μM unlabeled ATP), lysate from either the striatum, cortex, or cerebellum and 2 μCi Adenosine-5'triphosphate [γ -^{32}P] (Perkin Elmer) in a total reaction volume of 20 μL for 1 hour at 30°C. The peptides were separated from the rest of the reaction by adding 100 μL of cold 1X PBS and 20 μL high-capacity streptavidin beads (Pierce) to the reaction and incubating at 4°C while rocking for 2 h. The beads were washed with 1X PBS and the peptide was eluted with 8M guanidine at pH 1.5. For the immunoprecipitated htt, the kinase reaction was performed with htt attached to the beads. The beads were isolated from the reaction and washed with 1X PBS. Htt was eluted from the beads with 0.1 M glycine (pH 2.8). 2 μL of the eluate was spotted onto a nitrocellulose membrane and exposed to autoradiography film. Phosphorylation levels were quantified by adding 2 μL

of each reaction to 5 mL scintillation fluid (Ecolume) and counting the radioactive units with a liquid scintillation counter (Beckman LS 6500). All counts were measured in triplicate.

Immunoprecipitation - Mouse brain tissue was resuspended in Nonidet P-40 lysis buffer (50mM Tris-HCl (pH7.4), 50mM NaCl, 0.2% Triton X-100, 1% Nonidet P-40, 1mM PMSF, 1:100 protease inhibitor cocktail (P8340, Sigma), 10mM NaF and 0.2mM $NaVO_3$). The lysate was homogenized with a dounce homogenizer then cleared with 50 µL protein A beads (Sigma) for 1 hour at 4ºC. Cleared lysates were incubated overnight with mEM48 at a dilution of 1:10 at 4ºC while rocking. 25 µL of fresh protein A beads were added for 2 hours then washed 3 times with Nonidet P-40 buffer. 1% SDS was added to the beads which were then boiled and analyzed by western blotting or used for *in vitro* phosphorylation assays.

Nuclear fractionation - To isolate the nuclear and cytoplasmic fractions from mouse brain, tissue from mice of 4-8 months of age was homogenized for 20 strokes with a dounce homogenizer in homogenizing buffer at 0.1 g/mL (0.25 M sucrose, 15 mM Tris-HCl pH 7.9, 60 mM KCl, 5 mM EDTA, 1 mM EGTA, 100 µg/mL PMSF, 10 mM NaF, 0.2 mM $NaVO_3$ and 1:100 protease inhibitor cocktail (P8340, Sigma). After incubating on ice for 10 minutes, the intact nuclei were isolated by centrifuging at 2000 g for 5 minutes. The supernatant was clarified at 16,000 RPM for 5 minutes and saved as the cytoplasmic fraction. The nuclear pellet was washed twice with homogenizing buffer and then lysed in 1X PBS lysis buffer. The fractions were analyzed by western blotting.

Mouse brain lysate preparation and western blotting - Tissue from a WT or KI 140Q mouse was resuspended in RIPA buffer (50mM Tris pH 8.0, 150mM NaCl, 1mM EDTA pH 8.0, 1mM EGTA pH 8.0, 0.1% SDS, 0.5% DOC, 1% triton X-100, 10mM NaF, 0.2mM $NaVO_3$ and 1:100 protease inhibitor cocktail (P8340, Sigma)) at 0.1g/mL. Lysate was homogenized with a dounce homogenizer and clarified at 16,000g for 10 minutes. The lysate was diluted to a concentration of 4 μg/μL then added to SDS sample buffer and resolved on 4-12% tris-glycine polyacrylamide gels (Invitrogen). The proteins were transferred to nitrocellulose membrane and blocked with 5% milk in 1X PBS before incubation with primary antibody overnight in 3% BSA in 1X PBS. After washing, the membrane was incubated with HRP conjugated secondary antibody (Jackson Laboratories) at 1:5000 for 1 hour and exposed to ECL then autoradiography film (Denville Scientific). Band intensity was calculated with densitometry software (U-SCAN).

Immunocytochemistry - Male and female mice were anesthetized and perfused intracardially with phosphate-buffered saline (PBS, pH 7.2) for 30 seconds followed by 4% paraformaldehyde in 0.1 M phosphate buffer (PB) at pH 7.2. Brains were removed, cryoprotected in 30% sucrose at 4°C, and sectioned at 40 μm using a freezing microtome. Free-floating sections were in 4% paraformaldehyde in 0.1 M phosphate buffer for 10 minutes and preblocked in 4% normal goat serum in PBS, 0.1% Triton X, and then incubated with the anti-S16 or mEM48 antibody at 4°C for 48 h. The immunoreactive

product was visualized with the Avidin–Biotin Complex kit (Vector ABC Elite, Burlingame, CA, USA).

GST pulldown – Mouse brain tissue or transfected HEK 293 cells were lysed in Nonidet P-40 lysis buffer (50 mM Tris-HCl (pH7.4), 50 mM NaCl, 0.2% Triton X-100, 1% Nonidet P-40, 1 mM PMSF, 1:100 protease inhibitor cocktail (P8340, Sigma), 10 mM NaF and 0.2 mM $NaVO_3$). Mouse brain tissue was homogenized with 50 strokes of a dounce homogenizer. 50 µL of GSH beads (Sigma) were added to each reaction. The reactions were incubated at 4°C for 3 hours rocking. The beads were isolated by centrifugation at 1000 RPM for 30 seconds. The beads were washed 3 times with NP-40 buffer and resuspended in 1X SDS protein loading dye. The samples were analyzed by western blotting.

Statistical analysis - Results generated from three or more independent experiments and expressed as the mean ±SD and were analyzed for statistical significance using a two-tailed Student's t-test.

4.4 Results

Enrichment of phosphorylation activity in the striatal nuclei of WT mice

Based on the data presented in chapter 3, we know that the phosphorylation of serine 16 (S16) of htt is important for the nuclear accumulation of N-terminal mutant htt in the nucleus of cultured HEK 293 cells and cultured primary striatal neurons. The next

step was to verify the phosphorylation *in vivo* and also to look at phosphorylation levels in various brain regions. In order to do this we needed a reliable assay to measure phosphorylation levels. To this end, we generated two peptides with an N-terminal biotin tag. The sequence of the peptides was the first 17 amino acids of htt with either a serine or an alanine at the amino acid 16 position (**Figure 4-1A**). Then we designed a radioactive *in vitro* phosphorylation assay for which the substrate was either the S16 or A16 peptide and the kinase source was fresh brain lysate generated from a wild-type (WT) mouse. They were incubated for an hour at 30°C. The modified peptide was then purified from the reaction mixture using streptavidin beads followed by several washes (**Figure 4-2B**). Phosphorylation levels were analyzed qualitatively by dot blotting and quantitatively by liquid scintillation counting, which measures the amount of ^{32}P incorporated into the peptide in counts per minute (CPM). To verify the accuracy of the assay we performed a simple phosphorylation assay using total lysate from the brain of WT mouse as the kinase source and the S16 or A16 peptides and found by liquid scintillation counting robust phosphorylation of the S16 while only very minimal or background level of phosphorylation of the A16 peptide (**Figure 4-1C**).

Once the assay conditions were optimized for the S16 and A16 peptides, we wanted to see if the various brain regions had different levels of S16 phosphorylation. We prepared lysates from the striatum, cortex and cerebellum of a WT mouse as the kinase source. After a protein assay and adjustment of protein concentration to have the equal protein concentrations for each sample, western blotting with a γ-tubulin showed the striatum and cortex have about the same amount of protein, though the cerebellum is slightly less concentrated (**Figure 4-2A**). A dot blot of the *in vitro* phosphorylation assay

performed with these lysates showed that the striatum is enriched for S16 phosphorylation activity compared to the cortex and cerebellum (**Figure 4-2B**). Since the protein concentrations were equal for the striatum and cortex, there is, at least compared to the cortex, striatal enrichment of a kinase or factor that can increase S16 peptide phosphorylation. We verified the dot blot results by liquid scintillation counting and again found that the striatum shows significantly more S16 phosphorylation than the cortex or cerebellum (**Figure 4-2C**). To control for differences in raw CPM numbers due to varying ^{32}P-ATP activity, we normalized the raw CPM values for each sample to the CPM value for the control without peptide. Notably, while there were large differences in phosphorylation of the S16 peptide, the A16 peptide showed very low phosphorylation levels for all of the samples, thus verifying the specificity of the assay of S16 phosphorylation levels.

Secondary and tertiary protein structures can drastically affect post-translational modifications such as phosphorylation by either hiding or exposing a residue subject to modification. Therefore we wanted to look at phosphorylation of S16 in the context of N-terminal htt fragments. We immunoprecipitated transfected 23Q-N208-S16 or -S16A htt from HEK 293 cells, which was used as the substrate for the *in vitro* phosphorylation assay. Western blotting with the mEM48 antibody against N-terminal htt verified the immunoprecipitation of htt and showed that more S16A-htt was isolated than S16-htt (**Figure 4-3A**). Similar to the data from the peptide phosphorylation assay, the dot blot using the immunoprecipitated transfected htt showed that the striatum is also able to phosphorylate N-terminal htt to a greater extent than the cortex and cerebellum (**Figure 4-3B**). Liquid scintillation counting verified the results seen in the dot blot and also

demonstrated that S16 htt was significantly more phosphorylated by the striatal lysates whereas S16A htt showed no difference among the brain regions (**Figure 4-3C**). By normalizing the raw CPM values for each sample to the CPM value for the untransfected lysate control, we confirmed that the striatum can phosphorylate more S16-htt.

In order to narrow down the kinase or other factor that may be responsible for S16 phosphorylation and also to determine where the phosphorylation event occurs, we also used lysates obtained from the cytoplasmic and nuclear fractions of the striatum and cortex of a WT mouse. We verified the purity of these fractions by western blotting using antibodies against GAPDH as the cytoplasmic marker and Sp1 as the nuclear marker (**Figure 4-4A**). A dot blot of the kinase reaction using each fraction from the cortex or cerebellum and the S16 or A16 peptides showed that S16 phosphorylation was increased by nuclear lysates from the striatum (**Figure 4-4B**). Importantly, the greatest difference in S16 phosphorylation between the striatum and cortex was in the total fraction, as we saw in the previous kinase assays. The difference in S16 phosphorylation between the striatal and cortical nuclei, while significant, was less than that of the total fraction. This is most likely due to loss of kinase activity during the process of subcellular fractionation since kinases are highly sensitive to environmental changes. Liquid scintillation counting of the same samples showed the same trend that S16 phosphorylation is greatest in the striatal nuclear and total fractions (**Figure 4-4C**). This data suggest that a kinase or other factor influencing S16 phosphorylation is also localized to the nucleus of the striatal neurons.

Another group working on N-terminal htt phosphorylation found that ikB kinase (IKK) directly phosphorylates S13 (Thompson et al., 2009). To see if IKK can also

phosphorylate S16, we used recombinant IKKα or IKKβ and the S16 or A16 peptides for an *in vitro* phosphorylation assay. A dot blot of the phosphorylation reaction samples showed that neither IKKα nor IKKβ significantly increased S16 phosphorylation (**Figure 4-5A**). This was also verified by liquid scintillation counting (**Figure 4-5B**). Based on this data, we find no evidence for direct phosphorylation of S16 by IKKα or IKKβ. This finding, of course, does not exclude the possibility that S16 is indirectly phosphorylated by IKK as suggested by Thompson et al (2009).

Mutant huntingtin is phosphorylated at S16 *in vivo*

So far we have shown that compared to the cortex and cerebellum, the striatal nuclei show altered activity a kinase or factor, which leads to an increase of S16 phosphorylation of N-terminal htt. We wanted to show that striatal mutant htt is in fact phosphorylated *in vivo*. To do this we needed to generate a phosphospecific antibody against phosphorylated S16 of htt. We conjugated a peptide containing amino acids 5-22 of htt and phosphorylated S16 (LEKLMKAFESLKS$_p$FQQ) to Affigel to purify the phosphospecific antibody from serum obtained from a rabbit injected with the phosphorylated peptide (**Figure 4-6A**). Specificity of the antibody to phosphorylated S16 was verified by western blotting using lysates of HEK 293 cells transfected with either 23Q-S16 or -S16A N-terminal htt. Expression of htt was verified by probing the same blot with the mEM48 antibody against N-terminal htt (**Figure 4-6B**).

First we stained sections of the striatum, cortex and cerebellum of 6- and 24-month-old HD KI I40Q mice as well as a WT control with the phospho-S16 antibody (anti-S16). There was an age-dependent increase in anti-S16 staining that was more

specific to the striatum of the HD KI mice when compared to the cortical and cerebellar regions of the same mice (**Figure 4-7A**). An interesting observation is that when striatal and cortical sections were also stained with mEM48, anti-S16 only labeled very small aggregates or diffuse htt whereas mEM48 also labeled large aggregates (**Figure 4-7B**). We also performed fluorescent co-staining of striatal sections of the same mice with the mEM48 and anti-S16 (**Figure 4-8**). Importantly, we noted that while mEM48 labeled large nuclear aggregates, the phosphor-S16 antibody labeled smaller aggregates mainly localized to the perinucleus (marked by arrows). Interestingly, this finding suggests that phosphorylated htt accumulates or potentially becomes trapped around the nuclear membrane.

We also examined lysates prepared from the HD KI 140Q mice by performing subcellular fractionation and western blotting with 1C2, another antibody that recognizes the expanded polyQ tract of htt (**Figure 4-9**). The purity of the fractionation was verified by probing with antibodies to GAPDH, a cytoplasmic marker, and TBP, a nuclear marker. The localization of full-length htt (marked by the arrow) also allows us to assess the fractionation purity because full-length htt is mainly localized to the cytoplasmic fraction. We noted that N-terminal fragments shorter than about 75 kDa (marked by the bracket) are enriched in the nucleus. This is especially clear in the striatal fractionation because of its purity compared to the cortical fraction.

To show that the striatum of the HD KI 140Q mice is enriched for phosphorylated htt, we had to immunoprecipitate mutant htt and its N-terminal fragments using the 1C2 antibody. We initially tried analyzing the total lysate by western blotting but were unable to detect phosphorylated htt. This is likely due to a low level of or the instability of S16

phosphorylation. Even in the presence of phosphatase inhibitors there is also some loss of protein phosphorylation during the lysis and sample preparation procedures. After immunoprecipitation of htt from the cortex and striatum of KI and WT mice, the samples were analyzed by western blotting with the 1C2 antibody to verify the immnoprecipitation and phosphorylated htt (**Figure 4-10A**). As we expected based on the immunocytochemistry data, we noted striatal enrichment of phosphorylated fragments < 75 kDa as marked by the bracket. We also noted increased levels of phosphorylated full-length htt in the striatum compared to the cortex (**Figure 4-10B**). We used densitometry to measure the intensity of the full-length htt band (marked by the arrow) on both the 1C2 and anti-S16 blots. We determined the percentage of phosphorylated htt in the striatum and cortex of the KI mice by calculating the ratio of the phosphorylated htt detected in the sample to the total amount of htt immunoprecipitated and multiplying by 100. This is further evidence that the striatum of KI mice are enriched for phosphorylated mutant htt, which is consistent with our *in vitro* data.

Phosphorylation of mutant htt inhibits its interaction with the nuclear pore proteins

After showing preferential accumulation of mutant N-terminal htt phosphorylated at S16 in the striatum of HD KI 140Q mice we wanted to determine the mechanism by which this occurs. Previous data by Cornett et al showed that polyQ-expanded htt has a decreased affinity for Tpr compared to non-expanded htt, indicating that nuclear export rather than nuclear import is impaired. Based on the fact that the interaction between Tpr and htt occurs via the N-terminus of htt, we hypothesized that the phosphorylation state of S16 may influence this interaction and thus nuclear export. To this end, we analyzed

the binding of transfected S16- and S16A- htt to transfected GST tagged Tpr by a GST pulldown followed by western blotting with the mEM48 and anti-S16 antibodies (**Figure 4-11**). Equal GST-Tpr expression was also verified by probing the same blots with a GST antibody. The results clearly show that more S16A- than S16-htt binds to GST-Tpr, indicating that phosphorylation at S16 inhibits the interaction between Tpr and htt. This is consistent with the idea that htt phosphorylated at S16 can accumulate in the nucleus more readily than unphosphorylated S16-htt or S16A-htt.

Next we wanted to show that the above phenomenon also occurs *in vivo*. Due to the poor affinity of anti-S16 to mouse htt, we could not assess the *in vivo* association between Tpr and phosphorylated htt. We could, however, assess the interaction between Tpr and htt and how it varies between brain regions. A GST pulldown of mutant htt from a HD KI 140Q mouse with recombinant GST-Tpr showed that the interaction is weakest in the striatum compared to both the cortex and cerebellum (**Figure 4-12**). This difference in binding is potentially due to phosphorylation differences as the *in vitro* data convincingly shows that Tpr binding is dependent on S16 dephosphorylation. Nonetheless, the *in vivo* binding provides the novel and important finding that the interaction of Tpr and htt is decreased in the striatum, explaining why mutant htt preferential accumulates in striatal neurons.

Finally, we wanted to link the preferential association of Tpr with unphosphorylated htt to our finding that N-terminal fragment length influences the nuclear accumulation of htt, which is discussed in chapter two. Therefore, we co-transfected HEK 293 cells with 120Q- N500 or -N67 (exon 1) htt and GST-Tpr, treated them with either okadaic acid (OA) or DMSO as a control. A GST pulldown followed by

western blotting with the mEM48 antibody showed that although more N500-htt than exon-1 htt bound to transfected GST-Tpr, more small fragments produced from N500-htt than exon 1-htt interacted with GST-Tpr. This is consistent with the idea that smaller N-terminal htt fragments show more nuclear accumulation than longer fragments (**Figure 4-13**). The high propensity for nuclear exon 1-htt to aggregate probably inhibits our ability to detect its interaction with Tpr. Additionally, OA treatment decreased the association between both exon 1 and N500 htt and Tpr. Importantly, very little full-length htt (marked by the arrow) was precipitated by GST-Tpr. Altogether we show that small mutant N-terminal htt fragments bind to the nuclear export protein, Tpr, specifically in the striatum and in a length and dephosphorylation dependent manner, suggesting a mechanism by which phosphorylated mutant htt accumulates in the nucleus.

4.5 Discussion

These *in vitro* and *in vivo* experiments show that the striatum is enriched for mutant htt phosphorylated at S16. We also provide a novel mechanism for the preferential accumulation of mutant htt in the striatum whereby phosphorylation of mutant N-terminal htt inhibits the interaction between htt and the nuclear pore proteins. Presumably, phosphorylation of htt at S16 traps the N-terminal htt fragments in the nucleus in a length dependent manner. Based on the increase in phosphorylation seen in the striatum we can conclude that S16 phosphorylation of mutant htt contributes to the progressive nuclear accumulation in the striatum.

While we were not able to identify the kinase that directly phosphorylates S16, it is possible that the kinase activity is higher in the nucleus of striatal neurons. There was

some activity in the cytoplasm, which indicates that either that there was slight contamination of the cystolic proteins by the putative nuclear kinase as a result of the fractionation procedure or that there is a low level of cytoplasmic phosphorylation of N-terminal htt. If the latter is true, the role of phosphorylated htt in the cytoplasm remains to be investigated. Nonetheless, the striatal nucleus may be enriched for a kinase that phosphorylates S16 or other factors that promote S16 phosphorylation. Our data cannot exclude the possibility that a phosphatase has a lower expression level or is specifically inactivated in the striatum thereby increasing the S16 phosphorylation levels. Although such factors remain to be identified, the increased S16 phosphorylation observed in the striatal nuclei is consistent with the preferential nuclear accumulation on N-terminal mutant htt in striatum.

Regardless of whether altered activity of a phosphatase or kinase is responsible for the striatal specific S16 phosphorylation, there are several possible pathophysiological triggers that could lead to aberrant phosphorylation once nuclear translocation of mutant htt occurs. First, transcriptional dysregulation, reported by many groups to be a result of aberrant interactions between soluble mutant htt in the nucleus and various transcription factors, could alter the expression levels of a kinase or phosphatase that is important for modifying S16 of htt. It could also affect the expression of an upstream protein that regulates the activity of the putative kinase or phosphatase. A second possibility is that age-dependent cellular stressors, which can affect protein clearance mechanisms such as chaperone or UPS activity, alter kinase or phosphatase activity or expression. A third possibility is that htt misfolding leads to an aberrant interaction between mutant N-

terminal mutant htt and the kinase, phosphatase or regulatory protein thus altering their function.

Our proposed mechanism is consistent with immunocytochemistry data generated from various HD KI mouse models showing preferential accumulation of mutant in the striatum (Li et al., 2000; Lin et al., 2001; Wheeler et al., 2002). Interestingly, unpublished immunocytochemistry data from an HD KI 143Q N208 mouse model generated by our lab, which expresses the 208 amino acid fragment with 140 CAG repeats under the endogenous mouse htt promoter, also shows preferential accumulation of mutant htt in the striatum. This is significant to our work because it shows that without the context of the full-length protein, N-terminal mutant htt is sufficient for its preferential striatal nuclear accumulation and late-onset neurological symptoms. Other mouse models expressing smaller N-terminal htt, such as the R6/2 or N171-82Q models, are transgenic and overexpress htt at levels much higher than endogenous htt (Mangiarini et al., 1996). This overexpression causes nuclear accumulation of mutant htt in all brain regions, suggesting that overexpressed small N-terminal mutant htt fragments may not be able to show the preferential nuclear accumulation in the striatum. Based on the data generated from our *in vitro* work and the HD KI 140Q mouse model that expresses full-length htt at the endogenous level, we hypothesize that a large N-terminal htt fragment such as N208-htt with an expanded polyQ tract can preferentially accumulate in the nucleus of striatal neurons and that this nuclear localization can contribute to the selective HD neuropathology. It would be interesting in the future to use this mouse model to further study N-terminal phosphorylation since it expresses the same size fragment used for our *in vitro* studies at endogenous levels.

Figure 4-1

A

S16 Peptide: Biotin – LC – MATLEKLMKAFESLKSF - OH

S16A Peptide: Biotin – LC – MATLEKLMKAFESLKAF - OH

B

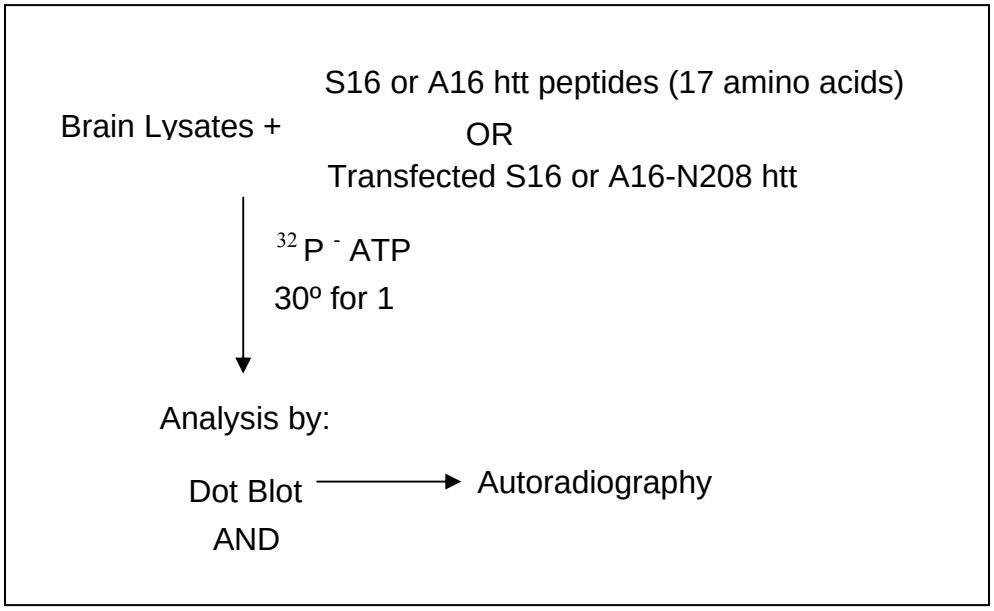

C

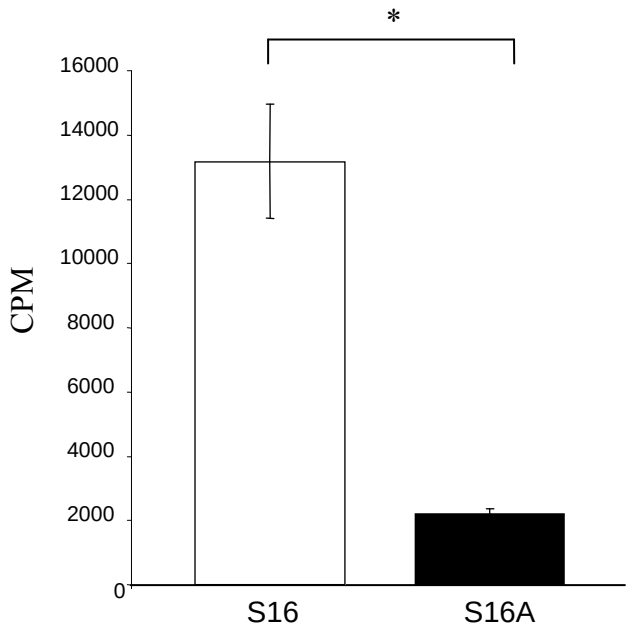

Figure 4-1. Phosphorylation assay for measuring htt S16 phosphorylation levels. **(A)** Two peptides consisting of the first 17 amino acids of htt were generated; one contained a serine at residue 16 and the other contained an alanine at the same residue. Both have an N-terminal biotin tag to allow for purification from the phosphorylation reaction mixture. **(B)** A flow chart describing the *in vitro* radioactive phosphorylation assay that was used to measure htt S16 phosphorylation levels in the peptide and transfected N-terminal htt. In the assay, the brain lysate was the kinase source and the peptide or transfected htt was the substrate. **(C)** The assay was performed as described above using the S16 and A16 peptides. The S16 peptide showed high levels of phosphorylation while the A16 peptide showed relatively little phosphorylation. * $p < 0.05$ (N=3).

Figure 4-2

A

B

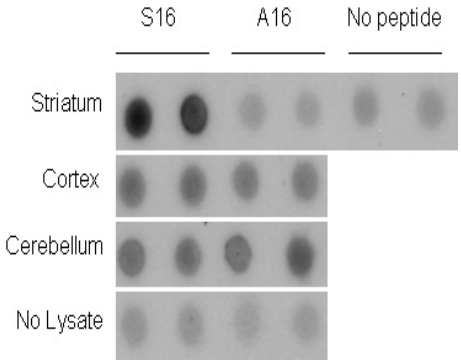

C

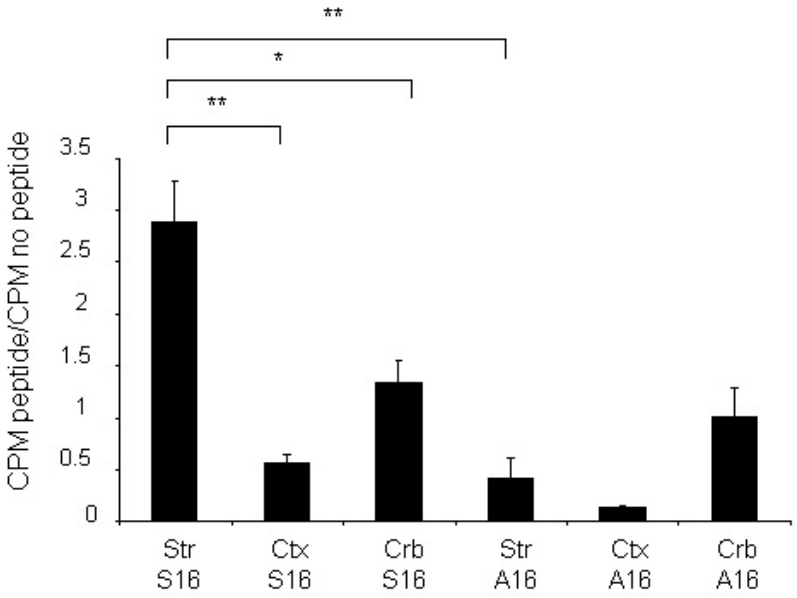

Figure 4-2. Phosphorylation levels of the peptides by various brain regions. (A) A WT mouse brain was dissected to isolate the striatum, cortex and cerebellum. Lysates from each region were carefully prepared in order to maintain kinase activity for use in the assay as the kinase source. A western blot probed with γ-tubulin was used to show the protein levels in each fraction. **(B)** The lysates from each brain region were incubated with the S16 or A16 peptides and ^{32}P-ATP. A small amount of each sample was dotted onto a nitrocellulose membrane and exposed to autoradiography film to visualize differences in S16 phosphorylation. The striatum showed a higher level of S16 phosphorylation compared to the cortex or cerebellum. **(C)** A small amount of each phosphorylation assay was also used for liquid scintillation counting in order to quantify phosphorylation levels. To normalize the raw CPM numbers, the ratio was taken of the CPM of the peptide sample: CPM of the no peptide control sample. The striatum showed a statistically significantly elevation of S16 phosphorylation compared to the cortex or cerebellum. The striatum S16 sample also showed significantly more phosphorylation than the A16 sample. * $p < 0.05$, ** $p < 0.01$ (N=3).

Figure 4-3

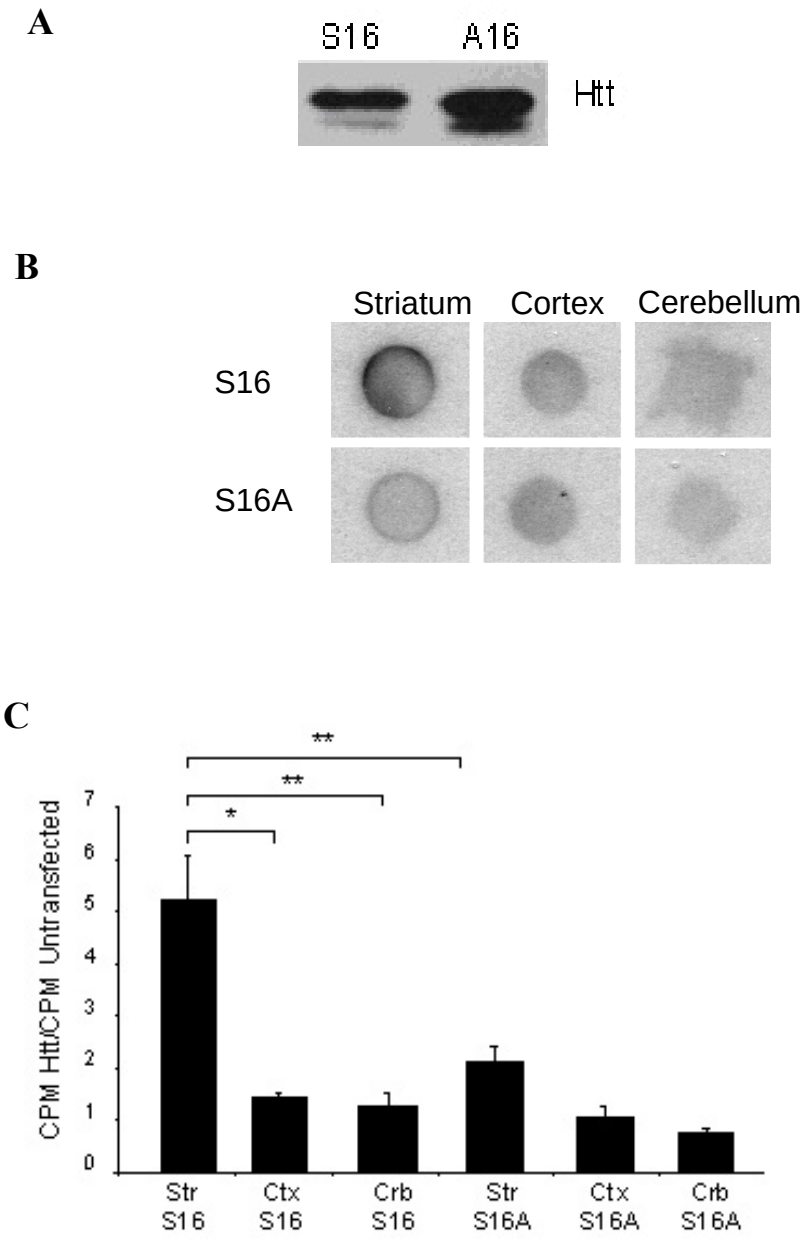
A
S16
A16
Htt
B
Striatum
Cortex
Cerebellum
S16
S16A
C
CPM Htt/CPM Untransfected
0
1
2
3
4
5
6
7
*
**
**
Str S16
Ctx S16
Crb S16
Str S16A
Ctx S16A
Crb S16A

Figure 4-3. Phosphorylation levels of transfected N-terminal htt by various brain regions. (A) HEK 293 cells were transfected with 23Q-S16 or S16A N-terminal htt for 48 hours. Immunoprecipitation with the mEM48 antibody was used to isolate the transfected N-terminal htt. The precipitated protein was analyzed by western blotting with the mEM48 antibody. **(B)** The phosphorylation assay was performed with the lysates of the different brain regions of a WT mouse as the kinase source and the immunoprecipitated htt as the substrate. A small portion of each sample was dotted on a nitrocellulose membrane to visualize the amount of phosphorylation. The striatum was able to phosphorylate S16 significantly more than the other brain regions. **(C)** A small portion of each phosphorylation assay sample was analyzed by liquid scintillation counting to quantify the S16 phosphorylation by each of the brain regional extracts. We normalized the raw CPM values for each sample to the CPM value for the untransfected control. The striatum was able to phosphorylate S16 significantly more than the other brain regions. * $p < 0.05$, ** $p < 0.01$ (N=3).

Figure 4-4

A

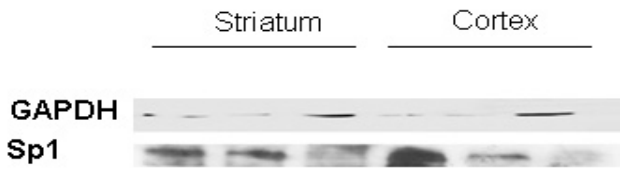

B

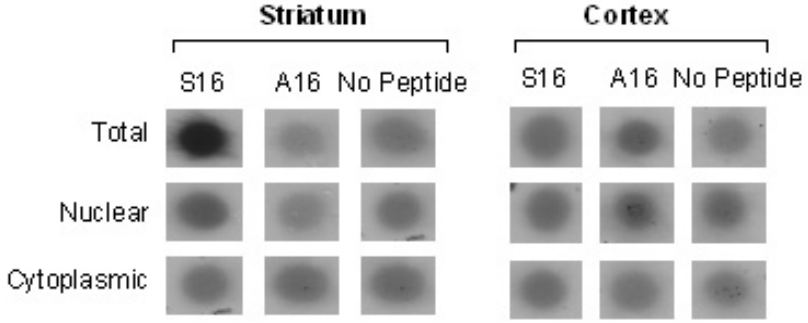

C

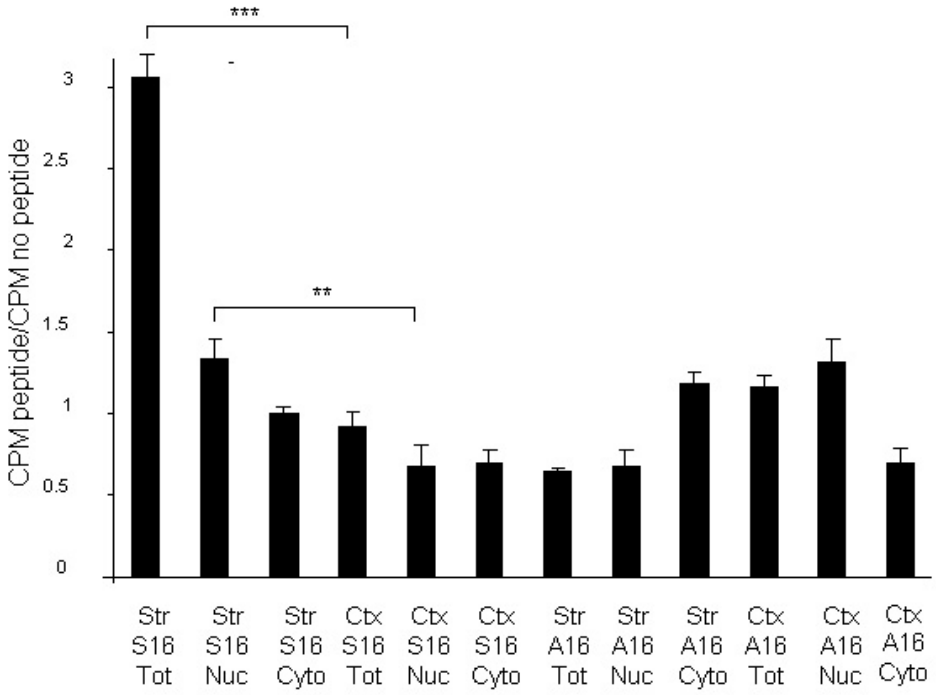

Figure 4-4. Phosphorylation levels of transfected N-terminal htt by subcellular fraction of the various brain regions. (A) A subcellular fractionation of the striatum, cortex and cerebellum of a WT mouse was used to separate the cytoplasm from the nucleus. The purity of the fractionation was verified by western blotting using GAPDH as a cytoplasmic marker and Sp1 as a nuclear marker. **(B)** The phosphorylation assay used the total, nuclear and cytoplasmic fractions from the striatum and cortex of a WT mouse as the kinase source and the N17 peptides as the substrate. A small portion of each reaction was spotted onto a nitrocellulose membrane to visualize differences in phosphorylation levels. The striatal nuclei appeared to have the greatest S16 phosphorylation activity aside from the striatal total fraction. **(C)** A portion of each reaction sample was analyzed by liquid scintillation counting to quantify the amount of phosphorylation activity in each fraction. We normalized the raw CPM values for each sample to the CPM value for the untransfected control. Aside from the striatal total fraction, the striatal nuclei had significantly higher S16 phosphorylation activity than the striatal cytoplasmic fraction or any fractions from the cortex. ** $p < 0.05$, *** $p < 0.001$ (N=3).

Figure 4-5

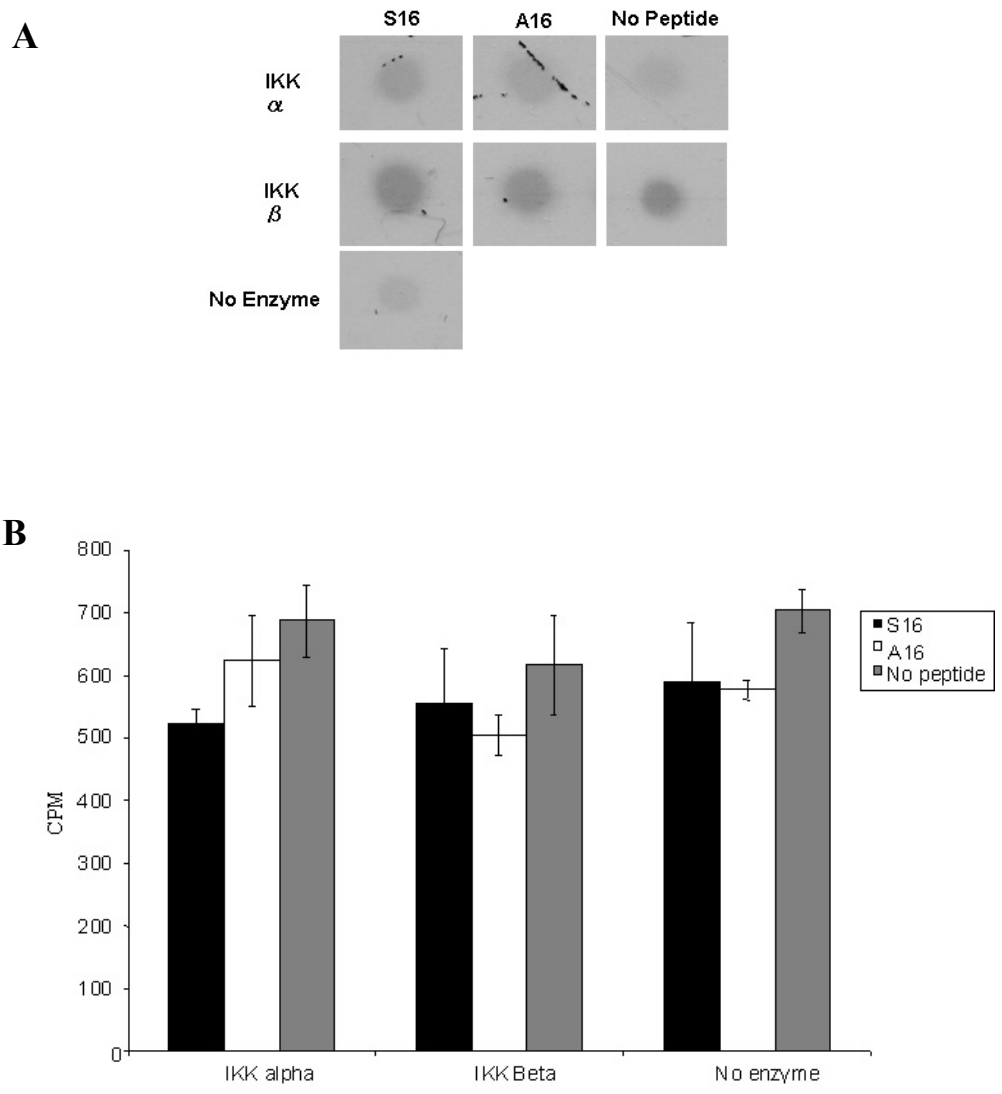
A
S16
A16
No Peptide
IKK α
IKK β
No Enzyme
B
CPM
800
700
600
500
400
300
200
100
0
IKK alpha
IKK Beta
No enzyme
S16
A16
No peptide

Figure 4-5. IKKα or IKKβ does not directly phosphorylate S16 of htt. (A) The phosphorylation assay was performed using recombinant IKKα or IKKβ as the kinase source and the N17 htt peptides as the substrate. The negative control was the same reaction but with no peptide added. A small portion of each reaction was spotted onto a nitrocellulose membrane to visualize the phosphorylation levels of the peptides. Neither IKKα nor IKKβ appeared to phosphorylate the S16 htt peptide. **(B)** A small portion of each reaction was also analyzed by liquid scintillation counting to quantify the amount of phosphorylation in each reaction. Again, neither IKKα nor IKKβ appeared to phosphorylate the S16 htt peptide (N=3).

Figure 4-6

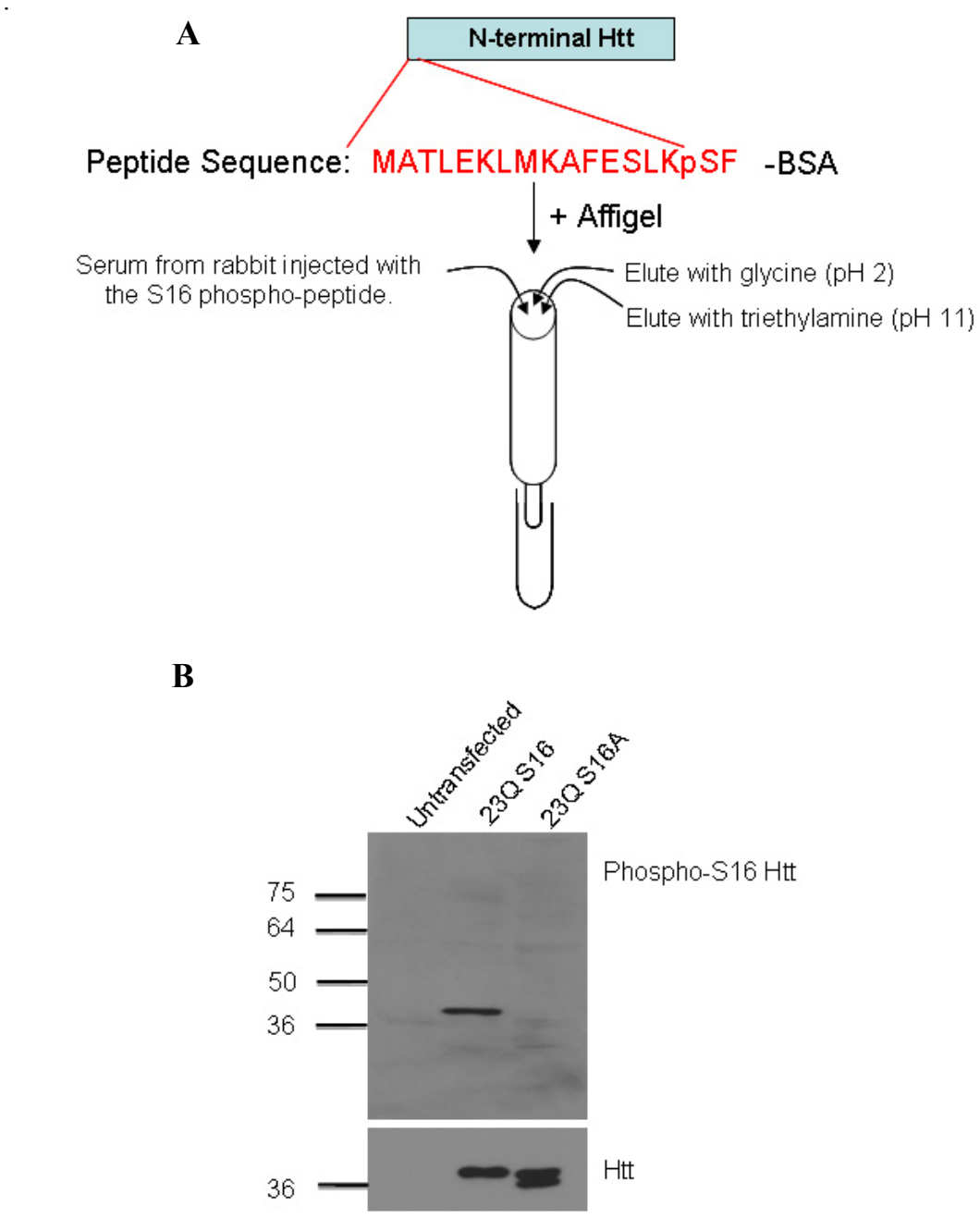
A
N-terminal Htt
Peptide Sequence: MATLEKLMKAFESLKpSF -BSA
+ Affigel
Serum from rabbit injected with the S16 phospho-peptide.
Elute with glycine (pH 2)
Elute with triethylamine (pH 11)
B
Untransfected
23Q S16
23Q S16A
75
64
50
36
Phospho-S16 Htt
36
Htt

Figure 4-6. Production of a phosphospecific antibody against S16 of htt (anti-S16). **(A)** A flow chart describing the production of a rabbit antibody that is specific to phosphorylated S16 of htt. **(B)** HEK 293 cells were transfected with either 23Q-N208-S16 or 23Q-N208-S16A htt for 48 hours. Htt expression was verified using the mEM48 antibody against htt. Specificity of the antibody against phosphorylated S16 was verified by western blotting of the cell lysates expressing 23Q-S16 or -S16A htt.

Figure 4-7

A

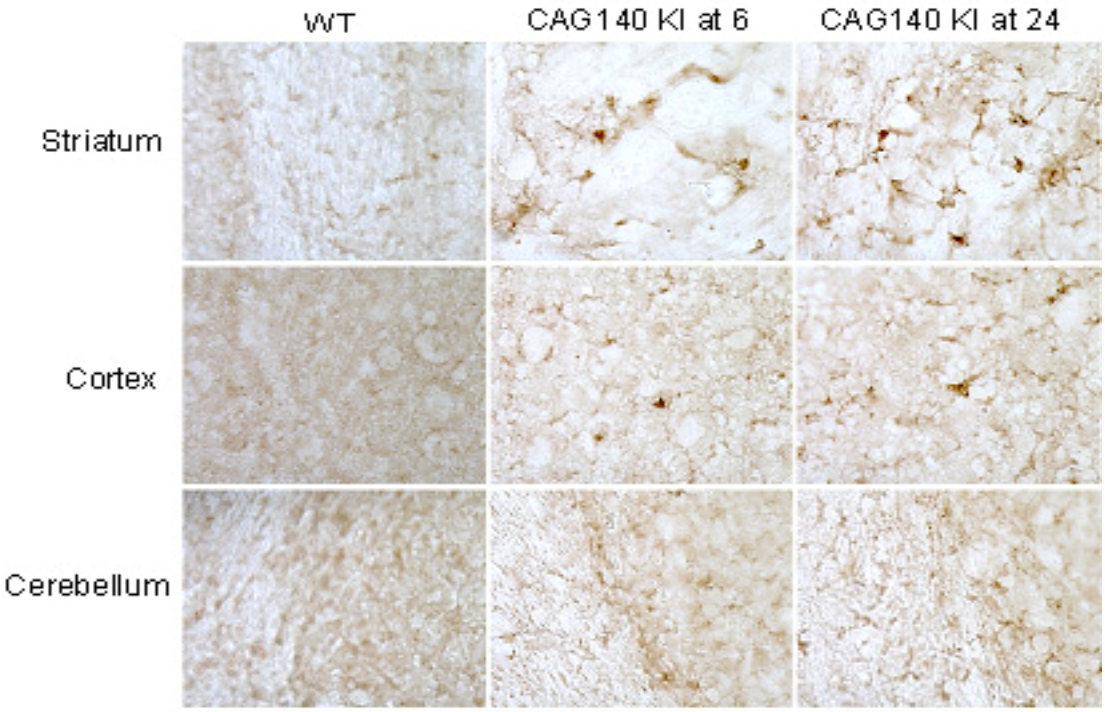
WT
CAG140 KI at 6
CAG140 KI at 24
Striatum
Cortex
Cerebellum

B

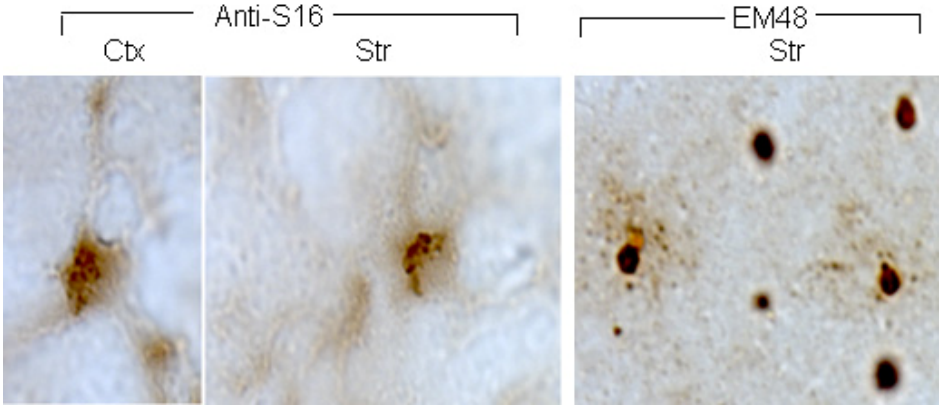
Anti-S16
Ctx
Str
EM48
Str

Figure 4-7. Staining of CAG140 KI mice of varying ages with the anti-S16 antibody. **(A)** Immunohistochemistry of the cortex, striatum and cerebellum of a WT, 6- month KI and 24-month KI mouse with the anti-S16 antibody showed increased levels of htt phosphorylated at S16 in the striatum as compared to the cortex and cerebellum. Additionally, the amount of htt phosphorylated at S16 appears to increase with the age of the mouse as the 24-month old KI mouse showed more striatal staining than the 6-month old mouse. **(B)** The anti-S16 antibody only recognized diffuse htt and small aggregated htt while mEM48 recognized large aggregates.

Figure 4-8

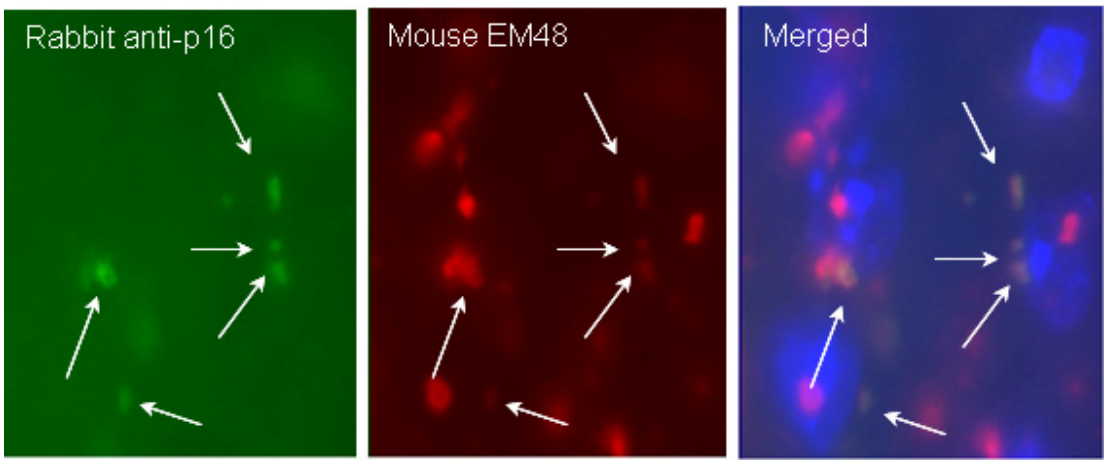

Figure 4-8. Htt phosphorylated at S16 colocalizes with EM48-positive small aggregates at the perinucleus. Double immunostaining was performed on the striatum of a CAG140 KI mouse with the anti-S16 antibody (green), the mEM48 antibody (red) and Hoechst to label the nucleus. The small aggregates (marked by the arrows), which localized to the perinucleus, were labeled with the anti-S16 antibody but the large nuclear aggregates were not.

Figure 4-9

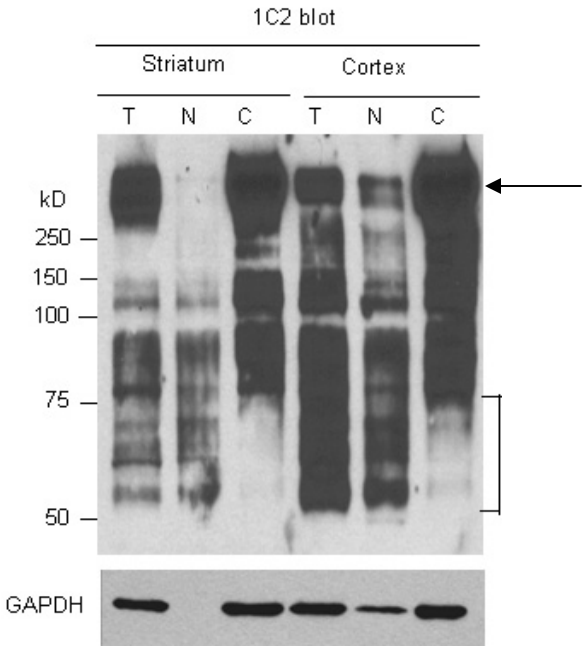

Figure 4-9. Small N-terminal fragments localize to the nuclear fraction. A subcellular fractionation was performed on a CAG140 KI mouse to separate the nucleus from the cytoplasm. The fractions were analyzed by western blotting with the 1C2 antibody against htt. The arrow marks full-length htt and the bracket marks the small N-terminal htt fragments (<75kD), which specifically localize to the nucleus of these mice. The purity of the fractionation was verified by western blotting for TBP as the nuclear marker and GAPDH as the cytoplasmic marker.

Figure 4-10

A

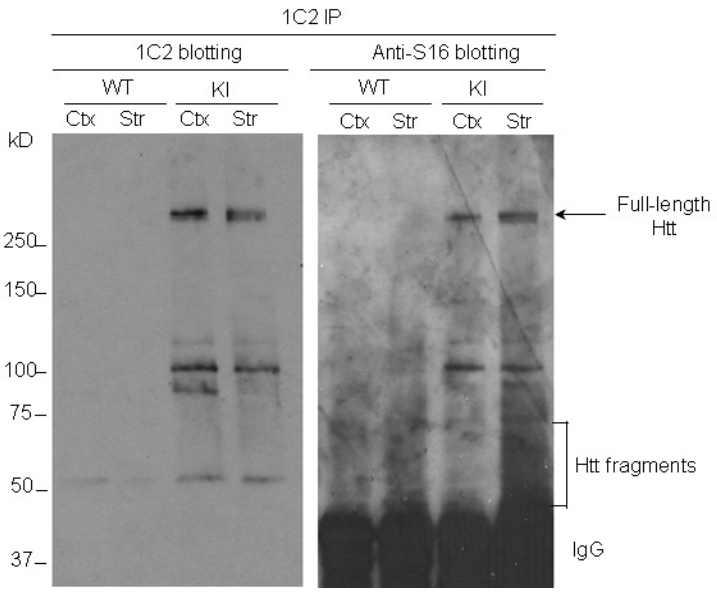

B

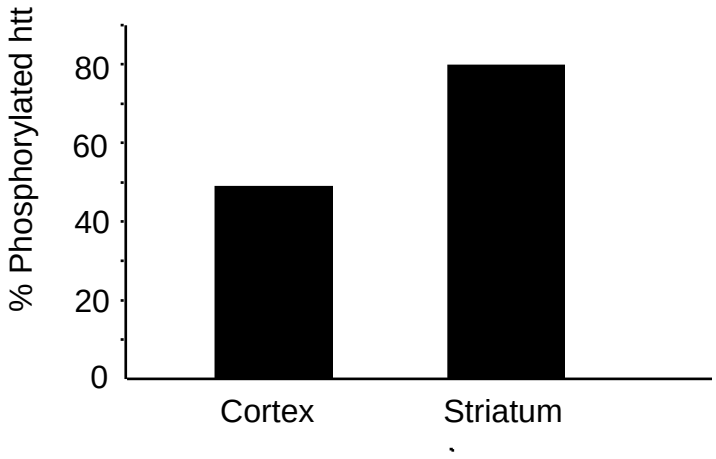

Figure 4-10. The striatum of CAG140 KI mice is enriched for htt phosphorylated at S16. (A) Lysates from the cortex and striatum of a CAG140 KI mouse were prepared and htt was immunoprecipitated from the lysates with the 1C2 antibody. The immunoprecipitates were analyzed by western blotting with the 1C2 antibody to determine total htt levels and with the phosphor-S16 antibody to determine phosphorylated htt levels. The arrow marks full-length htt while the bracket marks the small N-terminal htt fragments. Phosphorylated N-terminal htt fragments appear to be enriched in the striatum compared to the cortex. **(B)** The percentage of total full-length htt that is phosphorylated was calculated and determined to be higher in the striatum than the cortex.

Figure 4-11

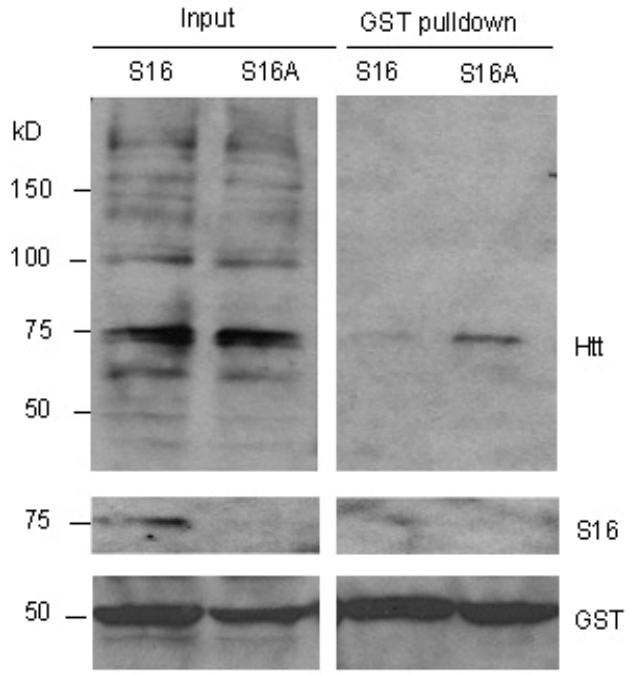
Input
GST pulldown
S16
S16A
S16
S16A
kD
150
100
75
50
Htt
75
S16
50
GST

Figure 4-11. Phosphorylation of S16 of htt inhibits the interaction between htt and Tpr. HEK 293 cells were co-transfected with Tpr-GST and 120Q-S16 or 120Q-S16A htt. A GST pulldown from the cell lysates showed that more 120Q-S16 N-terminal htt bound less Tpr than 120Q-S16A N-terminal htt, indicating that phosphorylation of S16 may inhibit its interaction with Tpr.

Figure 4-12

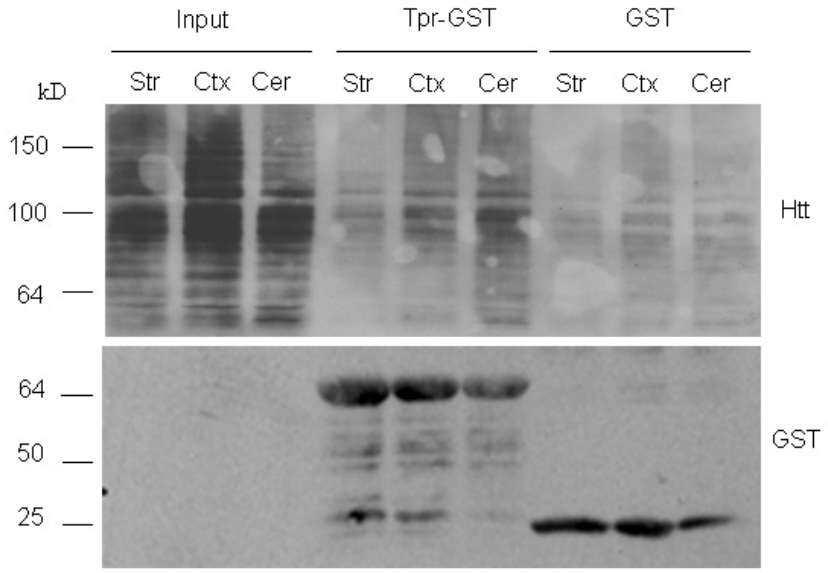
Input
Tpr-GST
GST
Str
Ctx
Cer
Str
Ctx
Cer
Str
Ctx
Cer
kD
150
100
64
Htt
64
50
25
GST

Figure 4-12. The interaction between N-terminal htt and Tpr in various brain regions of the CAG140 KI mice. Brain lysates were prepared from the striatum, cortex and cerebellum or a CAG140 KI mouse for a GST pulldown with recombinant Tpr-GST. Analysis of the samples by western blotting with the 1C2 antibody revealed that the interaction between the small N-terminal fragments (marked by the bracket) and Tpr is weakest in the striatum and strongest in the cerebellum. As a negative control, each sample was also used for a pulldown with GST only. In the lower panel, the same blot was re-probed for GST to show the amount of recombinant protein used for each sample.

Figure 4-14

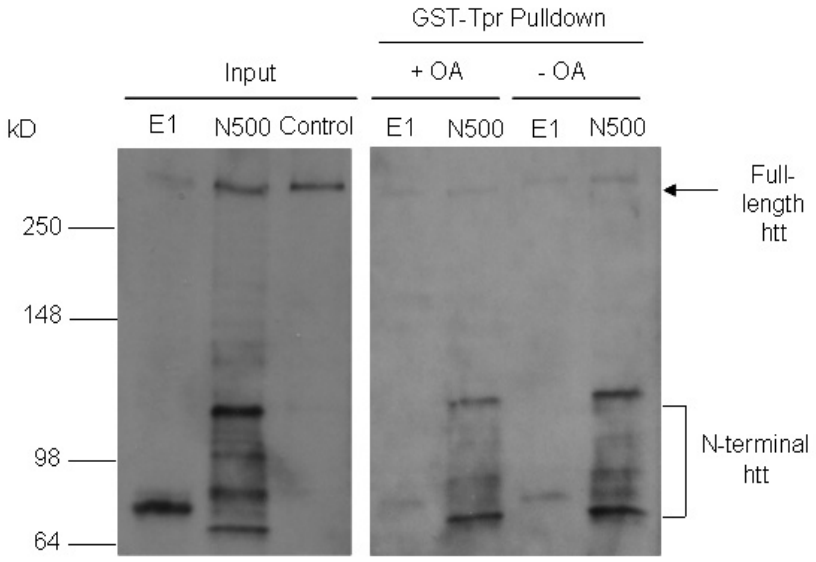
GST-Tpr Pulldown
Input
+ OA
- OA
kD
E1
N500
Control
E1
N500
E1
N500
250
148
98
64
Full-length htt
N-terminal htt

4-14. Phosphorylation of N-terminal htt decreases the interaction between htt and Tpr. HEK 293 cells were co-transfected with Tpr-GST and 120Q-exon1 or 120Q-N500 htt then treated with either 100 nM okadaic acid or DMSO for 4 hours. OA treatment decreased the interaction between all N-terminal htt fragments and Tpr. Among the OA treated samples, more 120Q-N500 htt and its degraded products (marked by the bracket) than 120Q-exon1 were precipitated by Tpr-GST. Also important to note is that very little full-length htt (marked by the arrow) was precipitated by the Tpr-GST.

CHAPTER 5

Conclusions and Future Directions

5.1 Summary

We have provided a novel mechanism for the preferential accumulation of N-terminal mutant huntingtin (htt) in the striatal nuclei (**Figure 5-1**). We show that full-length htt is cleaved into small N-terminal fragments that can enter the nucleus. Phosphorylation of S16 increased the nuclear accumulation and aggregation of htt specifically in the striatum by decreasing the interaction with the nuclear export proteins in a length dependent manner. This leaves phosphorylated htt trapped in the nucleus where it is able to accumulate and aggregate.

While it has been well established that N-terminal htt accumulates in the nucleus in postmortem human Huntington's disease (HD) brains (DiFiglia et al., 1997) and HD mouse models (Li et al., 2000; Lin et al., 2001; Wheeler et al., 2002), the mechanism and size of these pathological fragments that accumulate in the nucleus have not been determined. We analyzed the subcellular localization of polyQ expanded N-terminal htt fragments of 208, 300 or 500 amino acids (N208, N300, N500) containing a C-terminal HA tag in HEK 293 cells. Immunocytochemistry showed that N208 and N300 htt formed large nuclear aggregates while N500 htt remained cytoplasmic. This finding was confirmed by subcellular fractionation of HEK 293 cells transfected with the same constructs as well as by immunocytochemistry of transfected cultured neuronal cells. By immunocytochemistry of transfected HEK 293 cells, we found that the fragments comprising the nuclear aggregates were generated by proteolytic cleavage. We also found that cell viability was significantly decreased with the expression of 120Q N208-htt compared to N300- or N500-htt. Together these data show that N-terminal htt (208 amino acids) accumulates in the nucleus and causes cytotoxicity.

Other studies have shown that phosphorylation of N-terminal htt is important in HD pathogenesis (Gu et al., 2009; Thompson et al., 2009). These studies, however, focused on the phosphorylatable residues serine 13 and serine 16 in combination. Since serine 13 and 16 have not been studied individually, we wanted to first determine which residue (S13 or S16) was more important for the regulation of nuclear accumulation of N-terminal htt and how phosphorylation played a role. We created 23Q- and 120Q-N208 htt constructs where S16 or S13 was mutated to either alanine (S16A, S13A) to create an unphosphorylatable mutant or aspartic acid to create a phosphomimetic mutant (S16D, S13D). After determining by immunocytochemistry that S16 is more important for regulating the nuclear localization of N-terminal htt, we focused on the S16-htt constructs. S16 phosphorylation was found to be important in regulating not only nuclear localization of mutant htt but also its nuclear aggregation. This effect was confirmed by increasing cellular phosphorylation via treatment with the phosphatase inhibitor okadaic acid (OA).

In order to analyze phosphorylation of S16 in the brains of mice to confirm our HEK 293 cell data, we developed a radioactive *in vitro* phosphorylation assay using peptides of the first 17 amino acids of htt (N17) with S16 or A16 as well as immunoprecipitated N-terminal htt from transfected HEK 293 cells. Using lysates from the striatum, cortex and cerebellum of WT mice as the kinase source and either the N17 peptides or immunoprecipitated htt, we showed that the striatal nuclei display increased S16 phosphorylation. We generated an antibody that specifically recognizes phosphorylated S16 to analyze levels of htt phosphorylated at S16 in HD KI 140Q mice. Consistent with our *in vitro* phosphorylation assay data, we found that the striatum is

enriched for phosphorylated N-terminal htt as well as phosphorylated full-length htt compared to the cortex. This data is consistent with the observation that N-terminal htt preferentially accumulates in the striatal nuclei in several HD KI mouse models and the fact that the striatum is the brain region most vulnerable to neurodegeneration in HD.

To establish a mechanism for the striatal specific nuclear accumulation of phosphorylated N-terminal mutant htt, we expanded on previously published work by Cornett et al showing that polyQ expanded htt has a decreased affinity for the nuclear export protein, Tpr, compared to non-expanded htt. Using a GST pulldown approach, we showed that phosphorylated polyQ expanded N-terminal htt bound less unphosphorylated htt and that this binding is N-terminal length dependent. We also showed that the interaction between N-terminal htt and Tpr is weaker in the striatal region than the cortex and cerebellum, which is also consistent with the preferential accumulation of N-terminal phosphorylated htt in the striatum of HD KI mice.

5.2 Remaining questions and future directions

Based on my work, there are several important questions remaining that I will address in this section. The answers to these questions will more clearly define the role of the first 17 amino acids in HD pathogenesis. Clearly, the N17 region is important for the subcellular distribution of htt and understanding its role might provide several potential therapeutic targets for HD.

What is the kinase that phosphorylates S16 of N-terminal htt?

Previous work by Thompson et al showed direct phosphorylation of S13 and the potential for indirect phosphorylation of S16 by ikB kinase (IKK). Since our *in vitro* phosphorylation assay did not provide evidence for direct phosphorylation of S16 by IKKα or β, it would be interesting to identify the kinase that can directly phosphorylate S16. One common method for identifying kinases is to test a series of kinase inhibitors for the loss of phosphorylation. Several different inhibitor concentrations and treatment times will first be tested using our *in vitro* phosphorylation assay to determine the least amount of inhibitor and the shortest incubation time required for a loss of phosphorylation of the S16 peptide. Specifically, I would prepare striatal tissue lysates as the kinase source and do an *in vitro* phosphorylation assay as described in the materials and methods of chapter 4. Kinase inhibitors will be included in this *in vitro* phosphorylation assay to see which one can eliminate S16 phosphorylation. Using the identified conditions, an *in vitro* phosphorylation assay will also be performed using the identified kinase and N-terminal htt (S16-N208) immunoprecipitated from transfected HEK 293 cells to verify its effect on S16 phosphorylation. The products of the phosphorylation assay will also be analyzed with western blots, which will be probed with antibodies against htt or phosphorylated S16.

To verify the above results and to eliminate false positives obtained from the above experiment, I would order recombinant kinases for the candidate kinases and use them in an *in vitro* phosphorylation assay by incubating them directly with S16 or A16 peptides in the presence of ^{32}P -ATP. A kinase that can specifically phosphorylate the S16, but not A16, peptide is likely to be responsible for S16 phosphorylation. To further confirm this, I would co-transfect this kinase with S16-N208-htt or A16-N208-htt into

HEK 293 cells to see if the expression of this kinase can specifically enhance the phosphorylation of S16-N208-htt. Identifying the kinase responsible for S16 phosphorylation is critical for future work to elucidate the role of S16 phosphorylation in HD pathology. Furthermore, it will allow us to further explore why S16 phosphorylation is enriched in the striatum and its role in selective neurodegeneration.

Is the kinase enriched in the striatum of mouse brains?

The enrichment of phosphorylated N-terminal and full-length htt in the striatum of HD KI mice suggests that there may be striatal enrichment of the kinase that phosphorylates S16. To confirm this I would perform immunocytochemical staining with an antibody against the kinase, which may be identified in the above *in vitro* experiments. I would use the HD KI 140Q mice for this experiment because they show striatal specific nuclear accumulation of htt. The antibody against the putative kinase would also be used for immunoprecipitation to deplete the kinase in striatal lysates. This lysate would then be used for an *in vitro* phosphorylation assay to see if depleting the putative kinase reduces S16 peptide phosphorylation.

If the striatal enrichment of the kinase is not seen, one possibility is that the kinase activity rather than its expression is upregulated. To explore this possibility I would have to examine the signaling pathway responsible for regulating the kinase activity. Using antibodies against the regulatory proteins, the expression levels of these signaling molecules could be assessed by western blotting or immunocytochemistry. I would determine whether they show altered expression specific to the striatum, which could also be responsible for the increased S16 phosphorylation in the striatum. I would also look at

the activity of these regulatory proteins if I do not see changes in their expression levels. Protein activity can be regulated by mechanisms such as phosphorylation, cleavage or binding to another protein; all of which could be analyzed biochemically.

Another possibility is that there is a striatal specific reduction of activity or expression of the phosphatase responsible for removing phosphate from the S16 residue. Although phosphatase inhibitors are not as specific as kinase inhibitors, using their inhibitors in the assays similar to kinase inhibitor experiments may narrow down some candidates, likely specific to a class of phosphatases. Likewise, it is also important to look at the expression and functional regulation of the phosphatase to see if it is altered in the striatum compared to the other brain regions.

Determining why the striatum shows increased levels of htt phosphorylated at S16 is important for understanding the pathogenesis of HD and also for the development of therapeutics. Potentially, a drug that decreases S16 phosphorylation and thus prevents nuclear accumulation of htt may alleviate HD symptoms. A drug screen can be carried out on N17 peptides or HEK 293 cells transfected with N-terminal mutant htt to identify a drug that reduces htt phosphorylation at S16, assuming that increased nuclear accumulation of mutant htt by S16 phosphorylation is toxic, which as discussed previously, is still up for debate. If it turns out that S16 phosphorylation is in fact protective, the screen would search for drugs that increase S16 phosphorylation. Such a drug would also be very useful for understanding how S16 phosphorylation is regulated in the striatum.

Is the phosphorylation of S16 of huntingtin toxic or protective?

Since the toxicity data generated by me, Thompson et al, and Gu et al are contradictory, more work needs to be done to sort out the role of S16 phosphorylation in htt induced toxicity. As discussed in chapter 3, many factors influence *in vitro* htt toxicity data. Furthermore, the neurological phenotypes of transgenic mice are determined by the copy numbers and chromosomal insertion sites of transgenes. Thus, a rigorous experiment is to generate HD knock-in mice that express N-terminal mutant htt (N208-120Q) with either the S16A or S16D mutations at the endogenous level. These mice will be compared with regard to their neurological phenotypes as well as nuclear localization and aggregation of mutant htt. Neurological phenotypes would be assessed by analysis of their motor abilities, life span and weight changes. Phosphorylation of S16 in these mice could be unequivocally verified using mass spectrometry. The results of these experiments could provide strong *in vivo* evidence that phosphorylation of N-terminal fragments is important for regulating subcellular regulation and is involved in HD neuropathology.

Are the functions of the N-terminal post-translational modifications dependent on each other?

Since there are multiple known post-translational modifications (phosphorylation of T3, S13 and S16 and SUMOylation or ubiquitination of K6 and K9) that occur within the first 17 amino acids of htt, it is possible that the presence of one may enhance or inhibit the modification of a nearby residue due to changes in folding. It is also possible that the modification of one residue influences the function of another modified residue.

Since the phosphorylation of S16 of N-terminal htt has now been studied individually, the function of S13 phosphorylation should also be studied in a similar manner. Once we know the individual roles of the post-translational modifications we can start to determine how they influence each other and begin to understand the mechanisms by which N-terminal htt regulates subcellular localization and cell viability. This may resolve the discrepancies in toxicity and aggregation data observed between the different N-terminal phosphorylation studies.

Based on the previously published data showing that sumoylation of K6 and K9 increases htt toxicity while ubiquitination of the same residues protects cells from htt induced toxicity, it is possible that the phosphorylation of S16 prevents the sumoylation of K6 and/or K9 thereby reducing the nuclear toxicity. To test this, I would use an N17 peptide containing A16 as the substrate and mouse brain lysate as the kinase source for an *in vitro* phosphorylation assay. I would then perform mass spectrometry on the phosphorylation reaction samples to determine whether K6 and/or K9 are sumoylated. Alternatively, I could use S16-htt or S16A-htt immunoprecipitated from transfected HEK 293 cells as the substrate of the phosphorylation assay, run the samples on a western blot and probe with an antibody against SUMO. S16 phosphorylation induced inhibition of K6 and K9 sumoylation would support a protective role of S16 phosphorylated htt, which would be consistent with the toxicity studies by Gu et al (2009) and me. If S16 instead increases sumoylation of K6 or K9, S16 phosphorylation may be protective in the cytoplasm and toxic in the nucleus. Understanding how these N-terminal post-translational modifications influence one another is crucial to understanding HD pathogenesis, as the N17 region of htt has been shown by several groups to be crucial for

regulating the subcellular localization of htt. It would also allow us to define potential HD therapeutic targets aimed at altering the post-translational modification of htt.

What are some potential targets for developing Huntington's disease therapeutics?

Since there are currently no effective treatments or cures for Huntington's disease, it is important that more research is done to understand HD pathogenesis with the hope of finding a safe and effective therapeutic. Based on my findings and other reports, there are several potential targets for ameliorating HD symptoms. First, a drug that blocks the production of N-terminal fragments < 75 kDa or increases the efficiency of the removal of these fragments may help prevent the nuclear accumulation of mutant htt and subsequent transcriptional dysregulation.

As discussed earlier, a second possibility is to alter the phosphorylation status of S16 N-terminal mutant htt. Since our data clearly shows that S16 phosphorylation enhances nuclear accumulation of mutant htt fragments, it would be logical to find a drug that prevents S16 phosphorylation and thus nuclear accumulation; however, more research needs to be done to understand how all of the post-translational modifications of the N-terminus of htt influences htt-induced toxicity and HD pathogenesis.

5.3 Conclusions

Huntington's disease is a fatal, late-onset neurodegenerative disorder caused by an expansion of the polyQ tract in exon 1 of the protein. No effective treatment has been identified to date, and much more remains to be understood about HD pathogenesis. The work presented in this dissertation provides a novel mechanism for the preferential

accumulation of N-terminal mutant htt in the striatal nuclei. We present four important findings. First, due to the inverse correlation between nuclear htt levels and fragment length, the accumulation of small N-terminal htt fragments is likely due to a passive diffusion mechanism. Second, phosphorylation of serine 16 of N-terminal htt causes nuclear accumulation and aggregation of mutant N-terminal htt. Third, the striatal nuclei are enriched for htt phosphorylated at S16 compared to the cortex and striatum. Fourth, phosphorylation of htt at S16 interferes with the nuclear export proteins in a length dependent manner thus leaving it trapped in the striatal nuclei to accumulate. These insights provide potential therapeutic targets to be explored for the treatment of HD.

Figure 5-1

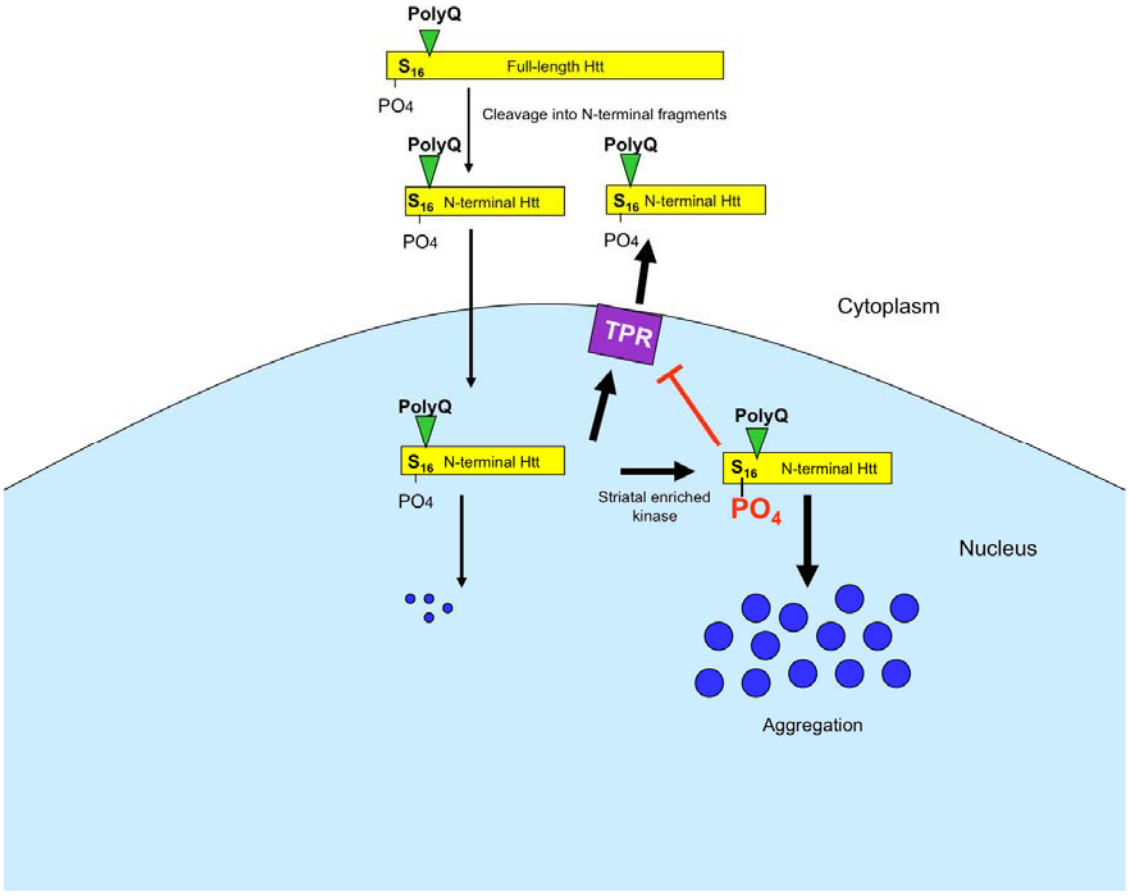
PolyQ
S16
Full-length Htt
PO4
Cleavage into N-terminal fragments
PolyQ
S16 N-terminal Htt
PO4
PolyQ
S16 N-terminal Htt
PO4
Cytoplasm
TPR
PolyQ
S16 N-terminal Htt
PO4
Striatal enriched kinase
PolyQ
S16 N-terminal Htt
PO4
Nucleus
Aggregation

Figure 5-1 A model for preferential striatal nuclear accumulation of htt phosphorylated at S16. In the cytoplasm, full-length mutant htt is proteolytically cleaved into small N-terminal htt fragments, which can enter the nucleus. Increased phosphorylation of S16 in N-terminal mutant htt enhances its aggregation and reduces its association with the nuclear pore complex protein Tpr, resulting in the accumulation of mutant htt in the nucleus. The size of N-terminal htt does not represent its actual proportion with respect to full-length htt.

References

Adachi, H., Katsuno, M., Minamiyama, M., Sang, C., Pagoulatos, G., Angelidis, C., Kusakabe, M., Yoshiki, A., Kobayashi, Y., Doyu, M.*, et al.* (2003). Heat shock protein 70 chaperone overexpression ameliorates phenotypes of the spinal and bulbar muscular atrophy transgenic mouse model by reducing nuclear-localized mutant androgen receptor protein. J Neurosci *23*, 2203-2211.

Aiken, C.T., Steffan, J.S., Guerrero, C.M., Khashwji, H., Lukacsovich, T., Simmons, D., Purcell, J.M., Menhaji, K., Zhu, Y.Z., Green, K.*, et al.* (2009). Phosphorylation of threonine 3: implications for Huntingtin aggregation and neurotoxicity. J Biol Chem *284*, 29427-29436.

Allen, T.D., Cronshaw, J.M., Bagley, S., Kiseleva, E., and Goldberg, M.W. (2000). The nuclear pore complex: mediator of translocation between nucleus and cytoplasm. J Cell Sci *113 (Pt 10)*, 1651-1659.

Arrasate, M., Mitra, S., Schweitzer, E.S., Segal, M.R., and Finkbeiner, S. (2004). Inclusion body formation reduces levels of mutant huntingtin and the risk of neuronal death. Nature *431*, 805-810.

Atwal, R.S., Xia, J., Pinchev, D., Taylor, J., Epand, R.M., and Truant, R. (2007). Huntingtin has a membrane association signal that can modulate huntingtin aggregation, nuclear entry and toxicity. Hum Mol Genet *16*, 2600-2615.

Benn, C.L., Landles, C., Li, H., Strand, A.D., Woodman, B., Sathasivam, K., Li, S.H., Ghazi-Noori, S., Hockly, E., Faruque, S.M.*, et al.* (2005). Contribution of nuclear and extranuclear polyQ to neurological phenotypes in mouse models of Huntington's disease. Hum Mol Genet *14*, 3065-3078.

Bennett, E.J., Shaler, T.A., Woodman, B., Ryu, K.Y., Zaitseva, T.S., Becker, C.H., Bates, G.P., Schulman, H., and Kopito, R.R. (2007). Global changes to the ubiquitin system in Huntington's disease. Nature *448*, 704-708.

Bett, J.S., Cook, C., Petrucelli, L., and Bates, G.P. (2009). The ubiquitin-proteasome reporter GFPu does not accumulate in neurons of the R6/2 transgenic mouse model of Huntington's disease. PLoS One *4*, e5128.

Bett, J.S., Goellner, G.M., Woodman, B., Pratt, G., Rechsteiner, M., and Bates, G.P. (2006). Proteasome impairment does not contribute to pathogenesis in R6/2 Huntington's disease mice: exclusion of proteasome activator REGgamma as a therapeutic target. Hum Mol Genet *15*, 33-44.

Boutell, J.M., Thomas, P., Neal, J.W., Weston, V.J., Duce, J., Harper, P.S., and Jones, A.L. (1999). Aberrant interactions of transcriptional repressor proteins with the Huntington's disease gene product, huntingtin. Hum Mol Genet *8*, 1647-1655.

Bowman, A.B., Yoo, S.Y., Dantuma, N.P., and Zoghbi, H.Y. (2005). Neuronal dysfunction in a polyglutamine disease model occurs in the absence of ubiquitin-proteasome system impairment and inversely correlates with the degree of nuclear inclusion formation. Hum Mol Genet *14*, 679-691.

Cattaneo, E., Rigamonti, D., Goffredo, D., Zuccato, C., Squitieri, F., and Sipione, S. (2001). Loss of normal huntingtin function: new developments in Huntington's disease research. Trends Neurosci *24*, 182-188.

Chai, Y., Wu, L., Griffin, J.D., and Paulson, H.L. (2001). The role of protein composition in specifying nuclear inclusion formation in polyglutamine disease. J Biol Chem *276*, 44889-44897.

Chan, E.Y., Luthi-Carter, R., Strand, A., Solano, S.M., Hanson, S.A., DeJohn, M.M., Kooperberg, C., Chase, K.O., DiFiglia, M., Young, A.B.*, et al.* (2002). Increased huntingtin protein length reduces the number of polyglutamine-induced gene expression changes in mouse models of Huntington's disease. Hum Mol Genet *11*, 1939-1951.

Chan, H.Y., Warrick, J.M., Gray-Board, G.L., Paulson, H.L., and Bonini, N.M. (2000). Mechanisms of chaperone suppression of polyglutamine disease: selectivity, synergy and modulation of protein solubility in Drosophila. Hum Mol Genet *9*, 2811-2820.

Chen-Plotkin, A.S., Sadri-Vakili, G., Yohrling, G.J., Braveman, M.W., Benn, C.L., Glajch, K.E., DiRocco, D.P., Farrell, L.A., Krainc, D., Gines, S., *et al.* (2006). Decreased association of the transcription factor Sp1 with genes downregulated in Huntington's disease. Neurobiol Dis *22*, 233-241.

Colin, E., Zala, D., Liot, G., Rangone, H., Borrell-Pages, M., Li, X.J., Saudou, F., and Humbert, S. (2008). Huntingtin phosphorylation acts as a molecular switch for anterograde/retrograde transport in neurons. EMBO J *27*, 2124-2134.

Cooper, J.K., Schilling, G., Peters, M.F., Herring, W.J., Sharp, A.H., Kaminsky, Z., Masone, J., Khan, F.A., Delanoy, M., Borchelt, D.R., *et al.* (1998). Truncated N-terminal fragments of huntingtin with expanded glutamine repeats form nuclear and cytoplasmic aggregates in cell culture. Hum Mol Genet *7*, 783-790.

Cornett, J., Cao, F., Wang, C.E., Ross, C.A., Bates, G.P., Li, S.H., and Li, X.J. (2005). Polyglutamine expansion of huntingtin impairs its nuclear export. Nat Genet *37*, 198-204.

Cornett, J., Smith, L., Friedman, M., Shin, J.Y., Li, X.J., and Li, S.H. (2006). Context-dependent dysregulation of transcription by mutant huntingtin. J Biol Chem *281*, 36198-36204.

Cummings, C.J., Sun, Y., Opal, P., Antalffy, B., Mestril, R., Orr, H.T., Dillmann, W.H., and Zoghbi, H.Y. (2001). Over-expression of inducible HSP70 chaperone suppresses

neuropathology and improves motor function in SCA1 mice. Hum Mol Genet *10*, 1511-1518.

Davies, S.W., Turmaine, M., Cozens, B.A., DiFiglia, M., Sharp, A.H., Ross, C.A., Scherzinger, E., Wanker, E.E., Mangiarini, L., and Bates, G.P. (1997). Formation of neuronal intranuclear inclusions underlies the neurological dysfunction in mice transgenic for the HD mutation. Cell *90*, 537-548.

de la Monte, S.M., Vonsattel, J.P., and Richardson, E.P., Jr. (1988). Morphometric demonstration of atrophic changes in the cerebral cortex, white matter, and neostriatum in Huntington's disease. J Neuropathol Exp Neurol *47*, 516-525.

De Rooij, K.E., Dorsman, J.C., Smoor, M.A., Den Dunnen, J.T., and Van Ommen, G.J. (1996). Subcellular localization of the Huntington's disease gene product in cell lines by immunofluorescence and biochemical subcellular fractionation. Hum Mol Genet *5*, 1093-1099.

DiFiglia, M., Sapp, E., Chase, K., Schwarz, C., Meloni, A., Young, C., Martin, E., Vonsattel, J.P., Carraway, R., Reeves, S.A., *et al.* (1995). Huntingtin is a cytoplasmic protein associated with vesicles in human and rat brain neurons. Neuron *14*, 1075-1081.

DiFiglia, M., Sapp, E., Chase, K.O., Davies, S.W., Bates, G.P., Vonsattel, J.P., and Aronin, N. (1997). Aggregation of huntingtin in neuronal intranuclear inclusions and dystrophic neurites in brain. Science *277*, 1990-1993.

Dragatsis, I., Levine, M.S., and Zeitlin, S. (2000). Inactivation of Hdh in the brain and testis results in progressive neurodegeneration and sterility in mice. Nat Genet *26*, 300-306.

Dunah, A.W., Jeong, H., Griffin, A., Kim, Y.M., Standaert, D.G., Hersch, S.M., Mouradian, M.M., Young, A.B., Tanese, N., and Krainc, D. (2002). Sp1 and TAFII130 transcriptional activity disrupted in early Huntington's disease. Science *296*, 2238-2243.

Duyao, M., Ambrose, C., Myers, R., Novelletto, A., Persichetti, F., Frontali, M., Folstein, S., Ross, C., Franz, M., Abbott, M.*, et al.* (1993). Trinucleotide repeat length instability and age of onset in Huntington's disease. Nat Genet *4*, 387-392.

Duyao, M.P., Auerbach, A.B., Ryan, A., Persichetti, F., Barnes, G.T., McNeil, S.M., Ge, P., Vonsattel, J.P., Gusella, J.F., Joyner, A.L.*, et al.* (1995). Inactivation of the mouse Huntington's disease gene homolog Hdh. Science *269*, 407-410.

Evert, B.O., Vogt, I.R., Vieira-Saecker, A.M., Ozimek, L., de Vos, R.A., Brunt, E.R., Klockgether, T., and Wullner, U. (2003). Gene expression profiling in ataxin-3

expressing cell lines reveals distinct effects of normal and mutant ataxin-3. J Neuropathol Exp Neurol *62*, 1006-1018.

Faber, P.W., Barnes, G.T., Srinidhi, J., Chen, J., Gusella, J.F., and MacDonald, M.E. (1998). Huntingtin interacts with a family of WW domain proteins. Hum Mol Genet *7*, 1463-1474.

Friedman, M.J., Shah, A.G., Fang, Z.H., Ward, E.G., Warren, S.T., Li, S., and Li, X.J. (2007). Polyglutamine domain modulates the TBP-TFIIB interaction: implications for its normal function and neurodegeneration. Nat Neurosci *10*, 1519-1528.

Gafni, J., and Ellerby, L.M. (2002). Calpain activation in Huntington's disease. J Neurosci *22*, 4842-4849.

Gafni, J., Hermel, E., Young, J.E., Wellington, C.L., Hayden, M.R., and Ellerby, L.M. (2004). Inhibition of calpain cleavage of huntingtin reduces toxicity: accumulation of calpain/caspase fragments in the nucleus. J Biol Chem *279*, 20211-20220.

Gauthier, L.R., Charrin, B.C., Borrell-Pages, M., Dompierre, J.P., Rangone, H., Cordelieres, F.P., De Mey, J., MacDonald, M.E., Lessmann, V., Humbert, S.*, et al.* (2004). Huntingtin controls neurotrophic support and survival of neurons by enhancing BDNF vesicular transport along microtubules. Cell *118*, 127-138.

Graham, R.K., Deng, Y., Slow, E.J., Haigh, B., Bissada, N., Lu, G., Pearson, J., Shehadeh, J., Bertram, L., Murphy, *Z., et al.* (2006). Cleavage at the caspase-6 site is required for neuronal dysfunction and degeneration due to mutant huntingtin. Cell *125*, 1179-1191.

Group, T.H.s.D.C.R. (1993). A novel gene containing a trinucleotide repeat that is expanded and unstable on Huntington's disease chromosomes. The Huntington's Disease Collaborative Research Group. Cell *72*, 971-983.

Gu, X., Greiner, E.R., Mishra, R., Kodali, R., Osmand, A., Finkbeiner, S., Steffan, J.S., Thompson, L.M., Wetzel, R., and Yang, X.W. (2009). Serines 13 and 16 are critical determinants of full-length human mutant huntingtin induced disease pathogenesis in HD mice. Neuron *64*, 828-840.

Gutekunst, C.A., Li, S.H., Yi, H., Mulroy, J.S., Kuemmerle, S., Jones, R., Rye, D., Ferrante, R.J., Hersch, S.M., and Li, X.J. (1999). Nuclear and neuropil aggregates in Huntington's disease: relationship to neuropathology. J Neurosci *19*, 2522-2534.

Haacke, A., Hartl, F.U., and Breuer, P. (2007). Calpain inhibition is sufficient to suppress aggregation of polyglutamine-expanded ataxin-3. J Biol Chem *282*, 18851-18856.

Hackam, A.S., Singaraja, R., Wellington, C.L., Metzler, M., McCutcheon, K., Zhang, T., Kalchman, M., and Hayden, M.R. (1998). The influence of huntingtin protein size on nuclear localization and cellular toxicity. J Cell Biol *141*, 1097-1105.

Hackam, A.S., Singaraja, R., Zhang, T., Gan, L., and Hayden, M.R. (1999). In vitro evidence for both the nucleus and cytoplasm as subcellular sites of pathogenesis in Huntington's disease. Hum Mol Genet *8*, 25-33.

Harper, P.S. (1992). The epidemiology of Huntington's disease. Hum Genet *89*, 365-376.

Hay, D.G., Sathasivam, K., Tobaben, S., Stahl, B., Marber, M., Mestril, R., Mahal, A., Smith, D.L., Woodman, B., and Bates, G.P. (2004). Progressive decrease in chaperone protein levels in a mouse model of Huntington's disease and induction of stress proteins as a therapeutic approach. Hum Mol Genet *13*, 1389-1405.

Hickey, M.A., Kosmalska, A., Enayati, J., Cohen, R., Zeitlin, S., Levine, M.S., and Chesselet, M.F. (2008). Extensive early motor and non-motor behavioral deficits are followed by striatal neuronal loss in knock-in Huntington's disease mice. Neuroscience *157*, 280-295.

Holbert, S., Denghien, I., Kiechle, T., Rosenblatt, A., Wellington, C., Hayden, M.R., Margolis, R.L., Ross, C.A., Dausset, J., Ferrante, R.J., *et al.* (2001). The Gln-Ala repeat transcriptional activator CA150 interacts with huntingtin: neuropathologic and genetic

evidence for a role in Huntington's disease pathogenesis. Proc Natl Acad Sci U S A *98*, 1811-1816.

Hoogeveen, A.T., Willemsen, R., Meyer, N., de Rooij, K.E., Roos, R.A., van Ommen, G.J., and Galjaard, H. (1993). Characterization and localization of the Huntington disease gene product. Hum Mol Genet *2*, 2069-2073.

Huang, C.C., Faber, P.W., Persichetti, F., Mittal, V., Vonsattel, J.P., MacDonald, M.E., and Gusella, J.F. (1998). Amyloid formation by mutant huntingtin: threshold, progressivity and recruitment of normal polyglutamine proteins. Somat Cell Mol Genet *24*, 217-233.

Iwata, A., Christianson, J.C., Bucci, M., Ellerby, L.M., Nukina, N., Forno, L.S., and Kopito, R.R. (2005). Increased susceptibility of cytoplasmic over nuclear polyglutamine aggregates to autophagic degradation. Proc Natl Acad Sci U S A *102*, 13135-13140.

Jackson, W.S., Tallaksen-Greene, S.J., Albin, R.L., and Detloff, P.J. (2003). Nucleocytoplasmic transport signals affect the age at onset of abnormalities in knock-in mice expressing polyglutamine within an ectopic protein context. Hum Mol Genet *12*, 1621-1629.

Jana, N.R., Tanaka, M., Wang, G., and Nukina, N. (2000). Polyglutamine length-dependent interaction of Hsp40 and Hsp70 family chaperones with truncated N-terminal

huntingtin: their role in suppression of aggregation and cellular toxicity. Hum Mol Genet *9*, 2009-2018.

Kalchman, M.A., Graham, R.K., Xia, G., Koide, H.B., Hodgson, J.G., Graham, K.C., Goldberg, Y.P., Gietz, R.D., Pickart, C.M., and Hayden, M.R. (1996). Huntingtin is ubiquitinated and interacts with a specific ubiquitin-conjugating enzyme. J Biol Chem *271*, 19385-19394.

Kazemi-Esfarjani, P., and Benzer, S. (2000). Genetic suppression of polyglutamine toxicity in Drosophila. Science *287*, 1837-1840.

Kegel, K.B., Meloni, A.R., Yi, Y., Kim, Y.J., Doyle, E., Cuiffo, B.G., Sapp, E., Wang, Y., Qin, Z.H., Chen, J.D., *et al.* (2002). Huntingtin is present in the nucleus, interacts with the transcriptional corepressor C-terminal binding protein, and represses transcription. J Biol Chem *277*, 7466-7476.

Kim, Y.J., Yi, Y., Sapp, E., Wang, Y., Cuiffo, B., Kegel, K.B., Qin, Z.H., Aronin, N., and DiFiglia, M. (2001). Caspase 3-cleaved N-terminal fragments of wild-type and mutant huntingtin are present in normal and Huntington's disease brains, associate with membranes, and undergo calpain-dependent proteolysis. Proc Natl Acad Sci U S A *98*, 12784-12789.

King, M.A., Hands, S., Hafiz, F., Mizushima, N., Tolkovsky, A.M., and Wyttenbach, A. (2008). Rapamycin inhibits polyglutamine aggregation independently of autophagy by reducing protein synthesis. Mol Pharmacol *73*, 1052-1063.

Kobayashi, Y., Kume, A., Li, M., Doyu, M., Hata, M., Ohtsuka, K., and Sobue, G. (2000). Chaperones Hsp70 and Hsp40 suppress aggregate formation and apoptosis in cultured neuronal cells expressing truncated androgen receptor protein with expanded polyglutamine tract. J Biol Chem *275*, 8772-8778.

Kuhn, A., Goldstein, D.R., Hodges, A., Strand, A.D., Sengstag, T., Kooperberg, C., Becanovic, K., Pouladi, M.A., Sathasivam, K., Cha, J.H.*, et al.* (2007). Mutant huntingtin's effects on striatal gene expression in mice recapitulate changes observed in human Huntington's disease brain and do not differ with mutant huntingtin length or wild-type huntingtin dosage. Hum Mol Genet *16*, 1845-1861.

Li, H., Li, S.H., Johnston, H., Shelbourne, P.F., and Li, X.J. (2000). Amino-terminal fragments of mutant huntingtin show selective accumulation in striatal neurons and synaptic toxicity. Nat Genet *25*, 385-389.

Li, H., Li, S.H., Yu, Z.X., Shelbourne, P., and Li, X.J. (2001). Huntingtin aggregate-associated axonal degeneration is an early pathological event in Huntington's disease mice. J Neurosci *21*, 8473-8481.

Li, S.H., Cheng, A.L., Li, H., and Li, X.J. (1999). Cellular defects and altered gene expression in PC12 cells stably expressing mutant huntingtin. J Neurosci *19*, 5159-5172.

Li, S.H., Cheng, A.L., Zhou, H., Lam, S., Rao, M., Li, H., and Li, X.J. (2002). Interaction of Huntington disease protein with transcriptional activator Sp1. Mol Cell Biol *22*, 1277-1287.

Li, S.H., Gutekunst, C.A., Hersch, S.M., and Li, X.J. (1998). Interaction of huntingtin-associated protein with dynactin P150Glued. J Neurosci *18*, 1261-1269.

Li, S.H., and Li, X.J. (1998). Aggregation of N-terminal huntingtin is dependent on the length of its glutamine repeats. Hum Mol Genet *7*, 777-782.

Li, X., Wang, C.E., Huang, S., Xu, X., Li, X.J., Li, H., and Li, S. (2010). Inhibiting the ubiquitin-proteasome system leads to preferential accumulation of toxic N-terminal mutant huntingtin fragments. Hum Mol Genet *19*, 2445-2455.

Li, X.J., Li, S.H., Sharp, A.H., Nucifora, F.C., Jr., Schilling, G., Lanahan, A., Worley, P., Snyder, S.H., and Ross, C.A. (1995). A huntingtin-associated protein enriched in brain with implications for pathology. Nature *378*, 398-402.

Lin, C.H., Tallaksen-Greene, S., Chien, W.M., Cearley, J.A., Jackson, W.S., Crouse, A.B., Ren, S., Li, X.J., Albin, R.L., and Detloff, P.J. (2001). Neurological abnormalities in a knock-in mouse model of Huntington's disease. Hum Mol Genet *10*, 137-144.

Lotz, G.P., Legleiter, J., Aron, R., Mitchell, E.J., Huang, S.Y., Ng, C., Glabe, C., Thompson, L.M., and Muchowski, P.J. Hsp70 and Hsp40 functionally interact with soluble mutant huntingtin oligomers in a classic ATP-dependent reaction cycle. J Biol Chem *285*, 38183-38193.

Lunkes, A., Lindenberg, K.S., Ben-Haiem, L., Weber, C., Devys, D., Landwehrmeyer, G.B., Mandel, J.L., and Trottier, Y. (2002). Proteases acting on mutant huntingtin generate cleaved products that differentially build up cytoplasmic and nuclear inclusions. Mol Cell *10*, 259-269.

Luthi-Carter, R., Hanson, S.A., Strand, A.D., Bergstrom, D.A., Chun, W., Peters, N.L., Woods, A.M., Chan, E.Y., Kooperberg, C., Krainc, D., *et al.* (2002a). Dysregulation of gene expression in the R6/2 model of polyglutamine disease: parallel changes in muscle and brain. Hum Mol Genet *11*, 1911-1926.

Luthi-Carter, R., Strand, A., Peters, N.L., Solano, S.M., Hollingsworth, Z.R., Menon, A.S., Frey, A.S., Spektor, B.S., Penney, E.B., Schilling, G., *et al.* (2000). Decreased expression of striatal signaling genes in a mouse model of Huntington's disease. Hum Mol Genet *9*, 1259-1271.

Luthi-Carter, R., Strand, A.D., Hanson, S.A., Kooperberg, C., Schilling, G., La Spada, A.R., Merry, D.E., Young, A.B., Ross, C.A., Borchelt, D.R., *et al.* (2002b). Polyglutamine and transcription: gene expression changes shared by DRPLA and Huntington's disease mouse models reveal context-independent effects. Hum Mol Genet *11*, 1927-1937.

Mangiarini, L., Sathasivam, K., Seller, M., Cozens, B., Harper, A., Hetherington, C., Lawton, M., Trottier, Y., Lehrach, H., Davies, S.W., *et al.* (1996). Exon 1 of the HD gene with an expanded CAG repeat is sufficient to cause a progressive neurological phenotype in transgenic mice. Cell *87*, 493-506.

Mao, Y., Senic-Matuglia, F., Di Fiore, P.P., Polo, S., Hodsdon, M.E., and De Camilli, P. (2005). Deubiquitinating function of ataxin-3: insights from the solution structure of the Josephin domain. Proc Natl Acad Sci U S A *102*, 12700-12705.

McGuire, J.R., Rong, J., Li, S.H., and Li, X.J. (2006). Interaction of Huntingtin-associated protein-1 with kinesin light chain: implications in intracellular trafficking in neurons. J Biol Chem *281*, 3552-3559.

Nasir, J., Floresco, S.B., O'Kusky, J.R., Diewert, V.M., Richman, J.M., Zeisler, J., Borowski, A., Marth, J.D., Phillips, A.G., and Hayden, M.R. (1995). Targeted disruption

of the Huntington's disease gene results in embryonic lethality and behavioral and morphological changes in heterozygotes. Cell *81*, 811-823.

Nucifora, F.C., Jr., Sasaki, M., Peters, M.F., Huang, H., Cooper, J.K., Yamada, M., Takahashi, H., Tsuji, S., Troncoso, J., Dawson, V.L., *et al.* (2001). Interference by huntingtin and atrophin-1 with cbp-mediated transcription leading to cellular toxicity. Science *291*, 2423-2428.

Ordway, J.M., Tallaksen-Greene, S., Gutekunst, C.A., Bernstein, E.M., Cearley, J.A., Wiener, H.W., Dure, L.S.t., Lindsey, R., Hersch, S.M., Jope, R.S., *et al.* (1997). Ectopically expressed CAG repeats cause intranuclear inclusions and a progressive late onset neurological phenotype in the mouse. Cell *91*, 753-763.

Orr, H.T., and Zoghbi, H.Y. (2007). Trinucleotide repeat disorders. Annu Rev Neurosci *30*, 575-621.

Perez, M.K., Paulson, H.L., Pendse, S.J., Saionz, S.J., Bonini, N.M., and Pittman, R.N. (1998). Recruitment and the role of nuclear localization in polyglutamine-mediated aggregation. J Cell Biol *143*, 1457-1470.

Peters, M.F., Nucifora, F.C., Jr., Kushi, J., Seaman, H.C., Cooper, J.K., Herring, W.J., Dawson, V.L., Dawson, T.M., and Ross, C.A. (1999). Nuclear targeting of mutant Huntingtin increases toxicity. Mol Cell Neurosci *14*, 121-128.

Ralser, M., Albrecht, M., Nonhoff, U., Lengauer, T., Lehrach, H., and Krobitsch, S. (2005). An integrative approach to gain insights into the cellular function of human ataxin-2. J Mol Biol *346*, 203-214.

Ratovitski, T., Gucek, M., Jiang, H., Chighladze, E., Waldron, E., D'Ambola, J., Hou, Z., Liang, Y., Poirier, M.A., Hirschhorn, R.R., *et al.* (2009). Mutant huntingtin N-terminal fragments of specific size mediate aggregation and toxicity in neuronal cells. J Biol Chem *284*, 10855-10867.

Ratovitski, T., Nakamura, M., D'Ambola, J., Chighladze, E., Liang, Y., Wang, W., Graham, R., Hayden, M.R., Borchelt, D.R., Hirschhorn, R.R., *et al.* (2007). N-terminal proteolysis of full-length mutant huntingtin in an inducible PC12 cell model of Huntington's disease. Cell Cycle *6*, 2970-2981.

Ravikumar, B., Imarisio, S., Sarkar, S., O'Kane, C.J., and Rubinsztein, D.C. (2008). Rab5 modulates aggregation and toxicity of mutant huntingtin through macroautophagy in cell and fly models of Huntington disease. J Cell Sci *121*, 1649-1660.

Ravikumar, B., Vacher, C., Berger, Z., Davies, J.E., Luo, S., Oroz, L.G., Scaravilli, F., Easton, D.F., Duden, R., O'Kane, C.J., *et al.* (2004). Inhibition of mTOR induces autophagy and reduces toxicity of polyglutamine expansions in fly and mouse models of Huntington disease. Nat Genet *36*, 585-595.

Rockabrand, E., Slepko, N., Pantalone, A., Nukala, V.N., Kazantsev, A., Marsh, J.L., Sullivan, P.G., Steffan, J.S., Sensi, S.L., and Thompson, L.M. (2007). The first 17 amino acids of Huntingtin modulate its sub-cellular localization, aggregation and effects on calcium homeostasis. Hum Mol Genet *16*, 61-77.

Saudou, F., Finkbeiner, S., Devys, D., and Greenberg, M.E. (1998). Huntingtin acts in the nucleus to induce apoptosis but death does not correlate with the formation of intranuclear inclusions. Cell *95*, 55-66.

Sawa, A., Nagata, E., Sutcliffe, S., Dulloor, P., Cascio, M.B., Ozeki, Y., Roy, S., Ross, C.A., and Snyder, S.H. (2005). Huntingtin is cleaved by caspases in the cytoplasm and translocated to the nucleus via perinuclear sites in Huntington's disease patient lymphoblasts. Neurobiol Dis *20*, 267-274.

Schilling, B., Gafni, J., Torcassi, C., Cong, X., Row, R.H., LaFevre-Bernt, M.A., Cusack, M.P., Ratovitski, T., Hirschhorn, R., Ross, C.A., *et al.* (2006). Huntingtin phosphorylation sites mapped by mass spectrometry. Modulation of cleavage and toxicity. J Biol Chem *281*, 23686-23697.

Schilling, G., Becher, M.W., Sharp, A.H., Jinnah, H.A., Duan, K., Kotzuk, J.A., Slunt, H.H., Ratovitski, T., Cooper, J.K., Jenkins, N.A., *et al.* (1999a). Intranuclear inclusions

and neuritic aggregates in transgenic mice expressing a mutant N-terminal fragment of huntingtin. Hum Mol Genet *8*, 397-407.

Schilling, G., Savonenko, A.V., Klevytska, A., Morton, J.L., Tucker, S.M., Poirier, M., Gale, A., Chan, N., Gonzales, V., Slunt, H.H., *et al.* (2004). Nuclear-targeting of mutant huntingtin fragments produces Huntington's disease-like phenotypes in transgenic mice. Hum Mol Genet *13*, 1599-1610.

Schilling, G., Wood, J.D., Duan, K., Slunt, H.H., Gonzales, V., Yamada, M., Cooper, J.K., Margolis, R.L., Jenkins, N.A., Copeland, N.G., *et al.* (1999b). Nuclear accumulation of truncated atrophin-1 fragments in a transgenic mouse model of DRPLA. Neuron *24*, 275-286.

Sharp, A.H., Loev, S.J., Schilling, G., Li, S.H., Li, X.J., Bao, J., Wagster, M.V., Kotzuk, J.A., Steiner, J.P., Lo, A., *et al.* (1995). Widespread expression of Huntington's disease gene (IT15) protein product. Neuron *14*, 1065-1074.

Shelbourne, P.F., Killeen, N., Hevner, R.F., Johnston, H.M., Tecott, L., Lewandoski, M., Ennis, M., Ramirez, L., Li, Z., Iannicola, C., *et al.* (1999). A Huntington's disease CAG expansion at the murine Hdh locus is unstable and associated with behavioural abnormalities in mice. Hum Mol Genet *8*, 763-774.

Shibata, M., Lu, T., Furuya, T., Degterev, A., Mizushima, N., Yoshimori, T., MacDonald, M., Yankner, B., and Yuan, J. (2006). Regulation of intracellular accumulation of mutant Huntingtin by Beclin 1. J Biol Chem *281*, 14474-14485.

Shimohata, T., Nakajima, T., Yamada, M., Uchida, C., Onodera, O., Naruse, S., Kimura, T., Koide, R., Nozaki, K., Sano, Y., *et al.* (2000). Expanded polyglutamine stretches interact with TAFII130, interfering with CREB-dependent transcription. Nat Genet *26*, 29-36.

Sipione, S., Rigamonti, D., Valenza, M., Zuccato, C., Conti, L., Pritchard, J., Kooperberg, C., Olson, J.M., and Cattaneo, E. (2002). Early transcriptional profiles in huntingtin-inducible striatal cells by microarray analyses. Hum Mol Genet *11*, 1953-1965.

Steffan, J.S., Agrawal, N., Pallos, J., Rockabrand, E., Trotman, L.C., Slepko, N., Illes, K., Lukacsovich, T., Zhu, Y.Z., Cattaneo, E., *et al.* (2004). SUMO modification of Huntingtin and Huntington's disease pathology. Science *304*, 100-104.

Steffan, J.S., Kazantsev, A., Spasic-Boskovic, O., Greenwald, M., Zhu, Y.Z., Gohler, H., Wanker, E.E., Bates, G.P., Housman, D.E., and Thompson, L.M. (2000). The Huntington's disease protein interacts with p53 and CREB-binding protein and represses transcription. Proc Natl Acad Sci U S A *97*, 6763-6768.

Subramaniam, S., Sixt, K.M., Barrow, R., and Snyder, S.H. (2009). Rhes, a striatal specific protein, mediates mutant-huntingtin cytotoxicity. Science *324*, 1327-1330.

Takano, H., and Gusella, J.F. (2002). The predominantly HEAT-like motif structure of huntingtin and its association and coincident nuclear entry with dorsal, an NF-kB/Rel/dorsal family transcription factor. BMC Neurosci *3*, 15.

Tam, S., Spiess, C., Auyeung, W., Joachimiak, L., Chen, B., Poirier, M.A., and Frydman, J. (2009). The chaperonin TRiC blocks a huntingtin sequence element that promotes the conformational switch to aggregation. Nat Struct Mol Biol *16*, 1279-1285.

Tanaka, Y., Igarashi, S., Nakamura, M., Gafni, J., Torcassi, C., Schilling, G., Crippen, D., Wood, J.D., Sawa, A., Jenkins, N.A., *et al.* (2006). Progressive phenotype and nuclear accumulation of an amino-terminal cleavage fragment in a transgenic mouse model with inducible expression of full-length mutant huntingtin. Neurobiol Dis *21*, 381-391.

Thompson, L.M., Aiken, C.T., Kaltenbach, L.S., Agrawal, N., Illes, K., Khoshnan, A., Martinez-Vincente, M., Arrasate, M., O'Rourke, J.G., Khashwji, H., *et al.* (2009). IKK phosphorylates Huntingtin and targets it for degradation by the proteasome and lysosome. J Cell Biol *187*, 1083-1099.

Tonoki, A., Kuranaga, E., Tomioka, T., Hamazaki, J., Murata, S., Tanaka, K., and Miura, M. (2009). Genetic evidence linking age-dependent attenuation of the 26S proteasome with the aging process. Mol Cell Biol *29*, 1095-1106.

Trottier, Y., Devys, D., Imbert, G., Saudou, F., An, I., Lutz, Y., Weber, C., Agid, Y., Hirsch, E.C., and Mandel, J.L. (1995). Cellular localization of the Huntington's disease protein and discrimination of the normal and mutated form. Nat Genet *10*, 104-110.

Tsai, C.C., Kao, H.Y., Mitzutani, A., Banayo, E., Rajan, H., McKeown, M., and Evans, R.M. (2004). Ataxin 1, a SCA1 neurodegenerative disorder protein, is functionally linked to the silencing mediator of retinoid and thyroid hormone receptors. Proc Natl Acad Sci U S A *101*, 4047-4052.

Turmaine, M., Raza, A., Mahal, A., Mangiarini, L., Bates, G.P., and Davies, S.W. (2000). Nonapoptotic neurodegeneration in a transgenic mouse model of Huntington's disease. Proc Natl Acad Sci U S A *97*, 8093-8097.

Tydlacka, S., Wang, C.E., Wang, X., Li, S., and Li, X.J. (2008). Differential activities of the ubiquitin-proteasome system in neurons versus glia may account for the preferential accumulation of misfolded proteins in neurons. J Neurosci *28*, 13285-13295.

Venkatraman, P., Wetzel, R., Tanaka, M., Nukina, N., and Goldberg, A.L. (2004). Eukaryotic proteasomes cannot digest polyglutamine sequences and release them during degradation of polyglutamine-containing proteins. Mol Cell *14*, 95-104.

Wacker, J.L., Huang, S.Y., Steele, A.D., Aron, R., Lotz, G.P., Nguyen, Q., Giorgini, F., Roberson, E.D., Lindquist, S., Masliah, E.*, et al.* (2009). Loss of Hsp70 exacerbates pathogenesis but not levels of fibrillar aggregates in a mouse model of Huntington's disease. J Neurosci *29*, 9104-9114.

Wang, C.E., Tydlacka, S., Orr, A.L., Yang, S.H., Graham, R.K., Hayden, M.R., Li, S., Chan, A.W., and Li, X.J. (2008a). Accumulation of N-terminal mutant huntingtin in mouse and monkey models implicated as a pathogenic mechanism in Huntington's disease. Hum Mol Genet *17*, 2738-2751.

Wang, J., Wang, C.E., Orr, A., Tydlacka, S., Li, S.H., and Li, X.J. (2008b). Impaired ubiquitin-proteasome system activity in the synapses of Huntington's disease mice. J Cell Biol *180*, 1177-1189.

Warrick, J.M., Chan, H.Y., Gray-Board, G.L., Chai, Y., Paulson, H.L., and Bonini, N.M. (1999). Suppression of polyglutamine-mediated neurodegeneration in Drosophila by the molecular chaperone HSP70. Nat Genet *23*, 425-428.

Wellington, C.L., Ellerby, L.M., Gutekunst, C.A., Rogers, D., Warby, S., Graham, R.K., Loubser, O., van Raamsdonk, J., Singaraja, R., Yang, Y.Z., *et al.* (2002). Caspase cleavage of mutant huntingtin precedes neurodegeneration in Huntington's disease. J Neurosci *22*, 7862-7872.

Wellington, C.L., Ellerby, L.M., Hackam, A.S., Margolis, R.L., Trifiro, M.A., Singaraja, R., McCutcheon, K., Salvesen, G.S., Propp, S.S., Bromm, M., *et al.* (1998). Caspase cleavage of gene products associated with triplet expansion disorders generates truncated fragments containing the polyglutamine tract. J Biol Chem *273*, 9158-9167.

Wellington, C.L., Singaraja, R., Ellerby, L., Savill, J., Roy, S., Leavitt, B., Cattaneo, E., Hackam, A., Sharp, A., Thornberry, N., *et al.* (2000). Inhibiting caspase cleavage of huntingtin reduces toxicity and aggregate formation in neuronal and nonneuronal cells. J Biol Chem *275*, 19831-19838.

Wheeler, V.C., Gutekunst, C.A., Vrbanac, V., Lebel, L.A., Schilling, G., Hersch, S., Friedlander, R.M., Gusella, J.F., Vonsattel, J.P., Borchelt, D.R., *et al.* (2002). Early phenotypes that presage late-onset neurodegenerative disease allow testing of modifiers in Hdh CAG knock-in mice. Hum Mol Genet *11*, 633-640.

Wood, J.D., Nucifora, F.C., Jr., Duan, K., Zhang, C., Wang, J., Kim, Y., Schilling, G., Sacchi, N., Liu, J.M., and Ross, C.A. (2000). Atrophin-1, the dentato-rubral and pallido-

luysian atrophy gene product, interacts with ETO/MTG8 in the nuclear matrix and represses transcription. J Cell Biol *150*, 939-948.

Wyttenbach, A., Carmichael, J., Swartz, J., Furlong, R.A., Narain, Y., Rankin, J., and Rubinsztein, D.C. (2000). Effects of heat shock, heat shock protein 40 (HDJ-2), and proteasome inhibition on protein aggregation in cellular models of Huntington's disease. Proc Natl Acad Sci U S A *97*, 2898-2903.

Wyttenbach, A., Swartz, J., Kita, H., Thykjaer, T., Carmichael, J., Bradley, J., Brown, R., Maxwell, M., Schapira, A., Orntoft, T.F., *et al.* (2001). Polyglutamine expansions cause decreased CRE-mediated transcription and early gene expression changes prior to cell death in an inducible cell model of Huntington's disease. Hum Mol Genet *10*, 1829-1845.

Xia, J., Lee, D.H., Taylor, J., Vandelft, M., and Truant, R. (2003). Huntingtin contains a highly conserved nuclear export signal. Hum Mol Genet *12*, 1393-1403.

Yamanaka, T., Miyazaki, H., Oyama, F., Kurosawa, M., Washizu, C., Doi, H., and Nukina, N. (2008). Mutant Huntingtin reduces HSP70 expression through the sequestration of NF-Y transcription factor. EMBO J *27*, 827-839.

Yang, D., Wang, C.E., Zhao, B., Li, W., Ouyang, Z., Liu, Z., Yang, H., Fan, P., O'Neill, A., Gu, W., *et al.* (2010). Expression of Huntington's disease protein results in apoptotic neurons in the brains of cloned transgenic pigs. Hum Mol Genet *19*, 3983-3994.

Yu, Z.X., Li, S.H., Nguyen, H.P., and Li, X.J. (2002). Huntingtin inclusions do not deplete polyglutamine-containing transcription factors in HD mice. Hum Mol Genet *11*, 905-914.

Zala, D., Colin, E., Rangone, H., Liot, G., Humbert, S., and Saudou, F. (2008). Phosphorylation of mutant huntingtin at S421 restores anterograde and retrograde transport in neurons. Hum Mol Genet *17*, 3837-3846.

Zeitlin, S., Liu, J.P., Chapman, D.L., Papaioannou, V.E., and Efstratiadis, A. (1995). Increased apoptosis and early embryonic lethality in mice nullizygous for the Huntington's disease gene homologue. Nat Genet *11*, 155-163.

Zhai, W., Jeong, H., Cui, L., Krainc, D., and Tjian, R. (2005). In vitro analysis of huntingtin-mediated transcriptional repression reveals multiple transcription factor targets. Cell *123*, 1241-1253.

Zhou, H., Cao, F., Wang, Z., Yu, Z.X., Nguyen, H.P., Evans, J., Li, S.H., and Li, X.J. (2003). Huntingtin forms toxic NH2-terminal fragment complexes that are promoted by the age-dependent decrease in proteasome activity. J Cell Biol *163*, 109-118.

Zhou, H., Li, S.H., and Li, X.J. (2001). Chaperone suppression of cellular toxicity of huntingtin is independent of polyglutamine aggregation. J Biol Chem *276*, 48417-48424.

Zuccato, C., Ciammola, A., Rigamonti, D., Leavitt, B.R., Goffredo, D., Conti, L., MacDonald, M.E., Friedlander, R.M., Silani, V., Hayden, M.R., *et al.* (2001). Loss of huntingtin-mediated BDNF gene transcription in Huntington's disease. Science *293*, 493-498.

Zuccato, C., Tartari, M., Crotti, A., Goffredo, D., Valenza, M., Conti, L., Cataudella, T., Leavitt, B.R., Hayden, M.R., Timmusk, T., *et al.* (2003). Huntingtin interacts with REST/NRSF to modulate the transcription of NRSE-controlled neuronal genes. Nat Genet *35*, 76-83.